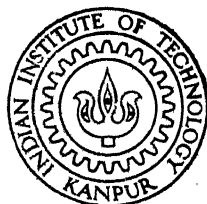


ANALYSIS OF FLUID FLOW AND HEAT TRANSFER IN A RECTANGULAR THERMOSYPHON LOOP

by

SANTOSH KUMAR KAR

**NETP
1990
M
KAR
ANA**



**NUCLEAR ENGINEERING AND TECHNOLOGY PROGRAMME
INDIAN INSTITUTE OF TECHNOLOGY KANPUR**

February, 1990

ANALYSIS OF FLUID FLOW AND HEAT TRANSFER IN A RECTANGULAR THERMOSYPHON LOOP

*A Thesis Submitted
in Partial Fulfilment of the Requirements
for the Degree of*
MASTER OF TECHNOLOGY

by
SANTOSH KUMAR KAR

to the
NUCLEAR ENGINEERING AND TECHNOLOGY PROGRAMME
INDIAN INSTITUTE OF TECHNOLOGY KANPUR
February, 1990

NETP-1990-M-KAR-ANA

30 JAN 1991

CENTRAL LIBRARY
IIT KANPUR

Acc. No. A.109995

ACKNOWLEDGEMENT

I take this opportunity to express my sincere thanks and heartfelt gratitude to Dr. K.SriRam, my thesis supervisor, whose constant encouragement, valuable suggestions and discussions regarding the problems at each stage of the thesis has made it a success. I express my thanks to Nuclear Power Corporation for suggesting this problem and financial assistance for my studies. I am also grateful to Dr. A. Sengupta, Dr. M. S. Kalra and Dr. P. Munshi who have taught me in my programme.

A lot of thanks to my classmates and other members of NET family whose cooperation and help has made the life easy going. The friendship of Sir, Rashmibhai, Mohanty, Silu, Ranjan, Aurobind and others deserves a special mention for the joyful and anxious moments enjoyed with them during my short stay.

Santosh Kumar Kar
Santosh Kumar Kar.

CONTENTS

<u>TITLE</u>	<u>PAGE</u>
LIST OF FIGURES	i
LIST OF GRAPHS	ii
SYNOPSIS	iii
<u>1. INTRODUCTION</u>	1
1.1 Definition	1
1.2 Classification	1
1.3 Application	2
1.4 Decay Heat Removal in Nuclear Power Plant	2
1.5 Review of Past Work	5
1.6 Scope of Present Work	8
<u>2. RECTANGULAR THERMOSYPHON WITH POINT SOURCE AND SINK</u>	10
2.1 Introduction	10
2.2 Formulation	10
2.3 Nondimensionalisation	13
2.4 Steady state solution	13
2.5 Transient Solution	13
2.5.1 Zvirin's Method	14
2.5.2 Numerical Solution by Finite Difference	16
2.6 Stability Characteristics	18
<u>3. RECTANGULAR THERMOSYPHON WITH EXTENDED SOURCE AND SINK</u>	22
3.1 Introduction	22
3.2 Formulation	22
3.3 Steady state Solution	23
3.4 Nondimensionalisation	25
3.5 Formulation for Different Heating Cases	26
3.5.1 Uniform Flux Case	26
3.5.2 Triangular Flux Case	26
3.5.3 Sinosidual Flux Case	27
3.6 Steady State Solutions	27
3.7 Finite Difference Formulation for Transient Analysis	28
3.7.1 Uniform Heating Case	29
3.7.2 Triangular Heating Case	30
3.7.3 Sinosidual Heating Case	30
3.8 Solution of Finite Difference Equations	30
3.9 Results and discussions	31

<u>4. Modelling with Heat Exchanger</u>	33
4.1 Introduction	33
4.2 Formulation	33
4.3 Nondimensionalisation	34
4.4 Steady State Solution	34
4.5 Finite Difference Formulation For Transient Analysis	35
4.6 Solution of Finite Difference Equations	37
4.7 Results and Discussions	37
<u>5. TWO DIMENSIONAL ANALYSIS OF THE PROBLEM</u>	38
5.1 Introduction	38
5.2 Formulation	38
5.3 Nondimensionalisation	39
5.4 Steady State Analysis	40
5.5 Solution for Steady State	41
5.6 Solution Techniques for Finite Difference Equations	43
5.7 Results and Discussions	44
<u>6. CONCLUSION</u>	45
APPENDIX-1	46
APPENDIX-2	47
APPENDIX-3	48
APPENDIX-4	50
REFERENCES	51

LIST OF FIGURES

Figure-1 Simplified CANDU Pressurised Heavy Water Flow Diagram

Figure-2.1 The Simplified Model

Figure-2.2 Tube Segment

Figure-2.3 Coordinate along the tube and anti-symmetry condition

Figure-2.4 Discretisation of the loop

Figure-2.5 Variation of total friction F and total buoyancy force B with Flow Rate

Figure-2.6 The function $A(T) = (1-T^{-2}) \ln (1-T)/(1+T)$

Figure-2.7 The function $-\omega \cot \omega/2$

Figure-2.8 The neutral curve in $(q-\omega)$ plane

Figure-3.1 Rectangular Thermosyphon Loop with heating at lower horizontal arm and cooling at upper horizontal arm

Figure-3.2 Heating Flux Distribution

Figure-4.1 Rectangular Thermosyphon with Heat-exchanger as heat sink

Figure-5.1 Discretisation of the loop for two-dimensional case

LIST OF GRAPHS

Graph 1.1-1.2	Nondimensional Flow Rate vs. Time
Graph 1.3-1.4	Nondimensional Source Temperature vs. Time
Graph 1.5-1.6	Nondimensional Sink Temperature vs. Time
Graph 1.7-1.8	Nondimensional Heated Height vs. Time
Graph 1.9-1.12	Nondimensional Flow Rate vs. Time
Graph 1.13-1.16	Temperature vs. time at different nodes
Graph 1.17-1.20	Temperature distribution at different times in the loop
Graph 3.1-3.3	Flow rate vs. time
Graph 3.4-3.6	Temperature distribution at different times
Graph 3.7-3.10	Temperature vs. time for uniform heat flux
Graph 3.11-3.14	Temperature vs. time for triangular heat flux
Graph 3.15-3.18	Temperature vs. time for sinusoidal heat flux
Graph 4.1	Flow rate vs. time
Graph 4.2	Source temperature vs. time
Graph 4.3	Hot segment temperature vs. time
Graph 4.4	Sink temperature vs. time
Graph 4.5	Cold segment temperature vs. time
Graph 5.1	Flow rate vs. iteration
Graph 5.2	Source temperature vs. iteration
Graph 5.3	Hot segment temperature vs. iteration
Graph 5.4	Sink temperature vs. iteration
Graph 5.5	Cold segment temperature vs. iteration

CHAPTER-1

INTRODUCTION

1.1 Definition

A thermosyphon is a circulating fluid system whose motion is caused by density differences in a body force field which result from heat transfer. This definition given by Davies and Morris[1] is so broad as to include all natural convection processes plus others. The system to which the name thermosyphon is applied in formal studies are in fact systems which has the intrinsic function of removing heat from a prescribed source and transporting heat and mass over a specific path(frequently a recirculating flow) and rejecting the heat and mass to a prescribed sink. Thus the path of the recirculating flow which transports the thermal energy is or can be totally prescribed. Thermosyphon flows are intrinsically driven by thermal buoyancy forces either locally or in an overall sense. A simple loop flow may be the result of local buoyancy force alone, but a multibranched flow circuit can incorporate sections in which the flow direction is contrary to local buoyancy force resulting from pressures created by the overall system buoyancy forces. Based on these factors, a thermosyphon is defined as a prescribed circulating fluid system driven by thermal buoyancy forces.

1.2 Classification

The thermosyphons can be classified into the following categories according to

- a) The nature of boundaries:
 - i) Open thermosyphon
 - ii) Closed thermosyphon
- b) The regime of heat transfer:
 - i) Purely natural convection
 - ii) Mixed natural and forced convection
- c) The number or types of phases present:
 - i) Single phase
 - ii) Two phase

d) The nature of the body force:

- i) Gravitational
- ii) Rotational

1.3 Application

The most common industrial thermosyphon applications include the following:

- i) Gas turbine blade cooling
- ii) Electrical machine rotor cooling
- iii) Transformer cooling
- iv) Nuclear reactor decay heat removal
- v) Heat exchanger fins
- vi) Cryogenic cool-down apparatus
- vii) Steam tubes for bakers' ovens
- viii) Cooling of internal combustion engines
- ix) Solar water heater
- x) Convection in the earth's mantle
- xi) Temperature distribution in earth drillings in steam power fields
- xii) Preservations for the conservation of permafrost under buildings in the Canadian Northland
- xiii) Maintenance of ice-free navigation buoys

A variety of thermosyphon characteristics are responsible for the applications found till now and can lead to numerous further applications.

- i) A thermosyphon can act as a thermal conductor with either a small or a large thermal impedance.
- ii) It can be used as a thermal diode or rectifier, or even as a thermal triode, permitting a variation in heat flow based on small changes in temperature.

1.4 Decay Heat Removal in Nuclear Power Plant

In a nuclear reactor core, enormous amount of heat is generated in the fuel element due to the fission of the fissionable material present in it. This heat is taken out of the reactor core by the coolant by forced convection by means of primary pumps. The primary coolant may exchange heat to the working fluid of the turbine-condenser combination in the heat exchanger. It may be the working fluid itself as in the direct-cycle BWR. In

normal operating conditions, the coolant flow rate and the coolant inlet temperature are so designed as to take out the heat from the fuel element in such a manner that the fuel element is not damaged due to excessive temperature.

However, a nuclear reactor is not only designed to work under normal conditions, but also it is to be seen that under accident conditions, the safety limits are not exceeded. As the nuclear industry came into recognition after a much horrified and fearful occurrence during the Second World war, the general faith of the ordinary public is very low with it. Again to avoid the dangers involved with the release of radio-activity, much care is taken in the design, construction, planning and operation of a nuclear power plant both under normal and accident conditions.

In nuclear reactors, loss of flow accidents (LOFA) is one of the major accidents, caused by a flow obstruction in the core or because of a decrease of pressure drop due to a pump failure. The pump may fail due to mechanical seizure or electrical supply failure. In the former case, the flow may be assumed to reduce to zero instantaneously whereas in the latter case, the flow deteriorates rather gradually due to the high inertia of the flywheels.

During the normal operations, fuel temperatures are controlled by the forced circulation of the coolant. However, during certain events postulated to occur during the life-time of a reactor, power to the primary pump, which maintains the forced flow, may be lost. As the forced flow tends to decrease, the plant protective system will, with extremely high reliability, shut down the plant. However, due to the generation of the radioactive material within the fuel and the structural components of the reactor during power operation, residual decay heat will be there even though the primary fission reactions have ceased. Therefore, there must be some continued circulation of coolant, though at much reduced rate, following this event to prevent overheating of the reactor.

Although the design of the plant will include back-up pumping systems such as redundant power supplies, the ultimate fall-back heat transport mechanism is natural circulation cooling. Provided the reactor has been shut down fast enough to prevent damage during the flow coast-down, a central question then becomes whether an equilibrium state can be established for the natural convection removal of decay heat without the occurrence of excessive temperatures.

The natural circulation decay heat removal in PHWR is discussed now. The PHWR has several modes of decay heat removal. The boilers and the primary pumps provide the normal mode. The shutdown cooling system has independent heat exchangers and pumps and can remove decay heat at pressures upto nominal primary system pressures. Thermosyphoning is the mode of heat transport to the boilers in the absence of any forced circulation of the primary coolant.

Thus thermosyphoning is defined as the natural convective flow of the primary coolant over the boilers. It is the predicted mode of heat transport in many postulated scenarios for PHWR safety analysis. The scenarios encompass a wide range of primary coolant inventories and secondary side conditions.

A typical figure-of-eight loop of a PHWR primary heat transport system is shown in Figure-1. It comprises two passes of the coolant past the fuel. Thus the coolant sees core1, boiler1, pump1, core2, boiler2, pump2, core1 etc.. Each core pass includes a large number of horizontal fuel channels each of which is connected by an inlet and an outlet feeder to large diameter inlet and outlet headers. Large diameter pipings are connecting the headers to the boilers and pumps. The tops of boiler U-tubes are located typically 11m. above the headers and the headers are located 7m. above the channels. The total height is 18m. and the density differences in this height provide the buoyancy force for thermosyphoning.

PHWR primary pumps are provided

with high inertia flywheels which on loss of electrical supply, provide a forced flow of coolant whilst power is reduced to decay level. Subcooled (single-phase) thermosyphoning is predicted thereafter for this and the more probable accident scenarios.

Boiling (two-phase) thermosyphoning is predicted either under reduced primary coolant inventory conditions or if the coolant make-up system is inoperative during boiler depressurisation. In the latter case, a pressurizer compensates, in part, for shrinkage of the primary coolant as it cools down. In any event, two-phase thermosyphoning is predicted for the less probable accident scenarios only.

Thermosyphoning requires a heat sink at the boilers. Water is provided either by the normal feedwater system, the auxiliary feedwater pumps or, on depressurisation of the secondary side, by an emergency supply system.

1.5 Review of past work

The problem of heat transfer and fluid flow in natural convection loops has stimulated considerable interest in the past due to its important applications in oceanographic and geophysical phenomena as well as in such practical systems as nuclear reactors and solar heaters. The early studies on such systems started with Rayleigh's analysis concerned with the stability of a fluid at rest and the onset of motion due to a temperature gradient in the direction of the body force. A review of external flows caused by buoyancy forces was presented in [2]. Another type of free convection flows is encountered in enclosures and cavities the review of which is given in [3] and [4]. An overall study of the buoyancy-induced flow and transport is given in the text [5] for various physical cases.

Some of the previous studies of natural circulation loops were concerned with the stability of the steady-state motion. Keller [6] and Welander [7] considered a simple rectangular thermosyphon consisting of

two insulated vertical branches with point heat source and sink at the centre of the lower and upper horizontal segments respectively. It was pointed out in these pioneering works that, when a certain parameter representing the ratio of the buoyancy force to the frictional force exceeds a critical value, an oscillatory motion of the fluid may occur. The work of Creveling et al. considered a toroidal loop and demonstrated experimentally and theoretically the presence of instabilities. Studies of stability behaviour of circular loops have also been done by Zvirin et al [9]. Zvirin et al. [10] have also studied the steady state, transient behaviour of a natural circulation loop with two vertical branches with point heat source and sink and have shown that the stability depends on the type of the temperature distribution assumed.

The loop configuration is one of the few alterable factors in thermosyphon design. A detailed study of this factor is done by Chen[11] for better understanding of the operational and safety problems caused by the periodic instability in the natural convection loops.

The instability associated with the onset of motion in a thermosyphon has been studied by Zvirin[12] to show that the rest state is always unstable as the Rayleigh number exceeds some critical value.

The above studies considered one dimensional analysis of the thermosyphon with the coordinate running along the loop. Mertol et al.[13] tried a two-dimensional analysis of the toroidal thermosyphon and Mallinson et al.[14] analysed the three-dimensional case of a rectangular thermosyphon.

Hart[15] gave a new approach to the thermosyphon analysis by solving the conservation equations by a set of coupled master and slave ordinary differential equations and by making the chaotic analysis, he claimed the instabilities to be chaotic rather than oscillatory.

The effect of viscous dissipation is studied by Zvirin[16]. The transient, steady state and

stability behaviour of a toroidal thermosyphon with throughflow is studied by Mertol et al.[17].

As far as the application of thermosyphon to decay heat removal in nuclear reactors is concerned, the text by Lewis[18] threw some light for the different formulations. The text by Guppy et al[19] discussed the decay heat removal in fast breeder reactors by natural convection in detail. Zvirin[20] reviewed the transient, steady state and stability behaviour of different natural circulation loops including PWRs.

Ghosh et al[21] studied the natural circulation cooling of PHWR for decay heat removal after a reactor trip under loss of class IV power. They showed that under bottled condition, thermosyphon cooling is adequate to remove upto 10% of full power without boiling and upto 12% with boiling in the primary coolant channels.

Spinks et al.[22] considered the thermosyphoning in CANDU reactor. Chato[23] studied the natural convection flows in parallel channel systems. Zvirin et al.[24] investigated a natural circulation system with parallel loops both analytically and experimentally. They studied the steady state and transient characteristics and the effects of core flow resistance, power distribution and upper plenum design. Flow oscillations were observed under certain conditions which were accompanied by instabilities and flow reversals.

The transition from forced flow to natural circulation was studied experimentally by Gillette et al[25]. They performed their experiment to simulate EBR-II, a liquid-metal-cooled fast breeder reactor. The test was initiated by abruptly tripping an electromagnetic pump which supplied 5-6% of the normal full operational primary flow rate. The flow coast-down reached a minimum after which the flow increased as natural circulation was established. The effect of secondary system flow through the IHX and reactor decay power level on minimum in-core flow rates and maximum in-core temperature were examined.

1.6 Scope of present work

In the present work,a nuclear reactor primary heat transport system has been simulated as a rectangular loop in a vertical plane the bottom segment of which is heated and the top horizontal segment is cooled by passing a coolant.In the present analysis,the approach is made initially by taking simplified assumptions and latter on the complexities being handled by relaxing the simple assumptions.

In Chapter-2,to get the feel of the complex nature of the problem as regards to stability,the simple case of a rectangular thermosyphon with point heat source and point heat sink has been analysed in detail.Two approaches have been made.In the first case,a linear temperature distribution is assumed which fails to give any information regarding the stability though steady state and transient behaviours are predicted correctly.In the second approach,a numerical solution of the equations show the instability associated with the problem.A linear stability analysis is also done.

Chapter-3 deals with the real situation of extended heat source and sink.For simplicity,the sink is assumed to be at constant temperature whereas three different types of heat source are chosen to give uniform,triangular and sinusoidal heat fluxes.The analysis is done considering one-dimensional flow with the coordinate along the loop.The fluid flow and heat transfer characteristics have been analysed for each case.

Chapter-4 takes into account the more practical situation by analysing the problem with the presence of a heat exchanger as the heat sink in stead of a constant temperature heat sink analysed in the previous chapters.

Experimentally the flow has been observed to be two-dimensional. Again for one-dimensional analysis, we have to use some correlations for the friction factor and heat transfer coefficient. As the appropriate correlations for the natural circulation flows have not been developed, we have to use the correlations available in forced convection flows for those quantities. Thus the combined effect of these two defects in our earlier models may be the cause for the discrepancies between the theoretical and the experimental results. So in Chapter-5, a two dimensional analysis of the problem is done.

Finally, Chapter-6 deals with the future scope of the work and draws some conclusions of the present work.

CHAPTER-2
RECTANGULAR THERMOSYPHON WITH
POINT SOURCE AND SINK

2.1 Introduction

Before analysing the real problem, it is advantageous to consider a simple model to have a better insight into the mechanism of convection. The model is materialised by taking a narrow tube of uniform cross-section and forming it into a closed loop. The tube is filled with fluid that is kept well mixed over the cross-section. The fluid is subjected to given heat sources and sinks along its path. The fluid motion is driven by buoyancy force and will also be retarded by frictional forces. The tube is considered to be insulated everywhere except at the top and bottom, where over short distances the temperature of the wall is kept at $-\Delta T$ and ΔT respectively. Thus we consider the limiting case where $\Delta s \rightarrow 0$ while $k \rightarrow \infty$ in such a way that the heat flux remains finite, i.e., point source and point sink.

In this chapter, the steady state, transient and stability behaviour of a system shown in Figure-2.1 as comprising of two vertical branches with point heat source and sink has been discussed.

2.2 Formulation

Let us consider a portion of the fluid with uniform cross-sectional area A and length L as shown in Figure-2.2. The fluid is driven by the pressure difference between the end points and by a buoyancy force and is retarded by frictional force. The following assumptions are made.

- 1) The fluid is incompressible due to the small pressure change encountered in natural convection.
- 2) The flow is one-dimensional and the coordinate runs along the loop.
- 3) All the fluid properties and heat transfer coefficients are constant.
- 4) Boussinesq approximation is valid, i.e., density is assumed to be constant in all the conservative equations except

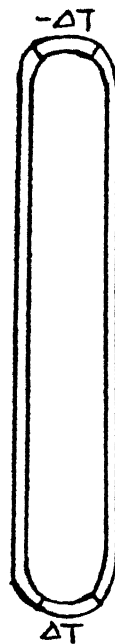


FIGURE 2.1. The Simplified model

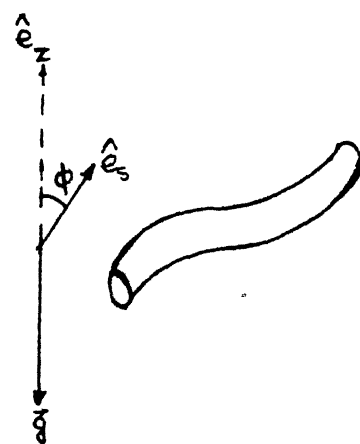


FIGURE 2.2. Tube segment

for the body force term, caused due to density difference, where linear variation of density is assumed,

$$i.e., \rho = \rho_0 [1 - \beta(T - T_0)] \quad \text{---(2.2.1)}$$

5) The fluid is well mixed over the cross-section. The characteristic time for mixing is small compared to the time required for the fluid to be advected an appreciable distance along the loop.

6) Due to well-mixing, the temperature is assumed uniform over the cross-section.

7) The tangential friction force is a function of the instantaneous flow rate. Here laminar flow is studied. Hence, a linear relation is assumed.

8) The heat flux between the tube and the fluid is proportional to the temperature difference between wall temperature T_0 and fluid temperature T .

Considering the tube segment in Figure-2.2, the following conservation equations are derived.

Continuity: $\nabla \cdot \mathbf{v} = 0 \quad \text{---(2.2.2)}$

Momentum:

$$\rho_0 \frac{d\mathbf{v}}{dt} = -\rho g \hat{\mathbf{e}}_z \nabla p + \mathbf{F} \quad \text{---(2.2.3)}$$

Energy:

$$\frac{dT}{dt} = k [T(s) - T_0] \quad \text{---(2.2.4)}$$

This constitute a set of 3 equations with 4 unknowns \mathbf{v}, T, p and ρ . So this equation set along with eq.(2.2.1) relating density and temperature constitute the total set of equations.

For one-dimensional case, eq.(2.2.2) gives :

$$\frac{\partial \mathbf{v}}{\partial s} = 0, i.e., \mathbf{v} = \mathbf{v}(t) \quad \text{---(2.2.5)}$$

So velocity is uniform along the loop.

Taking component of (2.2.3) along the loop,

$$\rho_0 \frac{d\mathbf{v}}{dt} = -\rho g \cos\phi - \frac{\partial p}{\partial s} + \mathbf{F}_s \quad \text{---(2.2.6)}$$

Integrating over the fluid volume,

$$\rho_0 \frac{\partial}{\partial t} \iint v dA ds = \iint -\rho g \cos\phi dA ds - \iint (\frac{\partial p}{\partial s}) dA ds + \iint \mathbf{F}_s dA ds$$

As flow rate $Q = \int v dA$ is constant by (2.2.5); $ds \cos\phi = dz$ and using (2.2.1) and assumptions (6) & (7), we get,

$$\rho_o L \frac{dQ}{dt} = \rho_o A \beta g T dz + C \int dz - A \beta dp - \rho_o L R Q \quad (2.2.7)$$

where R is a frictional coefficient

Now for a closed tube, eq.(2.2.7) reduces to

$$\rho_o L (dQ/dt) = \rho_o A \beta g T dz - \rho_o L R Q$$

as $\int dp = 0$ and $\int dz = 0$

$$\text{i.e., } dQ/dt = A \beta g / L \int T dz - R Q \quad (2.2.8)$$

The energy equation gives

$$(\partial T / \partial t) + Q/A (\partial T / \partial s) = k(T - T_o) \quad (2.2.9)$$

The tube is symmetrical with respect to the vertical. The temperature is antisymmetric with respect to the center of the loop, i.e., $T(s+L/2) = -T(s)$. These conditions are shown in Figure-2.3.

Applying the symmetry and antisymmetry conditions to the integral $\int T dz$, we get,

$$\int T dz = 2 \int_0^{L/2} T ds$$

Thus equation of motion becomes

$$dQ/dt = 2A \beta g / L \int_0^{L/2} T ds - R Q \quad (2.2.10)$$

The solution of (2.2.9) and (2.2.10) need some boundary conditions involving temp. The temperature of the fluid coming out of the source or sink depend on the temperature of the ingoing fluid and flow rate. Appendix-I proves that if a fluid particle passes through the source or sink for a time Δt , then the difference in temperature between the outgoing and incoming fluid is given by

$$T_{out} - T_{in} = (\Delta T - T_{in}) (1 - \exp(-\Delta t))$$

$$\text{i.e., } T_{out} - T_{in} = (\Delta T - T_{in}) (1 - \exp(-k \Delta s A / Q)) \text{ for source} \quad (2.2.11)$$

$$= (-\Delta T - T_{in}) (1 - \exp(k \Delta s A / Q)) \text{ for sink}$$

For the computation in the range $0 < s < L/2$, we need to know T_{in} at source when $Q > 0$ and at the sink when $Q < 0$.

$$\begin{aligned} \text{By antisymmetry, } T_{in} &= T(L - \Delta s/2) = -T((L - \Delta s)/2) \text{ for first case} \\ &= T((L + \Delta s)/2) = -T(\Delta s/2) \text{ for second case} \end{aligned}$$

$$\begin{aligned} \text{In the limit as } \Delta s \rightarrow 0, T_{in} &= -T(L/2) \text{ for first case} \\ &= -T(0) \text{ for second case} \end{aligned}$$

So, eq.(2.2.11) reduces to

$$\begin{aligned} T_{s=0} + T_{s=L/2} &= (\Delta T + T_{s=L/2}) (1 - \exp(-kA\Delta s / Q)), Q > 0 \\ &= (\Delta T + T_{s=0}) (1 - \exp(-kA\Delta s / Q)), Q < 0 \end{aligned} \quad (2.2.12)$$

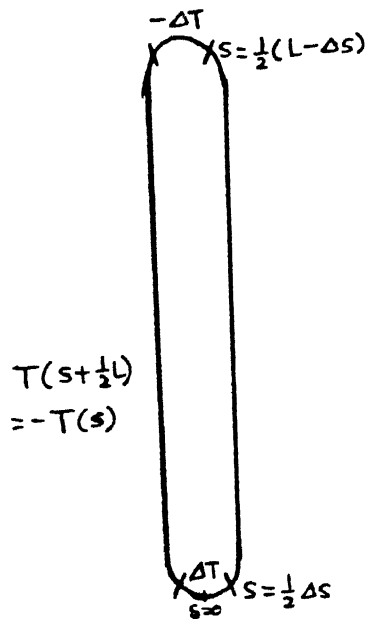


FIGURE 2.3 Coordinate along the tube and antisymmetry condition



FIGURE 2.4 Discretisation of the Loop

2.3 Non-dimensionalisation

The equations are non-dimensionalised by the transformation

$$s^* = L/2s \quad ; \quad t^* = (L/(2k\Delta s))t \quad ; \quad q^* = k\Delta s q \quad ; \quad T^* = \Delta T * T$$

and finally take the form

$$dQ/dt + \epsilon Q = \alpha \bar{T} \quad ds \quad \dots \quad (2.3.1)$$

$$\partial T/\partial t + Q \partial T/\partial s = 0 \quad \dots \quad (2.3.2)$$

$$\begin{aligned} T_{s=0} + T_{s=1} &= (1 + T_{s=1}) (1 - \exp(-1/\bar{Q})), \quad \bar{Q} > 0 \\ &= (-1 + T_{s=0}) (1 - \exp(-1/\bar{Q})), \quad \bar{Q} < 0 \end{aligned} \quad \dots \quad (2.3.3)$$

where the non-dimensional parameters are given by

$$\alpha = \text{Gravity parameter} = g\beta \Delta T L / (k\Delta s)^2$$

$$\epsilon = \text{Friction parameter} = RL / (2k\Delta s) \quad \dots \quad (2.3.4)$$

2.4 Steady state solution

We assume that $Q > 0$, hence the motion is upward in $0 < s < 1$. For steady state solution, the time derivative vanishes.

Eq. (2.3.2) reduces to $T = \text{constant} = \bar{T}$ \dots (2.4.1)

Eq. (2.3.1) results in $\epsilon \bar{Q} = \alpha \bar{T}$ \dots (2.4.2)

Eq. (2.3.3) gives $2\bar{T} = (1 + \bar{T}) (1 - \exp(-1/\bar{Q}))$ \dots (2.4.3)

Eliminating \bar{T} between (2.4.2) and (2.4.3), we get,

$$2\bar{Q}/(\bar{Q} + \alpha/\epsilon) = 1 - \exp(-1/\bar{Q}) \quad \dots \quad (2.4.4)$$

The LHS and RHS of (2.4.4) show that LHS is a monotonically decreasing and RHS is a monotonically increasing function of $1/\bar{Q}$. LHS decreases from 2 to 0 and RHS increases from 0 to 1 as \bar{Q} decreases from ∞ to 0. So there is a point where they intersect giving rise to steady state value \bar{Q} .

Eq. (2.4.4) also shows that the steady state solution is a function of α/ϵ . Table-1 gives different values of \bar{Q} for different α/ϵ ratios.

2.5 Transient solution

Eq. (2.3.1) and (2.3.2) form a set of coupled integro-differential equations in Q and T . The temperature being a function of both position and time needs a boundary condition in space given by Eq. (2.3.3). So to have a transient solution, we need initial conditions only. Here we consider the case where the motion starts from rest.

So at $t=0, Q=0$ and $T=1$ at $s=0$

$= 0$ at all other s

α/ϵ	\bar{q}	\bar{T}
0.100	0.100	1.000
0.500	0.417	0.834
1.000	0.648	0.648
2.000	0.958	0.479
10.000	2.218	0.222

TABLE 1. Values of non-dimensional flow rate and temperature in steady motion

The transient behaviour has been studied by two methods.

- 1) Zvirin's ordinary differential equation method
- 2) Numerical solution method by finite difference

2.5.1 Zvirin's method

This method comprises two stages. During the first stage, a linear temperature distribution is taken from the bottom to a penetration height $H(t)$ and $T=0$ for $0 < s < 1$. The penetration height increases with time and the first stage ends when $H(t)=1$ at some time $t=t^*$. Thus the second stage begins for $t > t^*$ when a linear temperature distribution is assumed over the whole range $0 < s < 1$.

Reduction of governing eq. into ODEs:

Integration of energy eq.(2.3.2) gives

$$\frac{d}{dt} \int_0^H T ds - QT_0 = 0$$

Assuming linear temperature variation, i.e., $T=T_0 - T_0 s/H$, we get

$$\frac{1}{2} \frac{d}{dt} (HT_0) = QT_0 \quad \text{---(2.5.1)}$$

Momentum equation (2.3.1) reduces to

$$\frac{dQ}{dt} + \varepsilon Q = 1/2 \alpha T_0 H \quad \text{---(2.5.2)}$$

The boundary condition (2.3.3) becomes

$$T_0 = 1 - \exp(-1/Q) \quad \text{---(2.5.3)}$$

The above equation set represents a set of ordinary coupled differential equations with 3 variables Q, T_0 and H with initial conditions $Q=0, T_0=1, H=H_1$ at $t=0$ ---(2.5.4)

where H_1 is a small value representing the initial asymmetry of heat source.

The above set can be reduced to a single equation by differentiating (2.5.3) with respect to t and substituting expression for T_0 from (2.5.3). This results in

$$\frac{d^2 Q}{dt^2} + \varepsilon \frac{dQ}{dt} = \alpha Q(1 - \exp(-1/Q)) \quad \text{---(2.5.5)}$$

with initial conditions $Q=0, dQ/dt=1/2 \alpha H_1$ at $t=0$ ---(2.5.6)

For the second stage, i.e., $t > t^*$
integration of (2.3.2) gives

$$\frac{d}{dt} \int_0^4 T ds - Q(T_4 - T_o) = 0 \quad \dots \quad (2.5.7)$$

With linear temperature distribution, $\int_0^4 T ds = 1/2(T_o + T_4) = T_m$

$$\text{Now using (2.3.3), } T_o = 1 - 2T_m \exp(-1/Q) / (1 - \exp(-1/Q)) \quad \dots \quad (2.5.8)$$

$$T_4 = 2T_m / (1 - \exp(-1/Q)) - 1$$

Now (2.5.7) reduces to

$$dT_m/dt = 2Q [1 - (1 + \exp(-1/Q)) * T_m / (1 - \exp(-1/Q))] \quad \dots \quad (2.5.9)$$

The momentum eq(2.3.1) reduces to

$$dQ/dt + \epsilon Q = \alpha T_m \quad \dots \quad (2.5.10)$$

These two coupled ordinary differential eq. in Q and T_m are to be solved with the initial condition

$$Q = Q_{\text{stage-1}}, \quad T_m = 1/2T_o \text{ at } t = t^*$$

Solution Technique:

The non-linearity of equation(2.5.5) in stage-1 and eq.s (2.5.9) and (2.5.10) in stage-2 eliminates any chance of analytical solution. So they are to be solved numerically. As the equations are ordinary differential equations and are of the initial value type, they are solved by Runge-Kutta method.

The solution algorithm first solves the equation for the 1st stage. Starting from $t=0$, at each time step, $Q, dQ/dt$ are calculated. From (2.5.3) T_o is found out and from (2.5.2) H is found. The first stage solution continues till $H=1$, the corresponding time being t^* . Taking the value of Q at $t=t^*$ as initial value, the coupled set (2.5.9) and (2.5.10) are solved at each time for Q and T_m . From (2.5.8), T_o and T_4 are found. The process continues till steady state is achieved.

Stability Characteristics

Let us consider small deviations from steady state in the form

$$Q(t) = \bar{Q} + Q'(t) \quad T_m(t) = \bar{T}_m + T_m'(t) \quad \dots \quad (2.5.11)$$

where \bar{T}_m and \bar{Q} are steady state values given in section 2.3.

Introducing (2.5.11) into (2.5.9) and (2.5.10), subtracting the steady state relations and using the linearized stability procedure, we get,

$$(1-m)dT_m'/dt = -2\bar{Q} [mQ'/\bar{Q}^2 (1+\bar{T}_m) + (1+m)\bar{T}_m'] \quad \dots \quad (2.5.12)$$

$$dQ'/dt = -\epsilon Q' + \alpha T_m' \quad \dots \quad (2.5.13)$$

where $m = \exp(-1/Q)$

To reduce the above equations into algebraic ones and to check their stability, we assume,

$$T_m' = \hat{T}_m \exp(\sigma t) \quad Q' = \hat{Q} \exp(\sigma t) \quad (2.5.14)$$

where σ , in general, is a complex number.

$$\text{Now, we get, } (1-m)\sigma \hat{T}_m' = -2\bar{Q} [\bar{m} \hat{Q}/\bar{Q}^2 (1+\hat{T}_m) + (1+m)\hat{T}_m'] \quad (2.5.15)$$

$$\sigma \hat{Q} = -\hat{Q} + \sigma \hat{T}_m \quad (2.5.16)$$

Elimination of \hat{T}_m and \hat{Q} gives rise to the

characteristic eq.

$$\sigma^2 + \sigma(\sigma + 2\bar{Q}/\bar{T}_m) + 2\bar{Q}[\bar{Q}/\bar{T}_m + 2m/(1-m)^2] = 0 \quad (2.5.17)$$

As the coefficients in the quadratic equation are always positive, there are no roots of σ with positive real part. Hence the solution is stable.

Results and Discussions

The plot of heated height H , flow rate Q , T_g and T_l as a function of time has been shown for various values of the parameters α, σ for different initial penetration depths in Graph 1.1 to 1.8. A close analysis of the results show the following:

(1) The time required for the full growth of the heated region of the loop is more for low initial penetration depth as expected. For high initial penetration depth, i.e., with some initial flow, the natural circulation flow establishes faster.

(2) As the ratio of gravity to friction parameter is increased, flow is established at much less time. This is due to the increase in the driving buoyancy force and decrease in the retarding friction force.

(3) The study with linear temperature distribution assumption explains steady state and transient behaviour well but fails to explain the instability associated with the flow. Thus it may be concluded that the stability of such a system depends on the assumed temperature distribution.

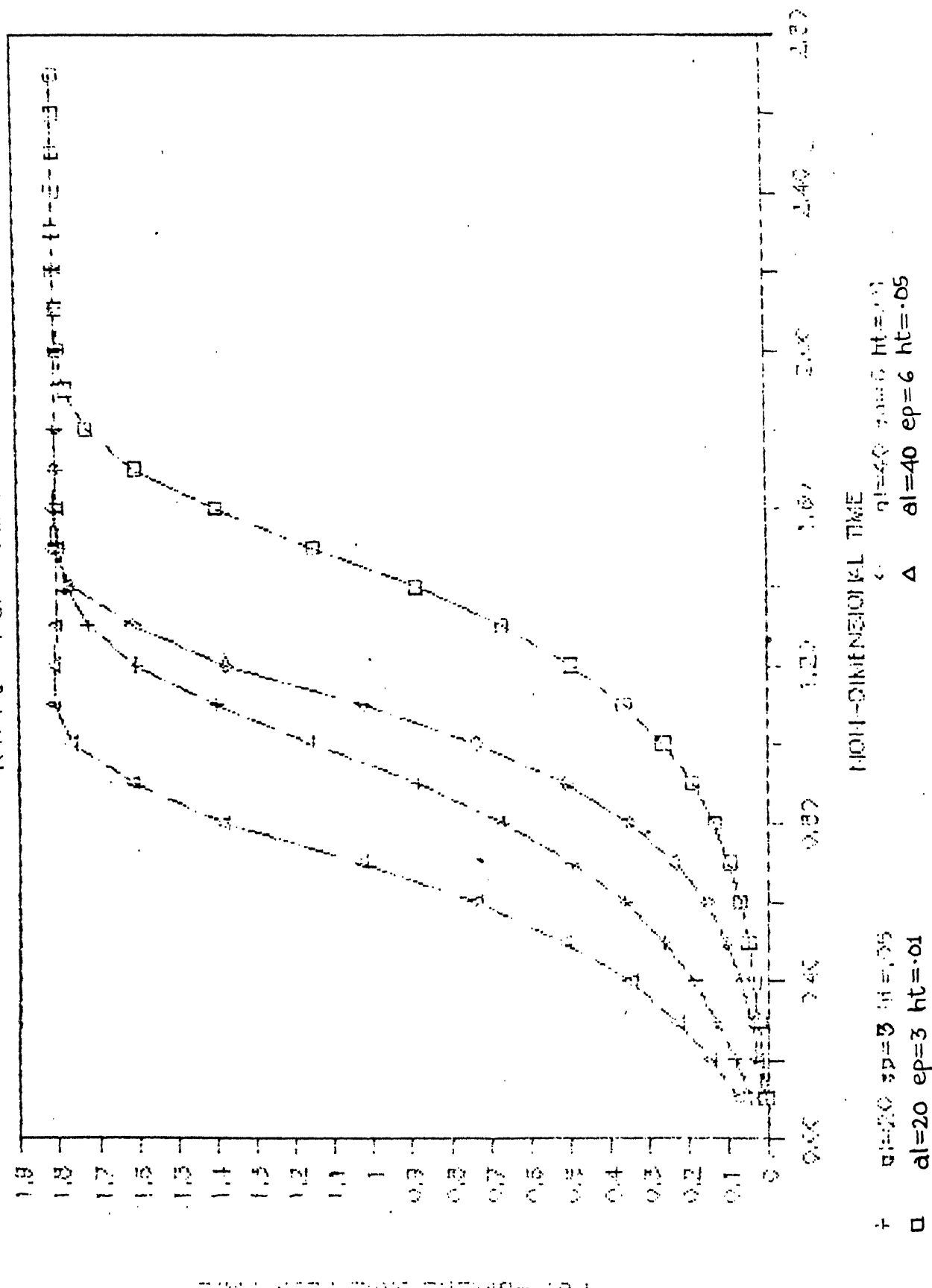
2.5.2: Numerical solution by Finite Difference :

Zvirin's method failed from certain drawbacks.

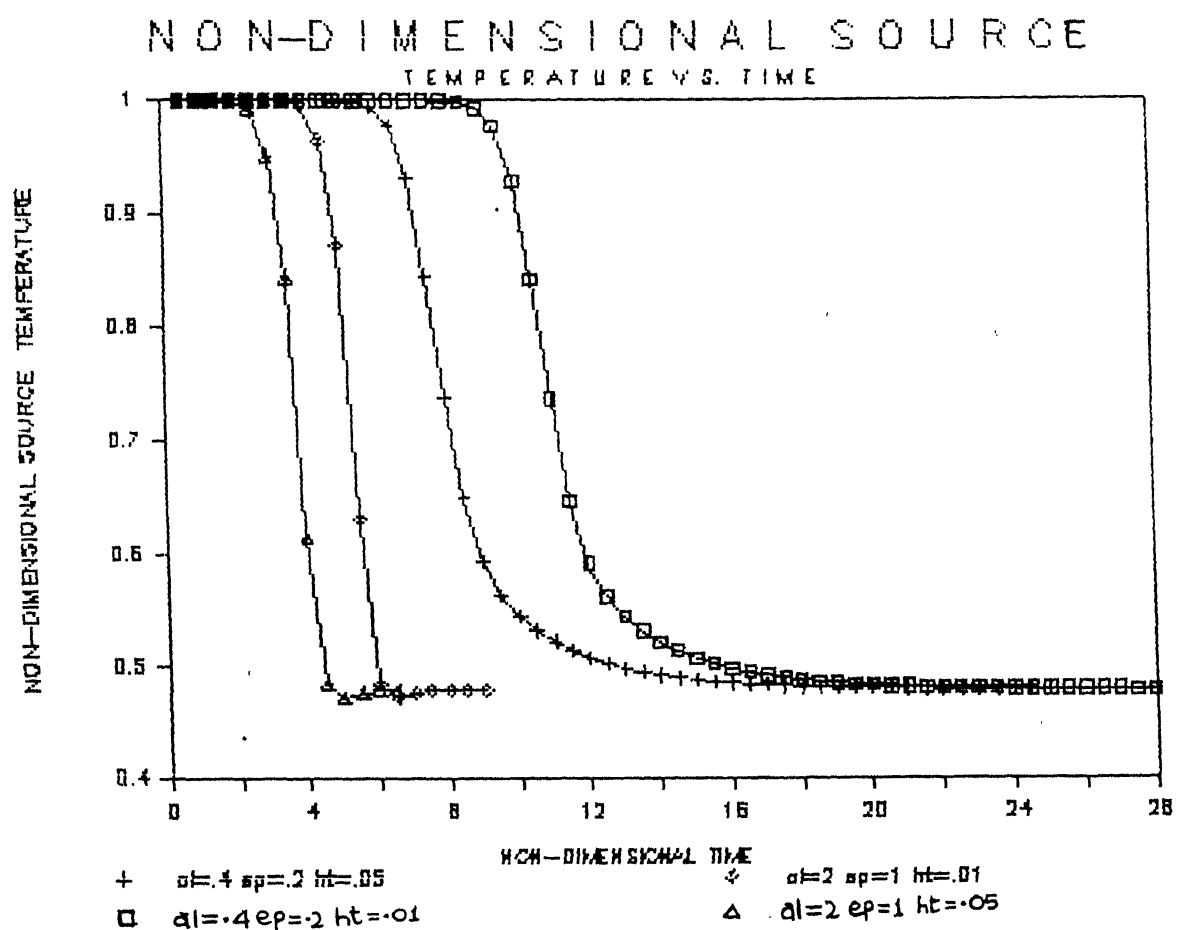
(1) The assumption of linear temperature profile is much a simplified assumption. The temperature distribution may be linear at the initial period when convection is not significant and the mode of heat transfer is conduction. But as natural circulation flow becomes significant, temperature distribution will not be

NON-DIMENSIONAL FLOW

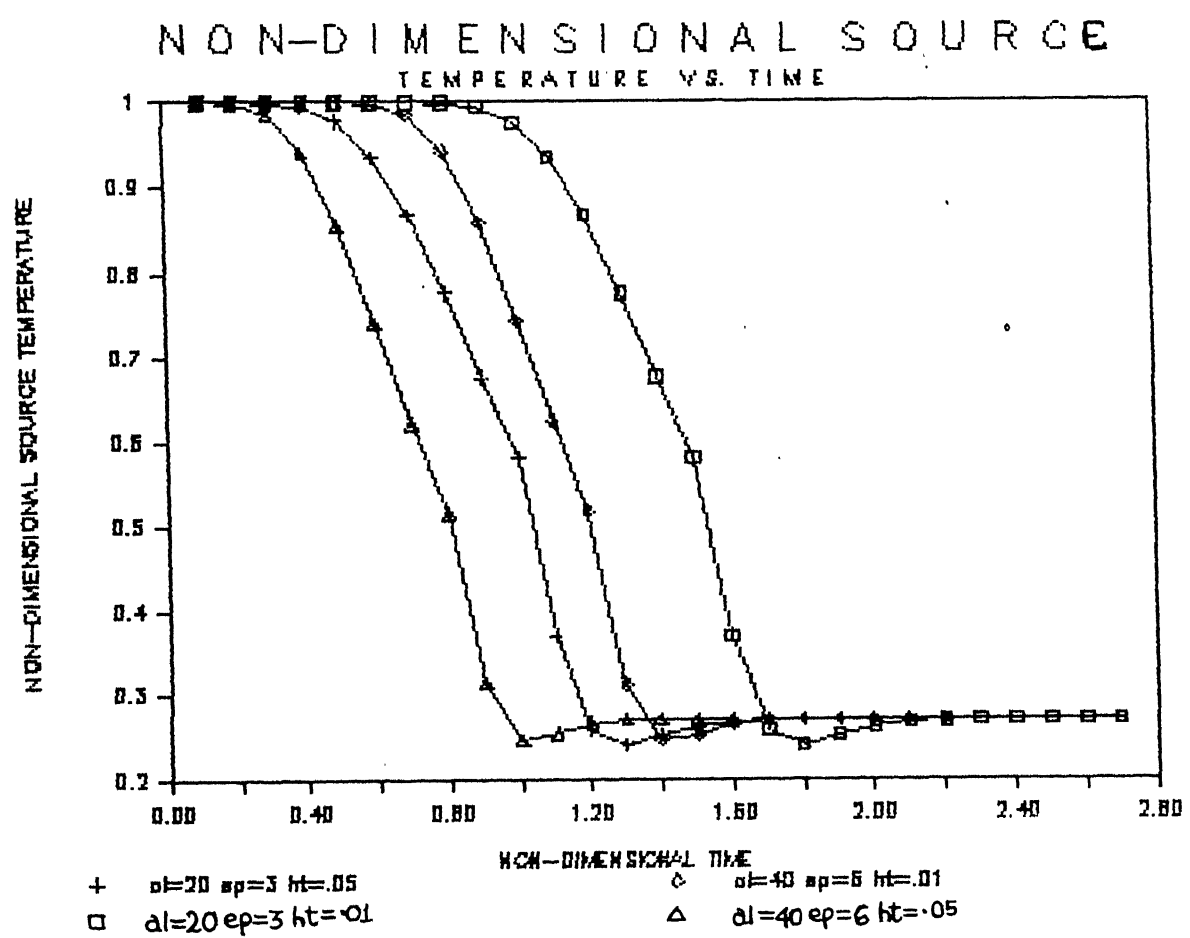
RATE VS. TIME



GRAPH 1.2

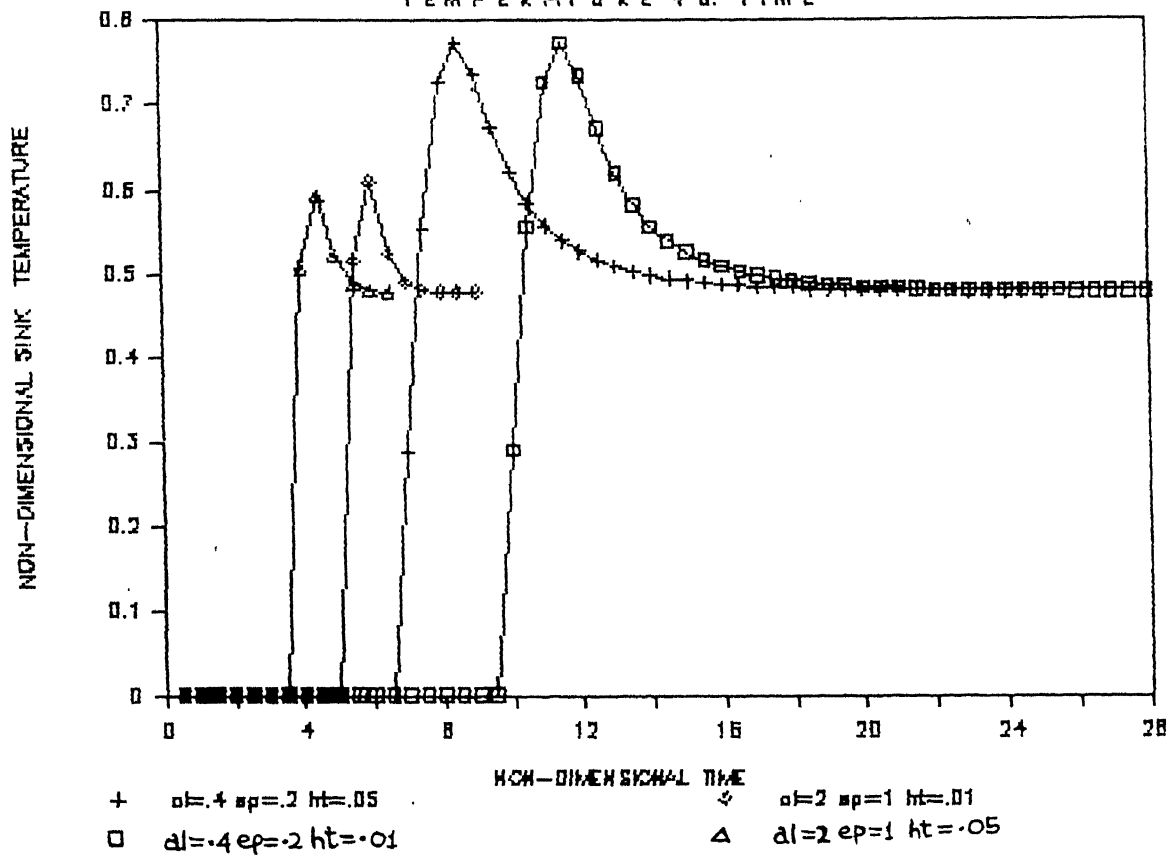


GRAPH 1.3



GRAPH 1.4

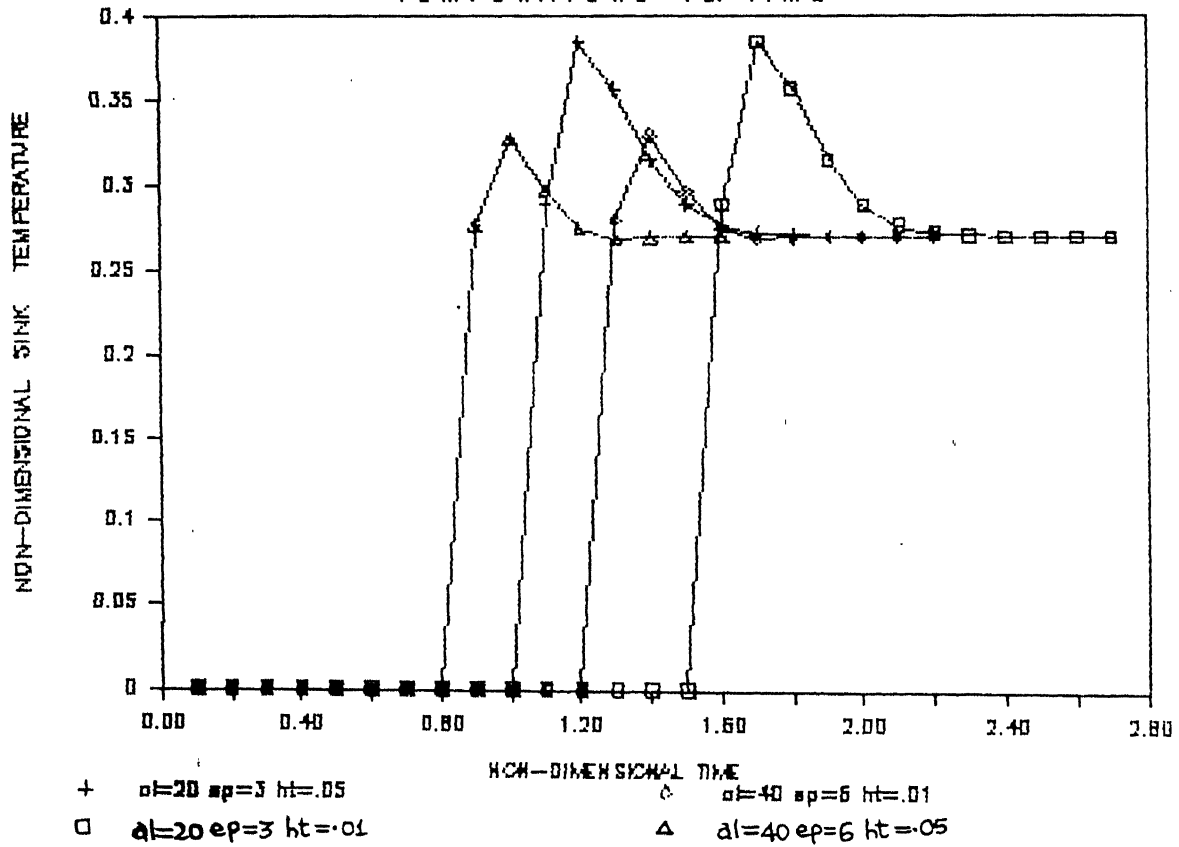
NON-DIMENSIONAL SINK TEMPERATURE V.S. TIME



GRAPH 1.5

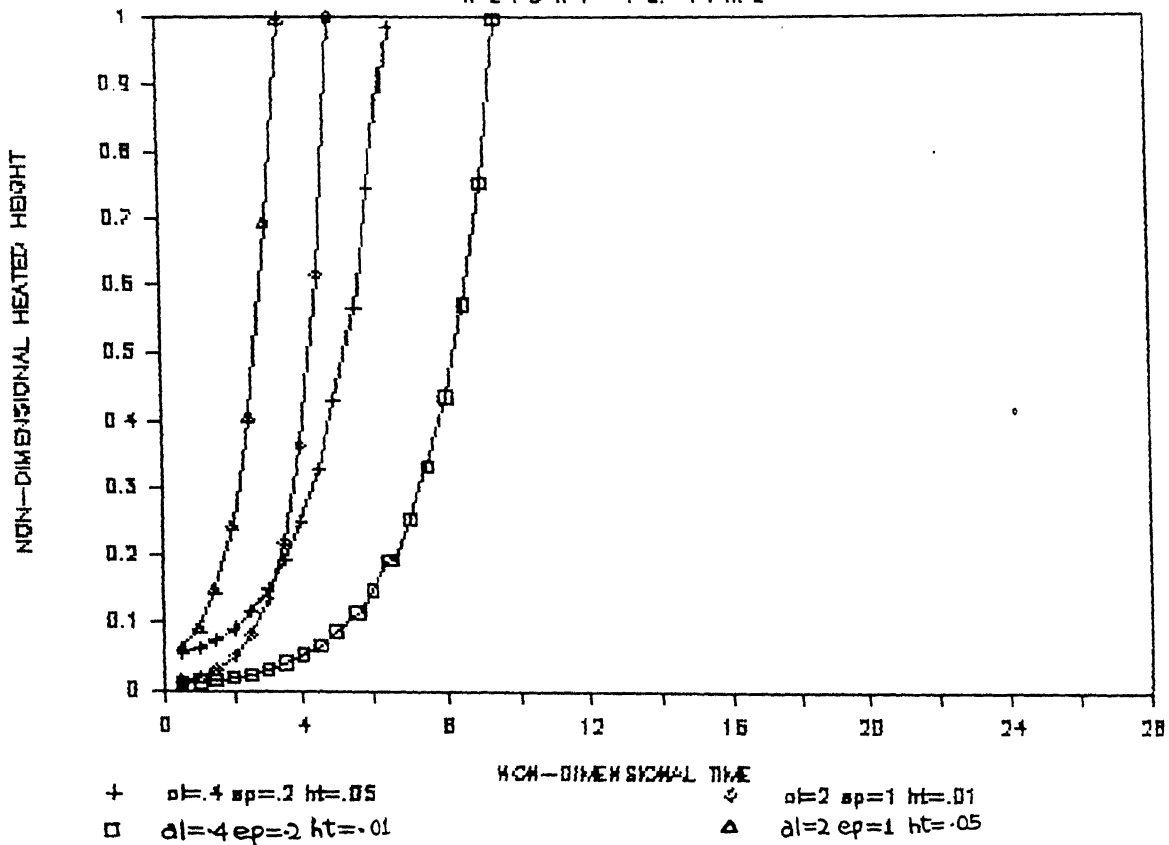
NON-DIMENSIONAL SINK

TEMPERATURE VS. TIME



GRAPH 1.6

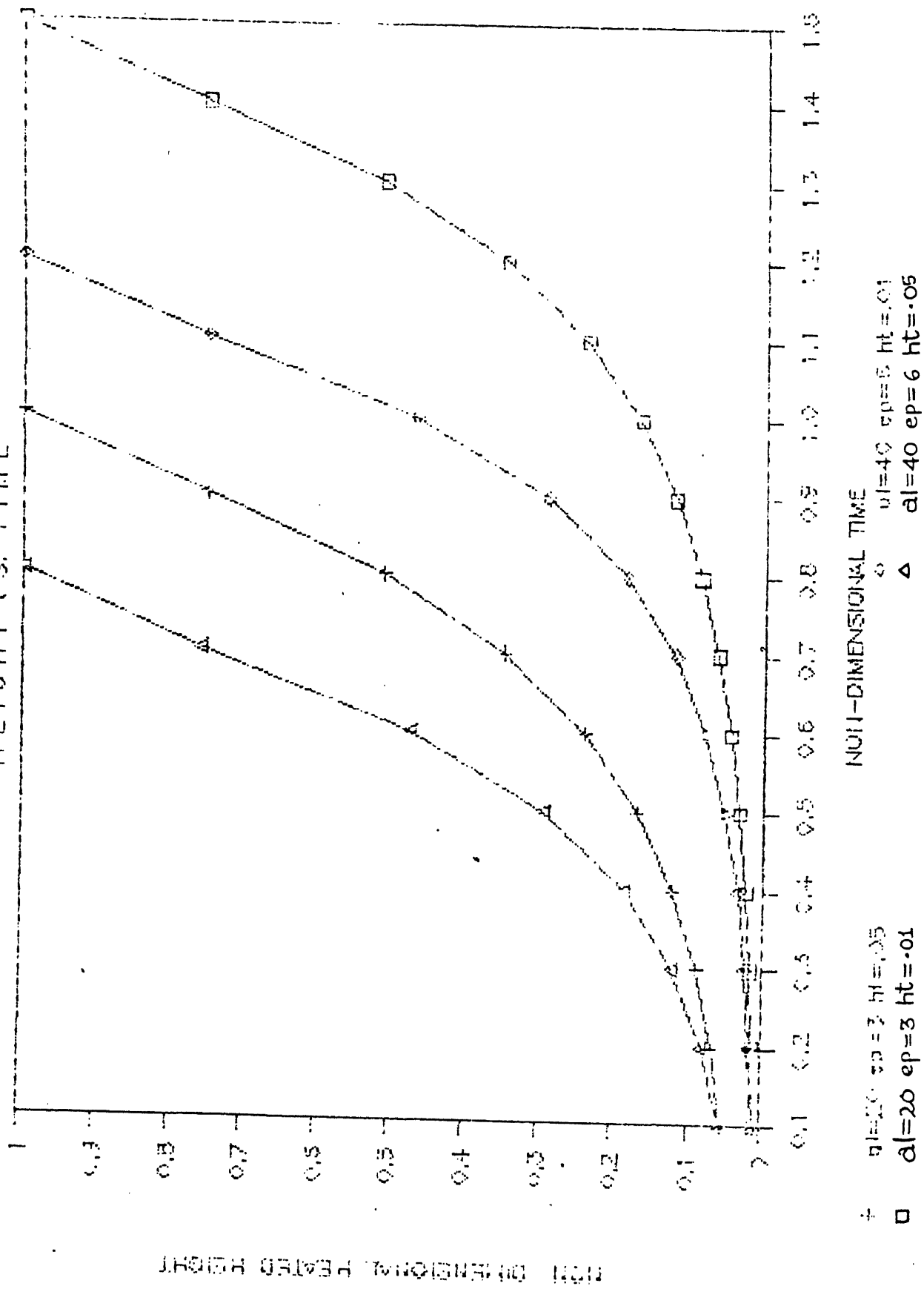
NON-DIMENSIONAL HEATED
HEIGHT VS. TIME



GRAPH 1.7

NON-DIMENSIONAL HEATED

HEIGHT VS. TIME



GRAPH 1.8

simply linear.

(2) The linear temperature profile assumption fails to explain the instability associated with the process as shown earlier.

In order to get a true picture as regards to stability, it is better to take up the original equations and make a numerical solution of these equations though it may require some additional mathematical analysis.

Solution Technique

The coupled non-linear integro-differential equation set (2.3.1) and (2.3.2) involving Q and T are solved by finite-difference scheme with the boundary condition and initial conditions as prescribed earlier. The discretisation of the loop is shown in Figure-2.4.

The integral in eq.(2.3.1) is decomposed by Simpson's rule. An implicit scheme is used for the time derivative. The upwind scheme is used for the space derivative, i.e., backward difference scheme in the present case.

Thus the finite-difference form of the eq.(2.3.1) and (2.3.2) are

$$(Q^{t+1} - Q^t) / \Delta t + \epsilon Q^{t+1} = \alpha \Delta s / 3 \sum_{i=1}^N a_i T_i^{t+1}$$

where $a_i = 1$ for $i=1$ and N

$=4$ for even i and 2 for odd i

$$(T_i^{t+1} - T_i^t) / \Delta t + Q^{t+1} (T_i^{t+1} - T_{i-1}^{t+1}) / \Delta s = 0 ; \text{ for } i=2,3,\dots,N$$

$$T_1^{t+1} + T_N^{t+1} = (1 + T_N^{t+1}) (1 - \exp(-1/Q^{t+1}))$$

$$\text{i.e., } Q^{t+1} = (Q^t + \alpha \Delta s \Delta t / 3 \sum_{i=1}^N a_i T_i^{t+1}) / (1 + \epsilon \Delta t) \quad \dots \quad (2.5.18)$$

$$T_i^{t+1} = (T_i^t + \Delta t Q^{t+1} T_{i-1}^{t+1} / \Delta s) / (1 + Q^{t+1} \Delta t / \Delta s); \text{ for } i=2,3,\dots,N \quad \dots \quad (2.5.19)$$

$$T_1^{t+1} = 1 - (1 + T_1^{t+1}) \exp(-1/Q^{t+1}) \quad \dots \quad (2.5.20)$$

For solution, first eq. set (2.5.19) is solved. The non-linearity arising is handled by taking $Q^{t+1} = Q^t$ and $T_1^{t+1} = T_1^t$. After finding $T_2^{t+1}, \dots, T_N^{t+1}$, corrected value of T_1^{t+1} is found from (2.5.20) and then corrected value of Q^{t+1} is found from (2.5.18). The process is repeated till convergence. The marching in

time is done till steady state is achieved or till a particular time to see the flow oscillations if there is no steady state.

Results and Discussions

The results are given as the plot of flow rate vs. time, temperature at various nodes vs. time and temperature distribution along the loop at different times for several sets of parameters α and ϵ in Graph 1.9 to 1.20. The flow rate curve shows monotonous increase till steady state for $\alpha=0.4$ and $\epsilon=0.2$ whereas for other ranges $\alpha=2, \epsilon=1; \alpha=20, \epsilon=3$ and $\alpha=40, \epsilon=6$ flow rate comes to steady state after some initial oscillations. So for some range of α and ϵ , we may encounter flow oscillations or even flow reversal.

The temperature distribution vs. time shows that near the source, temperature decreases gradually to steady state value whereas at other points temperature increases till a maximum and then falls to steady state value. This can be explained as follows. At initial time, when flow rate is small, i.e., natural convection has just been established, the temperature of the outgoing fluid from the source becomes close to the source temperature as the fluid takes more time to pass through it. As flow rate increases at subsequent time, the outgoing fluid temperature is nearer to the incoming fluid temperature which is relatively cold.

For other points, initially conduction is predominant mode of heat transfer. As convection is established, the temperature rises due to the advected hot fluid particles emanating from source till a time after which the temperature decreases due to relatively cold particles coming out of the source, mixing with the hot particles and being convected. Finally steady state is achieved when temperature throughout the loop is constant.

2.6 Stability Characteristics

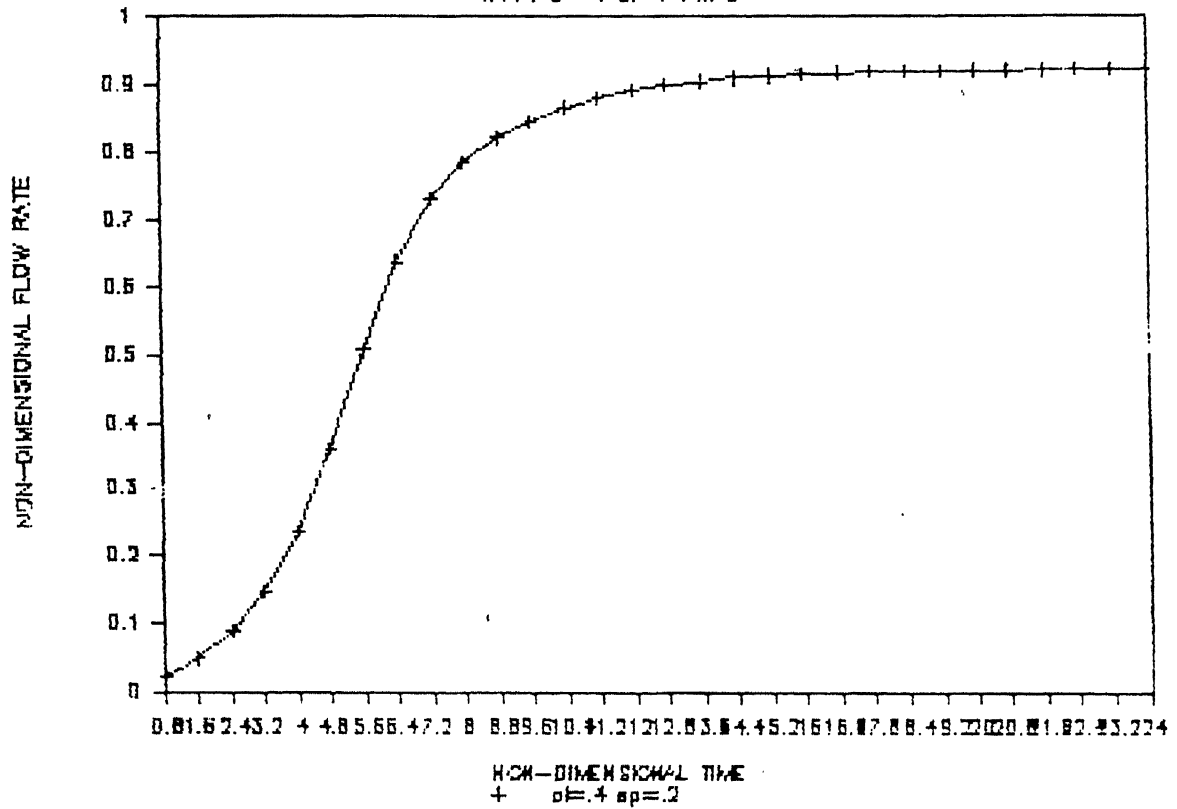
The fluid motion is driven by buoyancy force and retarded by friction force. The buoyancy force integrated around the loop is $\bar{B} = \rho_0 g A \int T dz$ ----- (2.6.1)

The temperature distribution of the fluid is solved from the energy equation $Q/A \partial T/\partial s = k [T_w(s) - T]$ ----- (2.6.2)

where $T_w(s)$ is prescribed wall temperature.

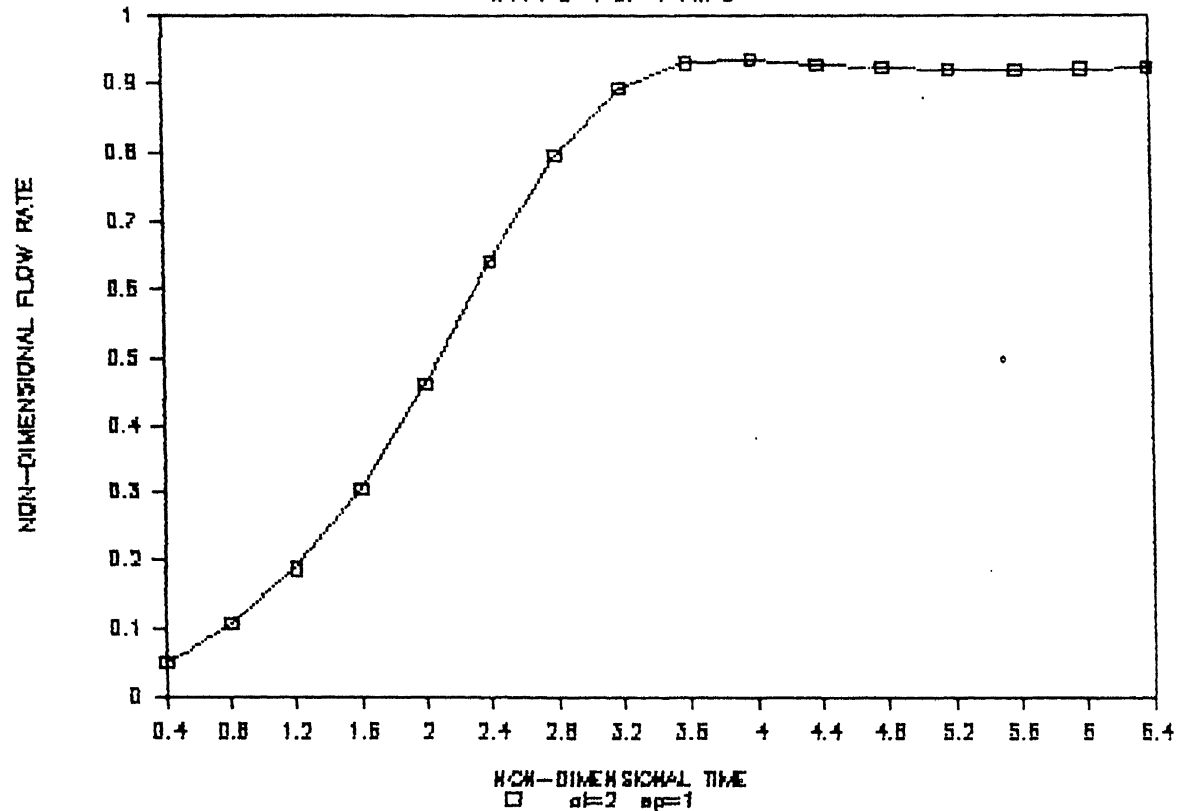
So temperature distribution is a function of Q and hence \bar{B} also. To find the behaviour of \bar{B} with Q , we find, from (2.6.2)

NON-DIMENSIONAL FLOW RATE VS. TIME



GRAPH 1.9

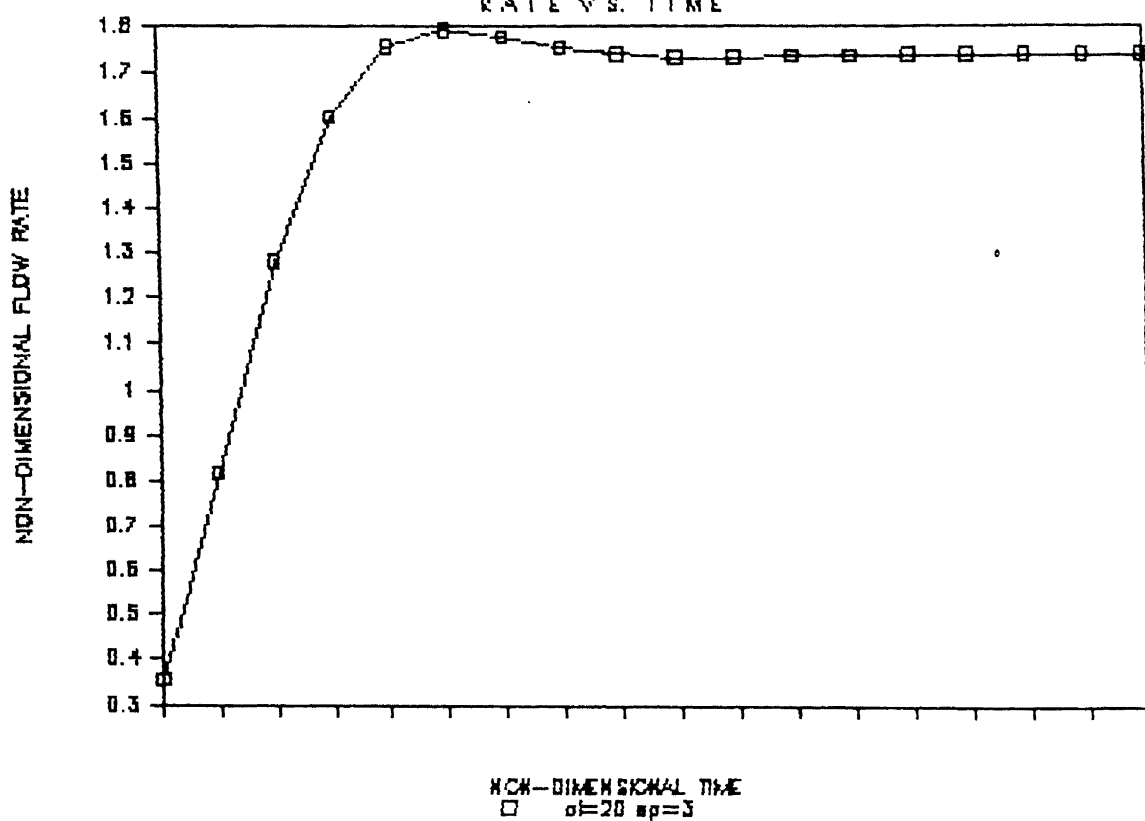
NON-DIMENSIONAL FLOW RATE VS. TIME



GRAPH 1-10

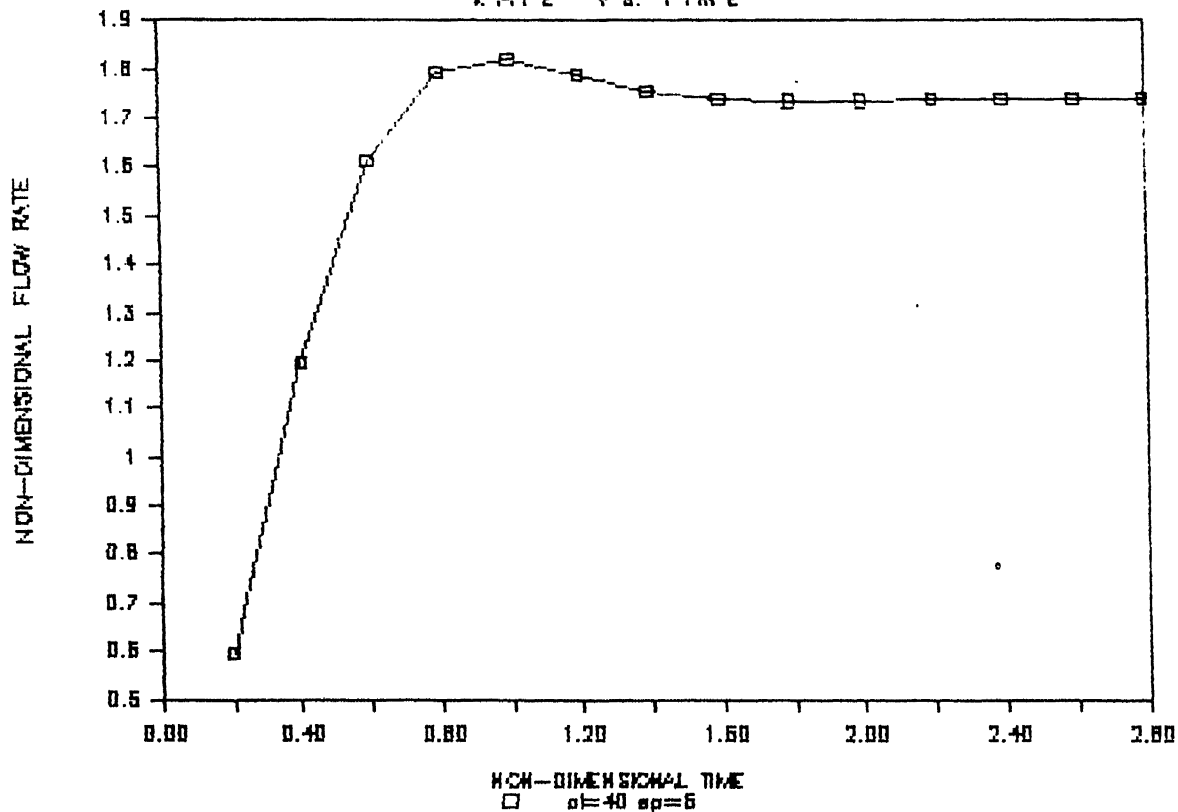
NON-DIMENSIONAL FLOW

RATE VS. TIME

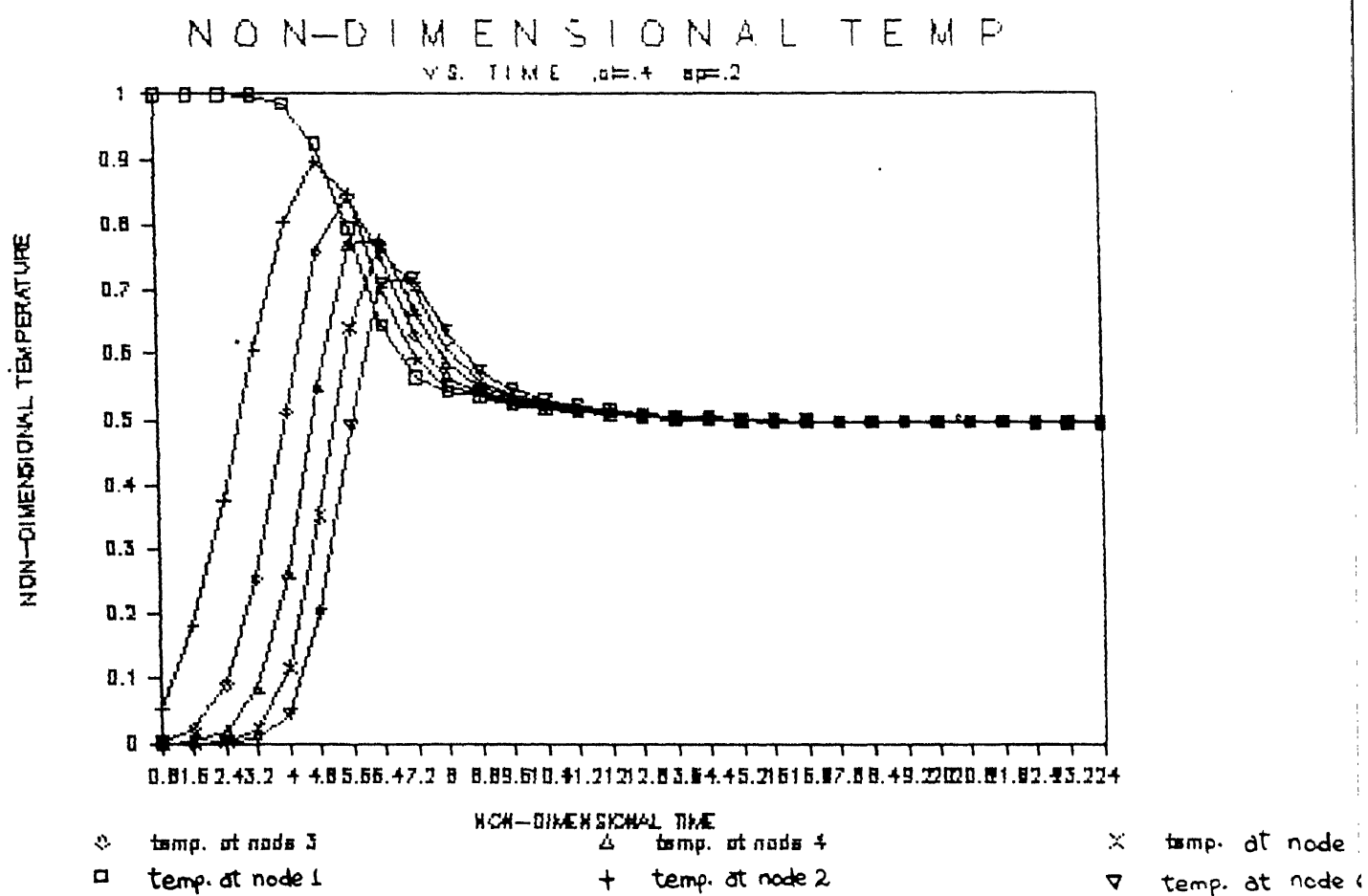


GRAPH 1.11

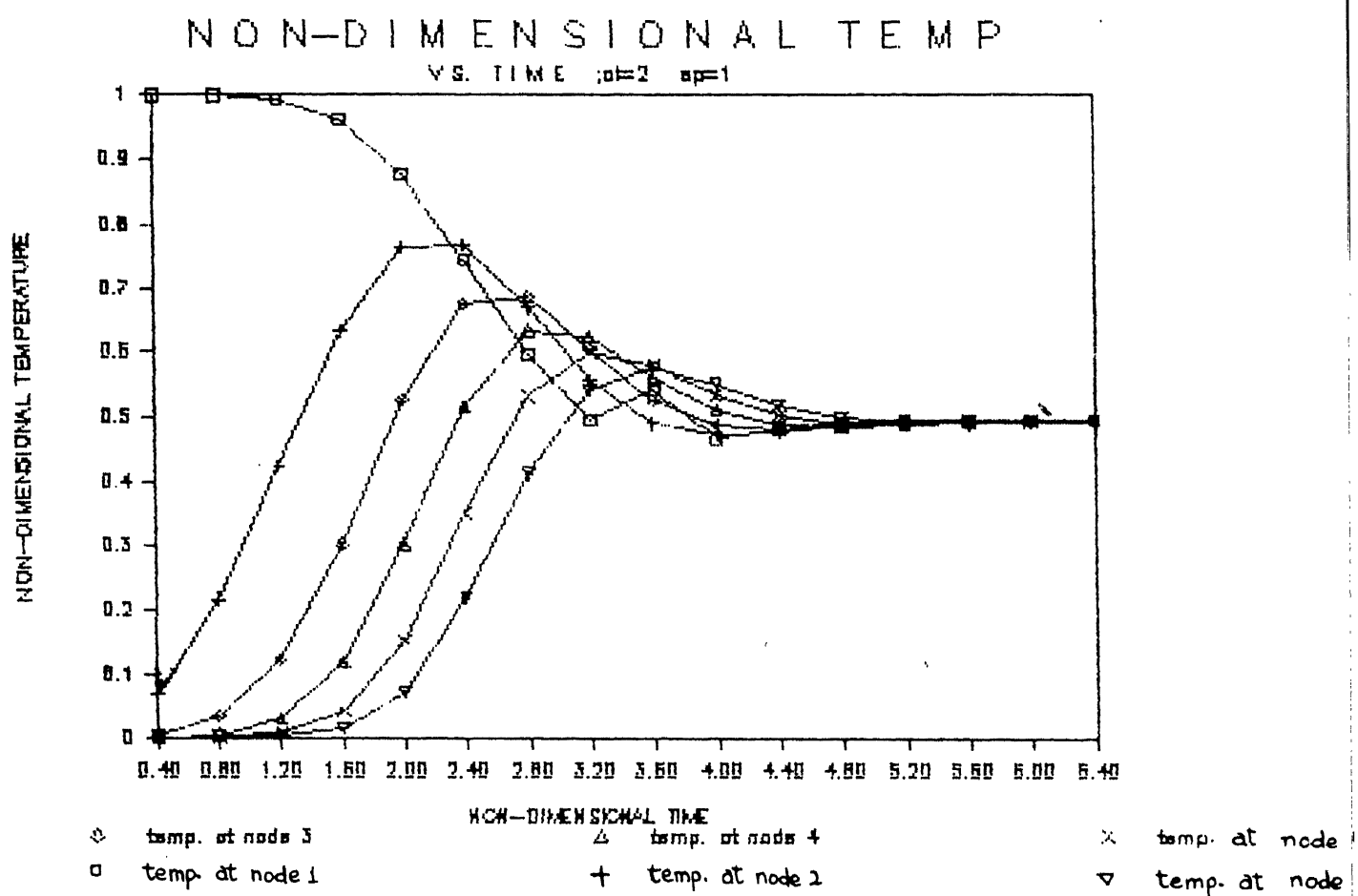
NON-DIMENSIONAL FLOW RATE VS. TIME



GRAPH 1-12

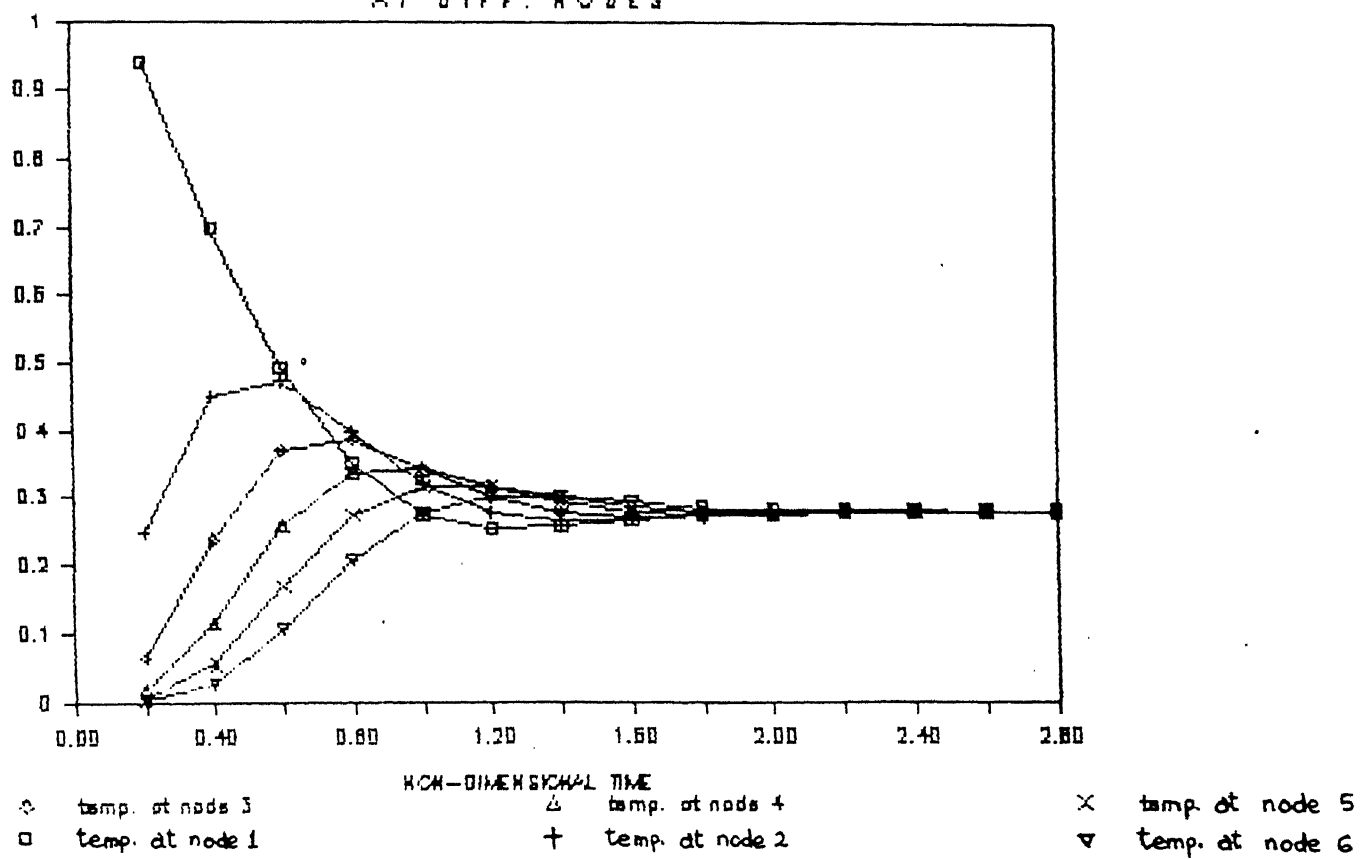


GRAPH 1.13



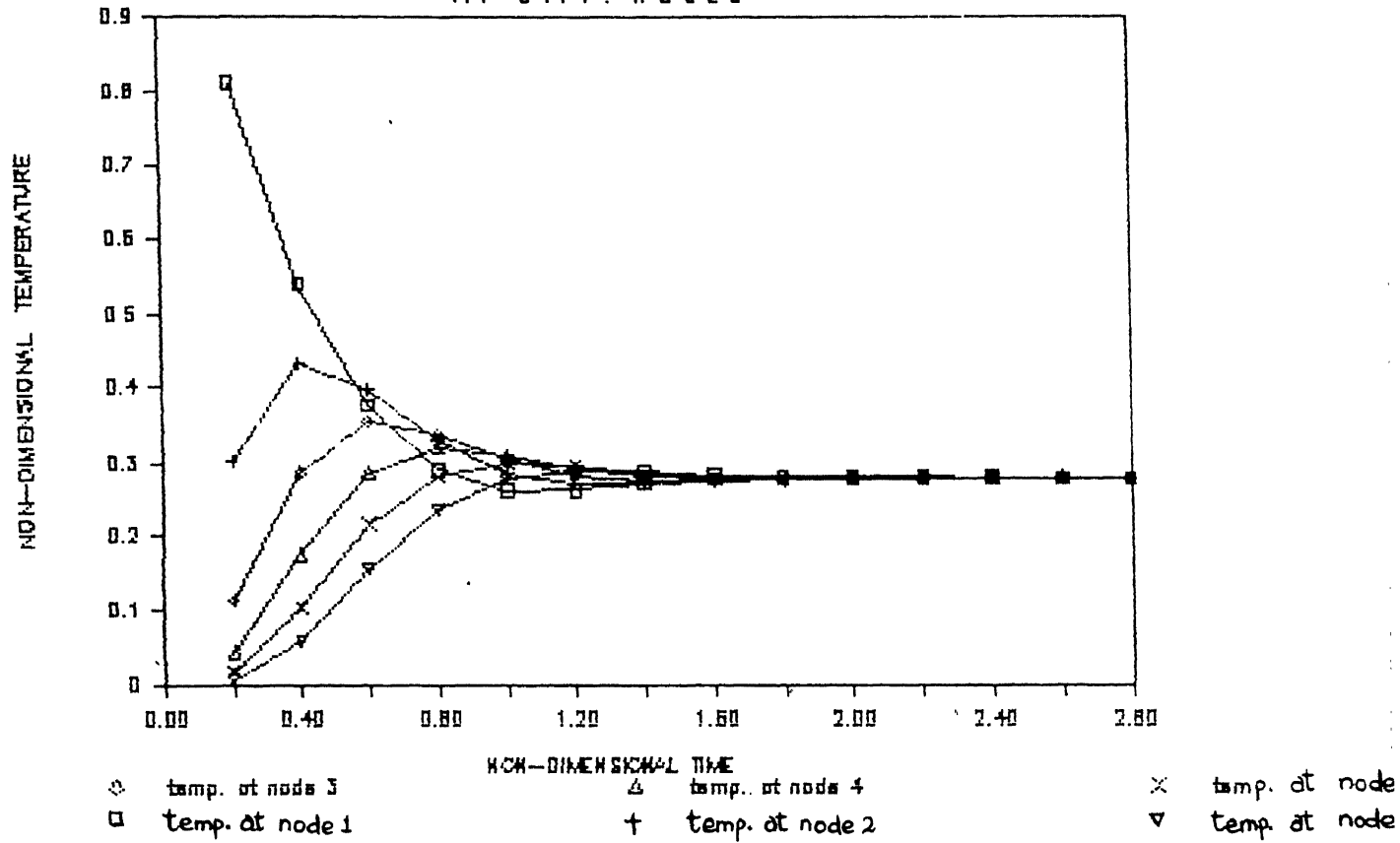
GRAPH 1.14

TEMPERATURE V.S. TIME
AT DIFF. NODES



GRAPH 1-15

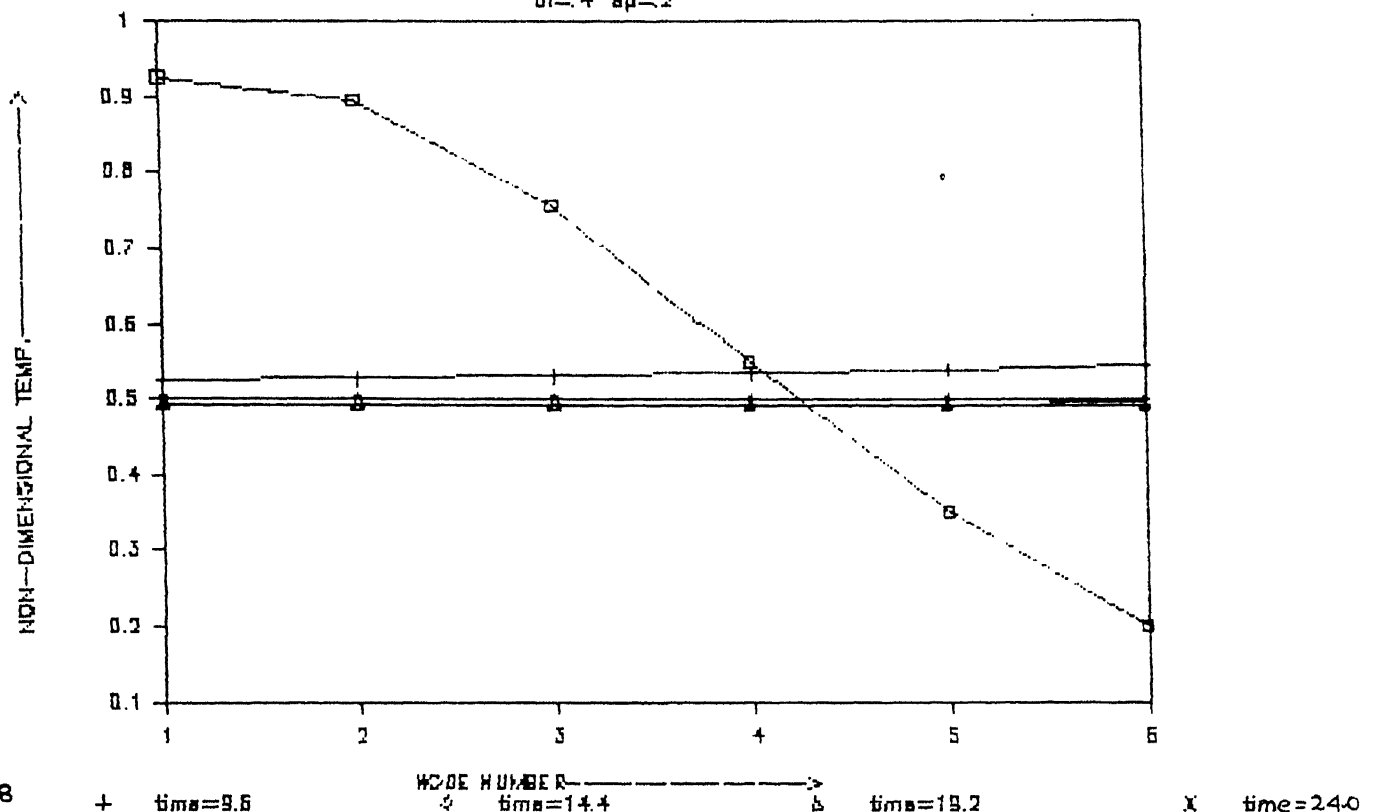
TEMPERATURE V.S. TIME
AT DIFF. NODES



GRAPH 1.16

TEMP. DIST. AT DIFF. TIMES IN LOOP

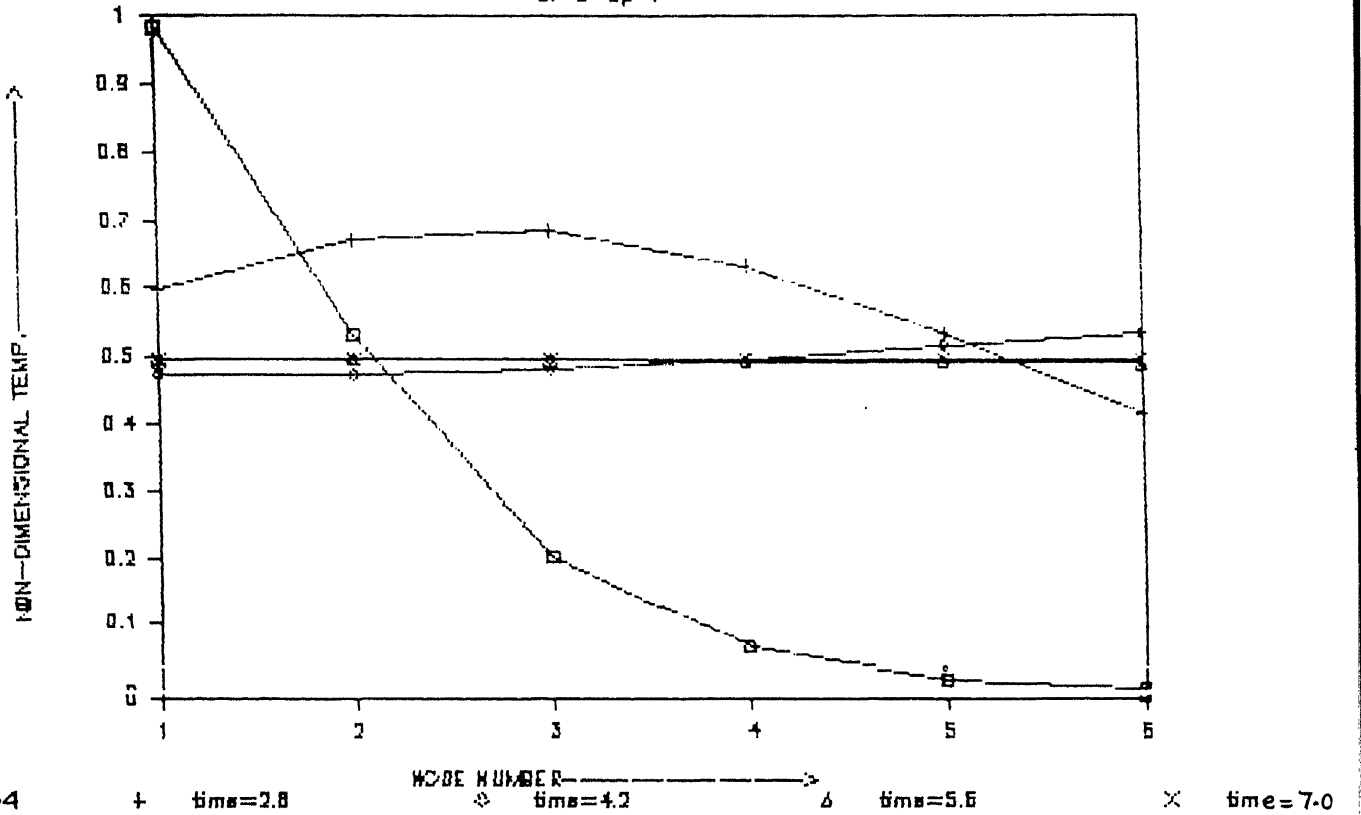
$\alpha l = 4 \quad \alpha p = 2$



GRAPH 1.17

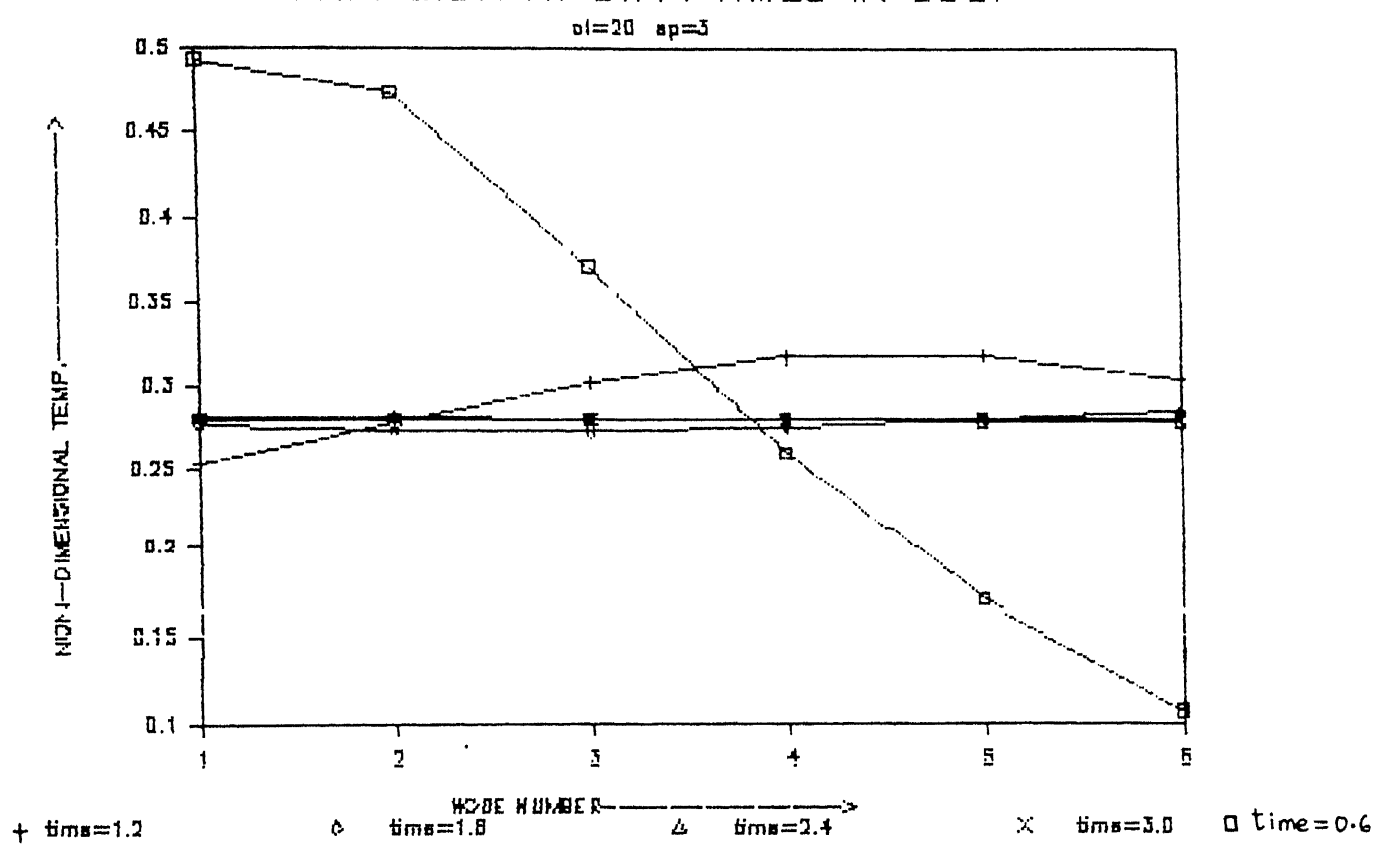
TEMP. DIST. AT DIFF. TIMES IN LOOP

$\alpha l=2 \quad \alpha p=1$

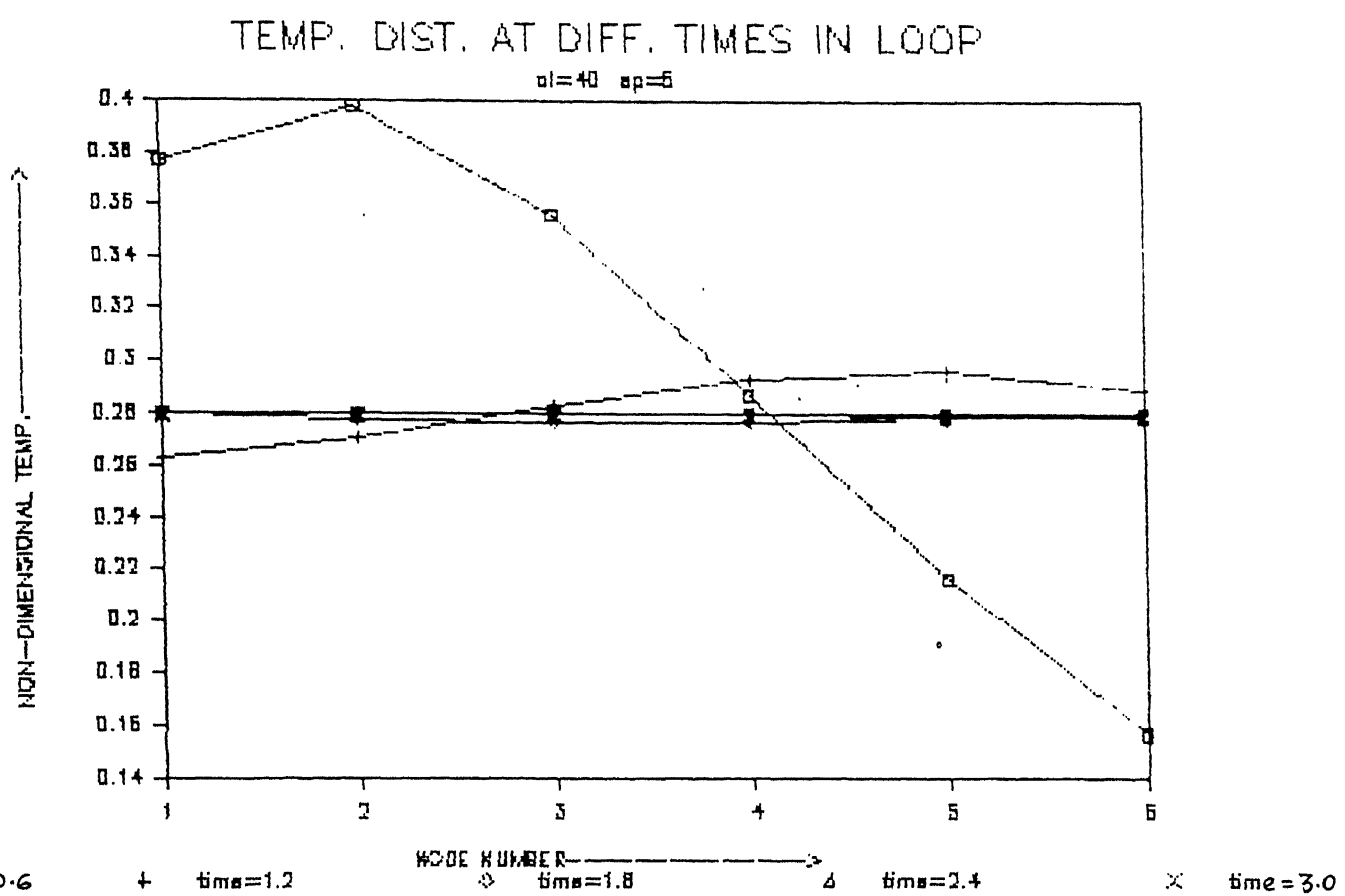


GRAPH 1.18

TEMP. DIST. AT DIFF. TIMES IN LOOP



GRAPH 1.19



GRAPH 1.20

as $Q \rightarrow \infty, \partial T / \partial s \rightarrow 0$, i.e., T is uniform and hence $B \rightarrow 0$

For $Q=0, T=T_0$ and hence B is non-zero if $\int T_0 dz$ is not zero (Case-1)
and $B=0$ if $\int T_0 dz=0$ (Case-2)

The frictional force F is a function of Q and increases with Q for any normal friction law. This is also shown in Figure 2.5.

Now, clearly in both cases, the two curves must meet at least in one point. In case-2, zero motion is also a possible steady solution.

In Figure-2.5a, as Q is increased above its balanced value, buoyancy force decreases and friction increases thereby counteracting the changes. Thus the system seems to be stable.

In figure-2.5b, if rate of increase of B is larger than that of F near $Q=0$, i.e., if $dF/dQ < dB/dQ$ at $Q=0$, then increase of Q results in larger increase of B than that of F . Hence instability may result. But as Q is increased further, we get a point after which steady state prevails. Thus it seems that the system would always end up in a stable situation. But experimentally instability has been observed when buoyancy forces are large. This is explained analytically in the following section by linear stability analysis.

Linear Stability Analysis

Let us analyse the equation set (2.3.1)-(2.3.3). By taking a first order perturbation,

$$Q(t) = \bar{Q} + \delta Q'(t) \quad T(t, s) = \bar{T}(s) + \delta T'(t, s) \quad (2.6.3)$$

and applying to (2.3.1)-(2.3.3), we get, by separation of zero and first order terms,

$$\varepsilon \bar{Q} = \alpha \int_0^s \bar{T}' ds \quad (2.6.4.a)$$

$$\bar{Q} \partial \bar{T} / \partial s = 0 \quad (2.6.4.b)$$

$$\bar{T}'_{s=0} + \bar{T}'_{s=1} = (1 + \bar{T}'_{s=1}) (1 - \exp(-1/\bar{Q})) \quad (2.6.4.c)$$

$$dQ'/dt + \varepsilon \bar{Q}' = \alpha \int_0^s \bar{T}' ds \quad (2.6.5.a)$$

$$\partial T' / \partial t + Q' \partial T' / \partial s = 0 \quad (2.6.5.b)$$

$$\underset{s=0}{T'} + \underset{s=1}{mT'} + \underset{s=1}{nQ'} = 0 \quad (2.6.5.c)$$

$$\text{where } m = \exp(-1/\bar{Q}) = (1-\bar{T})/(1+\bar{T})$$

$$n = (1+\bar{T}) \exp(-1/\bar{Q}) / (\bar{Q} * \bar{Q}) = (1-\bar{T}) / (\bar{Q} * \bar{Q}) \quad (2.6.5.d)$$

Equation (2.6.4) represents the steady state case whose solution is given in section (2.4). To solve (2.6.5), we take,

$$Q'(t) = \hat{Q} \exp(\sigma t) \quad T'(s, t) = \hat{T}(s) \exp(\sigma t) \quad (2.6.6)$$

where σ , the stability parameter, in general, is a complex number.

Applying in (2.6.5), we get,

$$(\sigma + \epsilon) \hat{Q} = \omega \int_0^1 \hat{T} ds \quad (2.6.7.a)$$

$$\sigma \hat{T} + \bar{Q} \frac{d\hat{T}}{ds} = 0 \quad (2.6.7.b)$$

$$\hat{T}(0) + m\hat{T}(1) + n\hat{Q} = 0 \quad (2.6.7.c)$$

By solving for \hat{T} and \hat{Q} ,

$$\hat{T} = C \exp(-\sigma s / \bar{Q})$$

$$\hat{Q} = \alpha / (\sigma + \epsilon) \int_0^1 \hat{T} ds = C \bar{Q} \alpha / [\sigma(\sigma + \epsilon)] (1 - \exp(-\sigma / \bar{Q}))$$

Now B.C. (2.6.7.c) becomes the characteristic equation

$$1 + m \exp(-\sigma / \bar{Q}) + n \bar{Q} / [\sigma(\sigma + \epsilon)] [1 - \exp(-\sigma / \bar{Q})] = 0 \quad (2.6.8)$$

For real, positive σ , all terms in LHS of (2.6.8) become positive and (2.6.8) does not hold. Hence there is no possibility of real, positive σ , hence no instability of exponential growth type. But there may be oscillatory instability. The neutral stability can be analysed by taking σ as a purely imaginary quantity $i\omega$.

Taking $\tilde{\alpha} = n\alpha / \bar{Q}$; $\tilde{\epsilon} = \epsilon / \bar{Q}$; $\tilde{\omega} = \omega / \bar{Q}$, we get,

$$(\exp(i\omega) + m) / (\exp(i\omega) - 1) + \tilde{\alpha} / (i\omega(i\omega + \tilde{\epsilon})) = 0$$

Separation of real and imaginary parts alongwith expressing $\tilde{\alpha}$ in terms of \bar{T} and $\tilde{\epsilon}$ only and substituting for m from (2.6.5.d), we get,

$$\tilde{\omega}^2 + (\tilde{\epsilon} - A/2)^2 = (A/2)^2 \quad (2.6.9)$$

$$\tilde{\epsilon} = -1/\bar{T} \tilde{\omega} \cot(\omega/2) \quad (2.6.10)$$

$$\text{where } A = A(\bar{T}) = -(1 - \bar{T}^2) / \bar{T}^2 \ln[(1 - \bar{T}) / (1 + \bar{T})] \quad (2.6.11)$$

The plot of A vs. \bar{T} and $\tilde{\omega} \cot(\omega/2)$ is shown in Figure-2.6 and 2.7. The curve represented by (2.6.9) is a circle and by (2.6.10) is a multi-branched curve, both being functions of \bar{T} in $\tilde{\omega} - \tilde{\epsilon}$ plane. Thus for certain $\bar{T} = 0.265$, both curves first touch each other. It is the largest \bar{T} for which flow becomes unstable

corresponding to smallest possible flow rate $Q=1.84$ and angular frequency of oscillation $3.6Q$. As angular frequency of fluid particle is $\bar{\Omega}Q$, thermal disturbance travels slightly faster than the fluid.

As \bar{Q} is increased, there are two intersection points of the curves of (2.6.9) and (2.6.10). Thus there are two values of ϵ for which neutral oscillations occur if the value of Q is above the critical value; in between these ranges the solutions are amplified. The neutral stability curve is shown in Figure-2.8 in $\bar{Q}-\epsilon$ plane.

Physical explanation of instability

The instability can be explained physically by considering the interplay of buoyancy and friction forces. The instability arises as these two forces may not be in phase at each time.

Let us consider the system to be operating in steady state. If a small thermal disturbance causes a pocket of fluid to emerge from the heated section slightly hotter than is normal for this steady state, the buoyancy is momentarily increased and the flow accelerates slightly. This hotter-than-normal pocket proceeds through the cooled section more rapidly than normal and is warmer than normal as it leaves the sink. The total buoyancy force is therefore decreased decelerating the flow. Thus the pocket enters the heated section once more, now at a higher inlet temperature and a lower velocity. These two effects combined together cause the pocket to emerge from the source at a higher temperature than before. The same logic applies for a pocket of fluid which initially emerges from the source cooler than normal leading to the same oscillatory result.

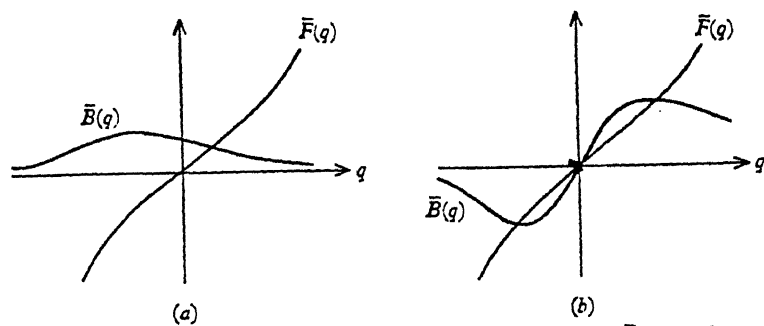


FIGURE 2.5 Variation of total friction \bar{F} and total buoyancy \bar{B} with flow rate;
(a) no equilibrium, (b) one unstable equilibrium. (Schematic picture.)

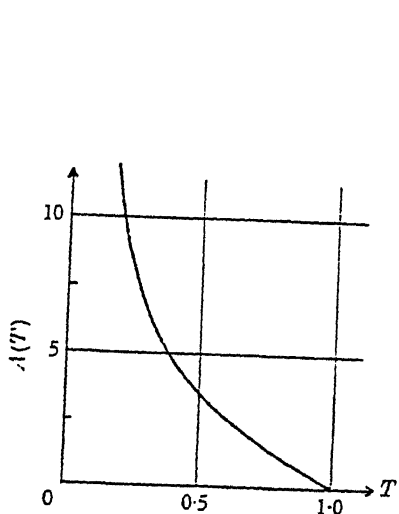


FIGURE 2.6. The function
 $A(T) = (1 - T^{-2}) \ln(1 - T)/(1 + T)$.

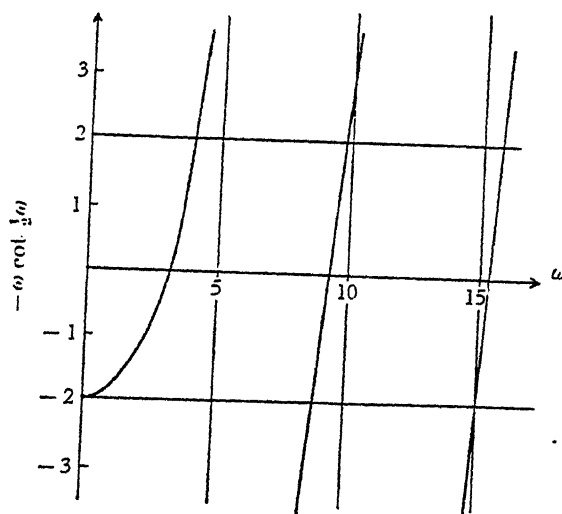


FIGURE 2.7 The function $-\omega \cot \frac{\pi}{2}\omega$.

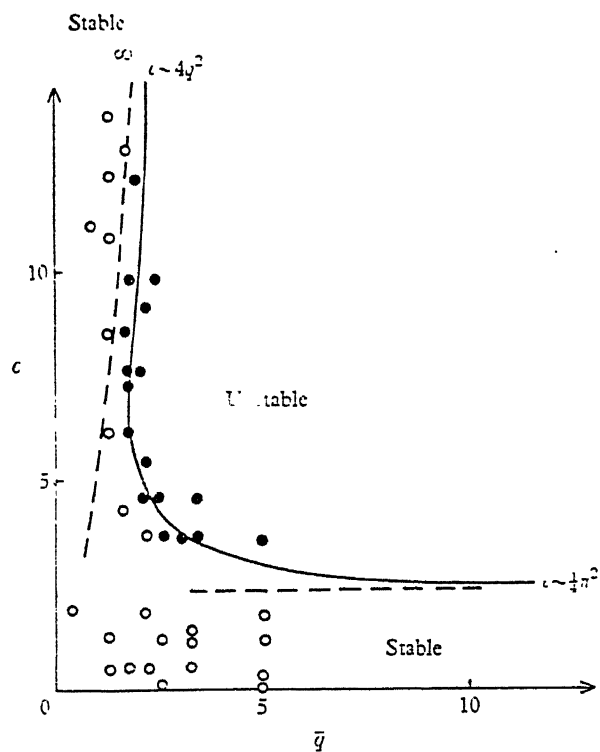


FIGURE 28. The neutral curve in a (\bar{q}, c) -plane, computed from the stability theory. The

CHAPTER-3
RECTANGULAR THERMOSYPHON WITH
EXTENDED SOURCE AND SINK

3.1:Introduction

The analysis of the previous chapter gives some insight into the complexity of the problem. However, the idea of a point source and point sink is not a real one, only assumed for mathematical simplicity in analysis. The real problem involves a line source and a line sink. So in this chapter, we consider a rectangular thermosyphon loop in vertical plane with insulated vertical branches whose lower segment is being heated and upper segment cooled. Here three types of heat fluxes are considered, i.e., uniform, triangular, sinusoidal. The heat sink has been assumed to be at constant temperature for simplicity.

3.2:Formulation

The loop to be analysed is shown in Figure-3.1. The following assumptions are made.

- (1) Due to small pressure changes in natural convection, the fluid is incompressible.
- (2) The flow is one-dimensional with the coordinate running around the loop.
- (3) The fluid properties and heat transfer coefficients are constant.
- (4) Boussinesq approximation is valid, i.e., density is assumed to be constant in all conservation equations except for the body force term in the momentum equation where linear variation of density with temperature is assumed, i.e., $\rho = \rho_0 [1 - \beta(T - T_0)]$ ----- (3.2.1)
- (5) The fluid is well mixed over the cross-section.
- (6) The temperature is uniform over the cross-section due to mixing.
- (7) The frictional force is a function of instantaneous flow rate.

Now, the governing equations are:

Continuity: $\partial v / \partial s = 0$, i.e., $v = v(t)$ ----- (3.2.2)

Velocity is uniform around the loop.

Momentum: $\rho v dv / dt = -\rho g \cos \theta - \partial p / \partial s - 4\tau_v / d$

where θ = Angle between vertical and tangent to the loop at a point.
Now to eliminate the pressure term, integration around the loop is

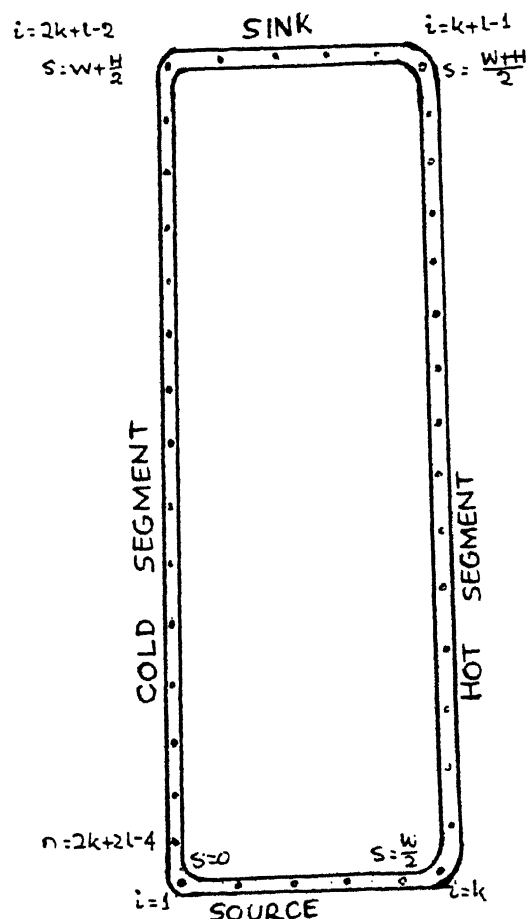


FIGURE 3.1 Rectangular Thermosyphon
 loop with heating at lower horizontal
 arm and cooling at upper horizontal arm.
 The dots denote discretization of the loop.

done. Thus, we get,

$$\rho_v dQ/dt + ds/A(s) = -g \rho dz - 4\tau_v / d ds$$

Now using the relation (3.2.1) and using $\tau_v = f/2 \rho_v Q^2 / A^2$,

$$\text{we get, } \rho_v dQ/dt + ds/A(s) = g \rho \beta T dz - 2f \rho_v Q^2 / (dA^2) ds$$

Now assuming uniform cross-sectional area around the loop

$$\rho_v dQ/dt L/A = \rho_v g \beta T dz - \rho_v / 2RQ^2$$

where $R = 4f / (dA^2) ds$ = Overall friction factor, which accounts for both friction and form losses

$$\text{Thus, } L/A dQ/dt = g \beta T dz - RQ^2 / 2 \quad \text{---(3.2.3)}$$

Energy: Neglecting viscous dissipation and axial conduction,

$$\begin{aligned} \rho_v c_p \left(\frac{\partial T}{\partial t} + \frac{Q}{A} \frac{\partial T}{\partial s} \right) &= \frac{4g}{d}, \quad 0 < s < W/2 \text{(Uniform heat flux)} \\ &= 0, \quad W/2 < s < (W+H)/2 \text{ and } W+H/2 < s < W+H \\ &= -\frac{4h(T - T_w)}{d}, \quad (W+H)/2 < s < W+H/2 \end{aligned} \quad \text{---(3.2.4)}$$

Eq.(3.2.3) and (3.2.4) represent a set of coupled integro-differential equations in two variables Q , a function of t only and T , a function of s and t . Hence we need boundary condition and initial condition.

B.C.: Continuity of T around the loop

I.C.: At time $t=0$, $Q=0$ and $T=T_o$ for all s ---(3.2.5)

3.3 :Steady state solution

The steady state equations are derived by making time derivative zero. So we get from (3.2.3), (3.2.4) and (3.2.5)

$$\text{Momentum: } g \beta T dz = RQ^2 / 2 \quad \text{---(3.3.1)}$$

$$\begin{aligned} \text{Energy: } \rho_v c_p \frac{Q}{A} \frac{\partial T}{\partial s} &= \frac{4g}{d}, \quad 0 < s < W/2 \text{(Source)} \\ &= 0, \quad W/2 < s < (W+H)/2 \text{ and } W+H/2 < s < W+H \text{(Vertical side)} \\ &= -\frac{4h(T - T_w)}{d}, \quad (W+H)/2 < s < W+H/2 \text{(Sink)} \end{aligned} \quad \text{---(3.3.2)}$$

B.C.: Continuity of T along the loop

To solve the above set of equations, we first solve the energy equation to find temperature distribution with Q as a parameter and then apply this distribution in (3.3.1) to find steady state values.

Solution of energy equation:

$$\text{Source } (0 < s < W/2) : T = \frac{4gAs}{\rho_v C_p dQ} + C_1$$

$$\begin{aligned} \text{Vertical branches } \left(\frac{W}{2} < s < \frac{W+H}{2}; W + \frac{H}{2} < s < W+H \right) : T &= \text{constant, say} \\ &= T_h \text{ for } \frac{W}{2} < s < \frac{W+H}{2} \text{ (Hot segment)} \\ &= T_c \text{ for } W + \frac{H}{2} < s < W+H \text{ (Cold segment)} \end{aligned}$$

$$\text{Sink } \left(\frac{W+H}{2} < s < W + \frac{H}{2} \right) : T = C_2 \exp \left(-\frac{4hAs}{\rho_v C_p Q d} \right) + T_w$$

To find the constants, we apply the boundary condition.

$$\text{Continuity at } s=W/2: \frac{4qAW}{\rho_v C_p dQ} + C_1 = T_H \quad \text{---(3.3.3)}$$

$$\text{at } s=\frac{W+H}{2} : C_2 \exp\left(-\frac{4hA(W+H)}{2\rho_v C_p Qd}\right) + T_v = T_H \quad \text{---(3.3.4)}$$

$$\text{at } s=W+\frac{H}{2} : T_c = C_2 \exp\left(-\frac{4hA(W+\frac{H}{2})}{2\rho_v C_p Qd}\right) + T_v \quad \text{---(3.3.5)}$$

$$\text{at } s=W+H: T_c = C_1 \quad \text{---(3.3.6)}$$

$$\text{Eq. (3.3.3) and (3.3.6) give } T_H - T_c = \frac{4qAW}{2\rho_v C_p dQ} = \frac{q\pi dW}{2\rho_v C_p Q}$$

Since, power = $P = q\pi dW/2$, ΔT_H = Temperature difference across heated

$$\text{section} = T_H - T_c = \frac{P}{\rho_v C_p Q} \quad \text{---(3.3.6)}$$

$$\text{Eq. (3.3.4) gives } C_2 = (T_H - T_v) \exp\left(\frac{h\pi d(W+H)}{2\rho_v C_p Q}\right)$$

$$\text{Eq. (3.3.5) gives } T_c = (T_H - T_v) \exp\left(-\frac{h\pi dW}{2\rho_v C_p Q}\right) + T_v \quad \text{---(3.3.7)}$$

Now temperature distribution is given by

$$T = \frac{2Ps}{\rho_v C_p WQ} + T_c \quad \text{(Source)} \quad \text{---(3.3.8)}$$

$$= T_H \quad \text{(Hot segment)} \quad \text{---(3.3.8)}$$

$$= (T_H - T_v) \exp\left(\frac{h\pi d(W+H)}{2\rho_v C_p Q}\right) + T_v \quad \text{(Sink)}$$

$$= T_c \quad \text{(Cold segment)}$$

Now momentum eq. (3.3.1) gives

$$g\beta(T_H - T_c)H/2 = RQ^2/2 \quad \text{---(3.3.9)}$$

Eq. (3.3.6), (3.3.7) and (3.3.9) are to be solved for unknowns T_H , T_c and Q .

$$\text{From (3.3.6), } \frac{g\beta PH}{2\rho_v C_p Q} = RQ^2/2$$

$$\text{So, } Q = \left(\frac{g\beta PH}{\rho_v C_p R}\right)^{1/3} \quad \text{---(3.3.10)}$$

Now T_H and T_c can be solved and temperature distribution in the loop can be found from (3.3.8).

3.4 Non-dimensionalisation:

The variables are non-dimensionalised as following :

$$T^* = \frac{T - T_w}{q/h} \quad s^* = \frac{s}{H/2} \quad Q^* = \frac{Q}{Q_{ch}} \quad t^* = \frac{t Q_{ch}}{(H+W)A}$$

$$\text{Now } \frac{dQ}{dt} = \frac{Q_{ch}}{(H+W)A} \frac{dQ^*}{dt^*} \quad \frac{\partial T}{\partial t} = \frac{Q_{ch} q}{hLA} \frac{\partial T^*}{\partial t^*}$$

$$\frac{\partial T}{\partial s} = \frac{2q}{hH} \frac{\partial T^*}{\partial s^*} \quad ds = H/2 \quad ds^*$$

Substituting these relations in (3.2.3)-(3.2.5), by dropping * from variables and defining aspect ratio $= B = W/H$, we get,

$$1/F = \frac{dQ}{dt} = G \left[\frac{1+B}{B} T ds - s \frac{2+2B}{1+2B} T ds \right] - Q^2$$

$$\begin{aligned} \frac{1}{2(1+B)} \frac{\partial T}{\partial t} + Q \frac{\partial T}{\partial s} &= M, 0 < s < B \text{(Source)} \\ &= 0, B < s < 1+B \text{(Hot segment)} \\ &= -MT, 1+B < s < 1+2B \text{(Sink)} \\ &= 0, 1+2B < s < 2+2B \text{(Cold segment)} \end{aligned} \quad (3.4.1)$$

with continuity of T along the loop and
initial condition of $Q=0$ and $T=0$ at $t=0$
with the non-dimensional parameters defined by

F =Friction parameter= $RA^2/2$

$$G=\text{Modified Grashof number}=\frac{2g\beta P}{RhQ_{ch}^2 \pi dB}=\frac{g\beta qH}{RhQ_{ch}^2} \quad (3.4.2)$$

$$M=\text{Geometry parameter}=\frac{2hHA}{\rho C_p Q_{ch} d}$$

In natural convection, the main problem encountered in non-dimensionalisation is the non-availability of a characteristic flow rate as compared to forced convection. Hence this problem is solved by taking the value of Q_{ch} to be equal to the steady state flow rate. Hence, $Q_{ch} = Q_{ss}$

To find the non-dimensional parameters, we need to know R , Q_{ch} and h . From definitions

$$R=\frac{4fL}{dA^2} \text{ where } f=\text{Friction factor, a function of Reynold's No.}$$

$$=\frac{a}{Re} = \frac{a \mu^b A^b}{(Q_{ch} \rho d)^b}$$

$$\text{So, } R=\frac{4AL\mu^b}{A^2 Q_{ch}^b \rho^b d^{1+b}} \quad (3.4.3)$$

The relations (3.3.10) and (3.4.3) involve two unknowns R and Q_{ch} .

$$\text{By solving, } Q_{ch} = \left(\frac{g\beta HPA}{4C_L \mu_p^b} \frac{d}{\rho^{1-b}} \right)^{1/(a-b)} \quad \text{--- (3.4.4)}$$

For laminar flow, $a=16$, $b=1$,

$$\text{So } Q_{ch} = \left(\frac{g\beta HPA d^2}{64C_L \mu_p} \right)^{1/2} = \left(\frac{\pi^2 g\beta H P d^4}{256C_L \mu_p} \right)^{1/2} \quad \text{--- (3.4.5)}$$

For turbulent flow, $a=f=f_v$, $b=0$

$$\text{So } Q_{ch} = \left(\frac{g\beta HPA^2 d}{4C_L f_v \mu_p} \right)^{1/8} = \left(\frac{\pi^2 g\beta H P d^5}{64C_L f_v \mu_p} \right)^{1/8} \quad \text{--- (3.4.6)}$$

Q_{ch} is substituted in (3.4.3) to find R .

To evaluate the heat transfer coefficient, the correlations used for forced convection are taken as there are no such correlations available for natural convection.

3.5 Formulation for differnt heating cases:

In this section, the formulation is done for the following three types of heating arrangements.

- (1) Uniform heat flux
- (2) Triangular heat flux
- (3) Sinosidual heat flux

The flux distributions have been shown in Figure-3.2. For all the cases, eq.(3.2.3) and (3.2.4) hold, the only change being in the source term of energy eq.(3.2.4).

3.5.1 Uniform heat flux case:

The governing equations are (3.2.3) and (3.2.4) which after being non-dimensionalised as shown before reduces to the set (3.4.1) with the non-dimensional parameters defined by (3.4.2).

3.5.2 Triangular flux case:

The governing equations are (3.2.3) and (3.2.4) except for the source portion, energy eq.(3.2.4) being

$$\rho_w C_p \left(\frac{\partial T}{\partial t} + \frac{Q}{A} \frac{\partial T}{\partial s} \right) = \frac{16}{dW} s q_{max} \quad , 0 < s < W/4 \\ = - \frac{16}{dW} q_{max} (s - W/2) \quad , W/4 < s < W/2$$

$$\text{In this case, power} = P = \int_0^{W/2} q \, ds \\ = 4/W \pi d q_{max} \left[\int_0^{W/4} s \, ds - \int_{W/4}^{W/2} (s - W/2) \, ds \right] \\ = W/4 \pi d q_{max}$$

Now making non-dimensionalisation as before except for $T^* = \frac{T - T_w}{q_{max}/h}$, we get,

$$1/F \frac{dQ}{dt} = G \left[\int_0^{1+b} T \, ds - \int_{1+b}^{2+2b} T \, ds \right] - Q^2$$

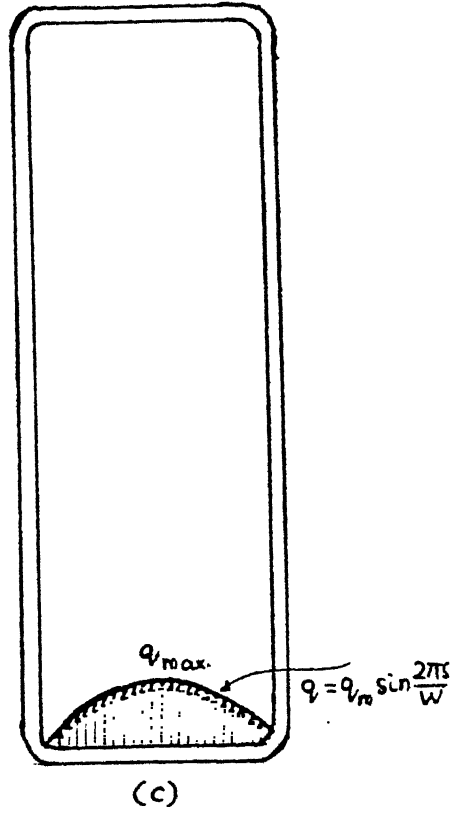
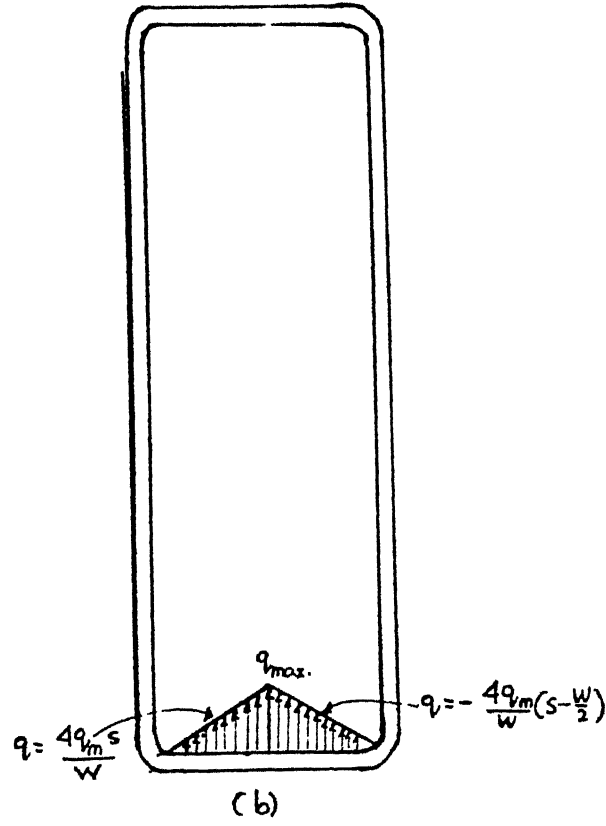
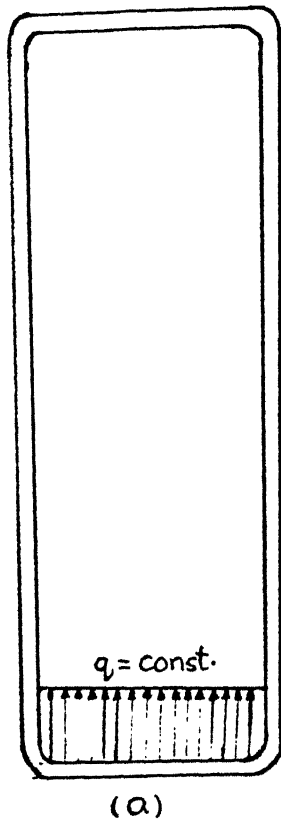


FIGURE 3.2

(a) Uniform heat flux (b) Triangular heat flux (c) Sinusoidal heat flux

$$\begin{aligned}
 \frac{1}{2(1+B)} \frac{\partial T}{\partial t} + Q \frac{\partial T}{\partial s} &= 2Ms/B, 0 < s < B/2 \\
 &= -2M(s-B)/B, B/2 < s < B \\
 &= 0, B < s < 1+B \\
 &= -MT, 1+B < s < 1+2B \\
 &= 0, 1+2B < s < 2+2B
 \end{aligned} \tag{3.5.2.1}$$

with continuity of T along the loop and initial condition of $Q=0$ and $T=0$ at $t=0$.

with the non-dimensional parameters given by

$$F = \text{Friction parameter} = RA^2/2$$

$$G = \text{Modified Grashof No.} = \frac{g^3 H}{R h Q_{ch}^2} q_{max} = \frac{4g^3 P}{R h \pi d B Q_{ch}^2} \tag{3.5.2.2.}$$

$$M = \text{Geometry parameter} = -\frac{2hHA}{\rho_w C_p d Q_{ch}}$$

3.5.3 Sinosidual flux case:

The governing equations are (3.2.3) and (3.2.4) except for the source portion, energy eq. there being

$$\rho_w C_p \left(\frac{\partial T}{\partial t} + Q \frac{\partial T}{\partial s} \right) = 4/d q_{max} \sin(2s\pi/W), 0 < s < W/2$$

$$\begin{aligned}
 \text{In this case, power} &= P = \int_0^{W/2} q \pi d ds = \int_0^{W/2} q_{max} \sin(2s\pi/W) \pi d ds \\
 &= dWq_{max}
 \end{aligned}$$

Now making non-dimensionalisation as above except for $T^* = \frac{T - T_w}{q_{max} / 7h}$, we get,

$$1/F \frac{dQ}{dt} = G \left[\int_0^{1+B} T ds - \int_{1+2B}^{2+2B} T ds \right] - Q^2$$

$$\begin{aligned}
 \frac{1}{2(1+B)} \frac{\partial T}{\partial t} + Q \frac{\partial T}{\partial s} &= M \sin(\pi s/B), 0 < s < B \\
 &= 0, B < s < 1+B \\
 &= -MT, 1+B < s < 1+2B \\
 &= 0, 1+2B < s < 2+2B
 \end{aligned} \tag{3.5.3.1}$$

with the non-dimensional parameters given by

$$F = RA^2/2 = \text{Frictional parameter}$$

$$G = \text{Modified Grashof No.} = \frac{g^3 P}{R h d B Q_{ch}^2} \tag{3.5.3.2}$$

$$M = \text{Geometry parameter} = -\frac{2hHA}{\rho_w C_p d Q_{ch}}$$

3.6 Steady state solutions:

The steady state equations are obtained for each case by making the time derivative zero in the equations (3.4.2), (3.5.2.1)

and (3.5.3.1). There exists analytical solutions for these cases which are given in detail in Appendix-2 for uniform heating, Appendix-3 for triangular heating and Appendix-4 for sinusoidal heating case. The results are summarised below.

For uniform heating, eq.set (3.6.1) are given as

$$\bar{Q}=1$$

$$\begin{aligned}\bar{T}(s) &= Ms + MB \frac{\exp(-MB)}{1-\exp(-MB)}, 0 \leq s \leq B \\ &= \frac{MB}{1-\exp(-MB)}, B \leq s \leq 1+B \\ &= \frac{MB \exp[M(1+B-s)]}{1-\exp(-MB)}, 1+B \leq s \leq 1+2B \\ &= \frac{MB \exp(-MB)}{1-\exp(-MB)}, 1+2B \leq s \leq 2+2B\end{aligned}\quad \text{----- (3.6.1)}$$

For triangular heating, eq. set (3.6.2) are given by

$$\bar{Q}=1$$

$$\begin{aligned}\bar{T}(s) &= \frac{Ms^2}{B} + K_1, 0 \leq s \leq B/2 \\ &= -2M/B (s/2-B)s + K_2, B/2 \leq s \leq B \\ &= K_4, B \leq s \leq 1+B \\ &= K_3 \exp(-Ms), 1+B \leq s \leq 1+2B \\ &= K_5, 1+2B \leq s \leq 2+2B\end{aligned}$$

$$\text{where } K_1 = BM/2 \frac{\exp(-MB)}{1-\exp(-MB)}$$

$$K_3 = BM/2 \frac{\exp[M(1+B)]}{1-\exp(-MB)}$$

$$K_2 = K_1 - MB/2$$

$$K_4 = K_1 + MB/2$$

For sinusoidal heating, eq. set (3.6.3) are given by

$$\bar{Q}=1$$

$$\begin{aligned}\bar{T}(s) &= K_1 - MB/\pi \cos(\pi s/B), 0 \leq s \leq B \\ &= K_2, B \leq s \leq 1+B \\ &= K_3 \exp(-Ms), 1+B \leq s \leq 1+2B \\ &= K_4, 1+2B \leq s \leq 2+2B\end{aligned}$$

$$\text{where } K_3 = 2MB/\pi \frac{\exp[M(1+B)]}{1-\exp(-MB)}$$

$$K_4 = K_3 \exp[-M(1+2B)]$$

$$K_2 = K_3 \exp[-M(1+B)]$$

$$K_1 = K_4 + MB/\pi$$

3.7 Finite difference formulation for transient analysis:

For solving the transient equations, we use finite difference method. Implicit scheme has been used for the time derivative part and upwind scheme, here, backward difference, is used for the space

derivative part. The integro-differential equation is solved by using Simpson's rule for the integrals. The finite difference equations for the three cases are given below. The discretisation of the loop is shown in Figure-3.3.

3.7.1 Uniform heating case:

Let k , l and n represent the no. of nodes in horizontal direction, no. of nodes in vertical direction and total no. of nodes respectively. Source is nodalised from 1 to k ; hot segment from node $(k+1)$ to $(k+l-2)$; sink from node $(k+l-1)$ to $(2k+l-2)$ and cold segment from $(2k+l-1)$ to $n = (2k+2l-4)$.

Now, taking eq.(3.4.1) and discretising as said above, we get,

$$1/F \frac{Q^{t+1} - Q^t}{\Delta t} = \frac{GA_s}{3} \sum_{i=k}^{k+l-4} a_i T_i^{t+1} - \sum_{i=2k+l-2}^n [a_i T_i^{t+1} - a_{i-1} T_{i-1}^{t+1}] - Q^{t+1}$$

$$\frac{1}{2(1+B)} \frac{T_i^{t+1} - T_i^t}{\Delta t} + Q^{t+1} \frac{T_i^{t+1} - T_{i-1}^{t+1}}{\Delta s} = M, \quad i=2 \text{ to } k$$

$$= 0, \quad i=k+1 \text{ to } k+l-1$$

$$= -MT_{i-1}^{t+1}, \quad i=k+1 \text{ to } 2k+l-2$$

$$= 0, \quad i=2k+l-1 \text{ to } n$$

$$\frac{1}{2(1+B)} \frac{T_1^{t+1} - T_1^t}{\Delta t} + Q^{t+1} \frac{T_1^{t+1} - T_n^{t+1}}{\Delta s} = 0, \quad i=1$$

$$\text{Thus } Q^{t+1} = \frac{Q^t + \frac{FGA_s \Delta t}{3} \left[\sum_{i=k}^{k+l-4} a_i T_i^{t+1} - \sum_{i=2k+l-2}^n a_i T_i^{t+1} - a_{i-1} T_{i-1}^{t+1} \right]}{1 + F \Delta t Q^{t+1}} \quad (3.7.1.1)$$

$$T_i^{t+1} \left[1 + \frac{2(1+B) \Delta t Q^{t+1}}{\Delta s} \right] - \frac{2(1+B) \Delta t Q^{t+1}}{\Delta s} T_{i-1}^{t+1}$$

$$= T_i^t + 2(1+B)M \Delta t, \quad i=2 \text{ to } k \quad (3.7.1.2.b)$$

$$= T_i^t, \quad i=k+1 \text{ to } k+l-1 \quad (3.7.1.2.c)$$

$$, \quad i=2k+l-1 \text{ to } n \quad (3.7.1.2.e)$$

$$T_i^{t+1} \left[1 + \frac{2(1+B) \Delta t}{\Delta s} Q^{t+1} + 2(1+B)M \Delta t \right] - T_{i-1}^{t+1} \frac{2(1+B) \Delta t Q^{t+1}}{\Delta s}$$

$$= T_i^t, \quad i=k+1 \text{ to } 2k+l-2 \quad (3.7.1.2.d)$$

$$T_i^{t+1} \left[1 + \frac{2(1+B) \Delta t Q^{t+1}}{\Delta s} \right] - \frac{2(1+B) \Delta t Q^{t+1}}{\Delta s} T_n^{t+1}$$

$$= T_i^t + 2(1+B)M\Delta t, i=1 \dots (3.7.1.2.a)$$

where $a_i = 1$ for $i=1, k, k+1-1, 2k+1-2$
 $= 4$ for odd $k-i$ and $2k+1-2-i$
 $= 2$ for even $k-i$ and $2k+1-2-i$

3.7.2 Triangular heating case:

The finite difference equations are exactly same as in (3.7.1) except at the source portion. Hence in place of (3.7.1.1), a new set is obtained from (3.5.2.1). The finite difference form for source portion gives,

$$\frac{1}{2(1+B)} \frac{T_i^{t+1} - T_i^t}{\Delta t} + Q_i^{t+1} \frac{T_i^{t+1} - T_{i-1}^{t+1}}{\Delta s} = \frac{2M}{B} (i-1)\Delta s, i=2 \text{ to } (k+1)/2$$

$$= -\frac{2M}{B} [(i-1)\Delta s - B], i=(k+3)/2 \text{ to } k$$

Thus eq.(3.7.1.2.b) is replaced by

$$T_i^{t+1} \left[1 + \frac{2(1+B)\Delta t}{\Delta s} Q_i^{t+1} \right] - \frac{2(1+B)\Delta t}{\Delta s} Q_i^{t+1} T_{i-1}^{t+1}$$

$$= T_i^t + \frac{4M(1+B)\Delta t}{B} (i-1)\Delta s, i=2 \text{ to } (k+1)/2 \quad (3.7.1.2.b1)$$

$$= T_i^t - \frac{4M(1+B)\Delta t}{B} [(i-1)\Delta s - B], i=(k+3)/2 \text{ to } k \quad (3.7.1.2.b2)$$

3.7.3 Sinusoidal heating case:

The finite difference equations are exactly same as in (3.7.1) except at the source portion. So in place of (3.7.1.2.b), a new equation is framed up from (3.5.3.1).

$$\frac{1}{2(1+B)} \frac{T_i^{t+1} - T_i^t}{\Delta t} + Q_i^{t+1} \frac{T_i^{t+1} - T_{i-1}^{t+1}}{\Delta s} = M \sin \frac{\pi(i-1)\Delta s}{B}, i=2 \text{ to } k$$

Thus eq.(3.7.1.2.b) is replaced by

$$T_i^{t+1} \left[1 + \frac{2(1+B)\Delta t}{\Delta s} Q_i^{t+1} \right] - \frac{2(1+B)\Delta t}{\Delta s} Q_i^{t+1} T_{i-1}^{t+1}$$

$$= T_i^t + 2(1+B)M\Delta t \sin \frac{(i-1)\pi\Delta s}{B}, i=2 \text{ to } k \quad (3.7.3.2.b)$$

3.8 Solution of finite difference eq.s:

The finite difference equation set represent a coupled non-linear equation set in Q^{t+1} and T^{t+1} . To solve them, first energy equation is solved for T_i^{t+1} knowing T_i^t . Then the value of

T_i^{t+1} are substituted in momentum equation to find Q^{t+1} where Q^t is known.

The energy equation set except for $i=1$ represent a bidiagonal matrix with subdiagonal and diagonal elements. Initially to make the system linear, $Q^{t+1} = Q^t$ and $T_i^{t+1} = T_i^t$. Knowing Q^{t+1} , T_i^{t+1} we find T_i^{t+1} for $i=2,3,\dots,n$. After knowing T_n^{t+1} , T_i^{t+1} is found from the energy equation with $i=1$.

Now after getting all the T_i 's at $(t+1)$, we solve the momentum equation for Q^{t+1} . The guessed values of Q^{t+1} and T_i^{t+1} are compared with the fresh values for convergence within the required tolerance. The process is repeated till we get the converged solution for $(t+1)$ th time step.

Marching in the time direction is done till the steady state values are obtained, i.e., the error between the values of Q and T at two consecutive time steps agree within prescribed tolerance.

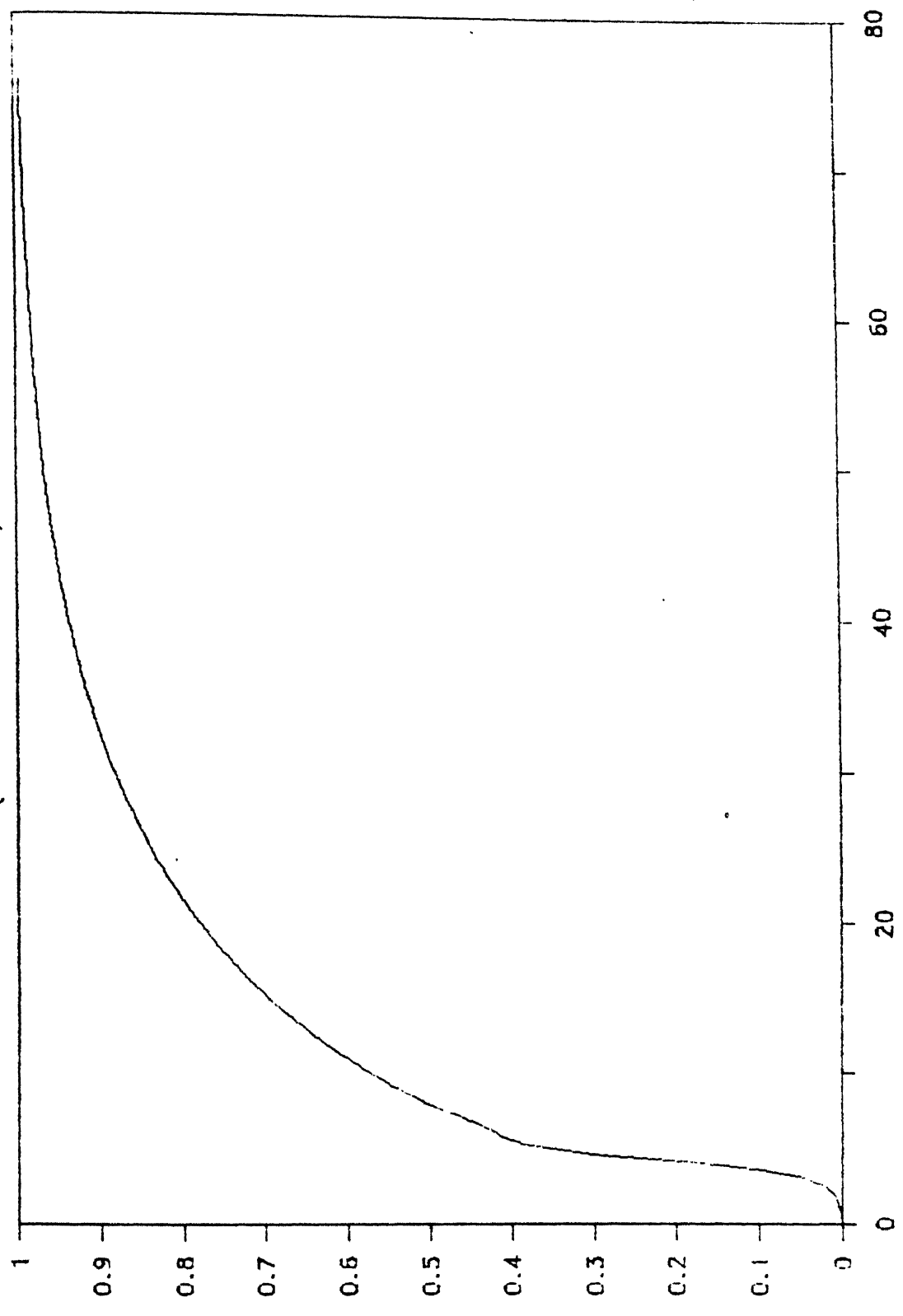
3.9 Results and Discussions

The results are shown in Graphs 3.1 to 3.18 as the plots of flow rate vs. time ; temperature distribution at different times in the loop ; source temperature, hot segment temperature, sink temperature and cold segment temperature vs. time for each of the heating cases. The flow rate curves show almost monotonous increase till steady state. The temperature vs. time curves show some initial oscillations before finally coming to a steady state. Initially, when there is no flow, introduction of uniform source results in uniform rise in temperature in the source portion and triangular and sinusoidal sources result in temperature being higher at middle and lower at ends for source portion. For this initial period, conduction is the mode of heat transfer. As time advances, due to buoyancy, flow is established. Now, relatively cold fluid enters the source and hence the temperature in the source portion decreases. To explain the attainment of steady state, let us consider a hot packet of fluid emerging from the source and a cold packet of fluid from the sink. At initial time, when flow rate is low, the hot packet passing through the sink suffers larger temperature loss whereas the cold packet passing through source gains larger temperature. Now when the hot packet again comes to enter the source and the cold packet

to the sink, flow rate has increased. This results in less temperature gain for the hot packet and less temperature loss for the cold packet. The cycle repeats till steady state is achieved. As can be seen from the results, the initial non-uniformity in the source portion in triangular and sinusoidal source cases gradually vanishes as natural convection is established. The temperature of the fluid increases from entry to exit in source portion. Similar explanation can be given for the other portions.

FLOW RATE VS. TIME

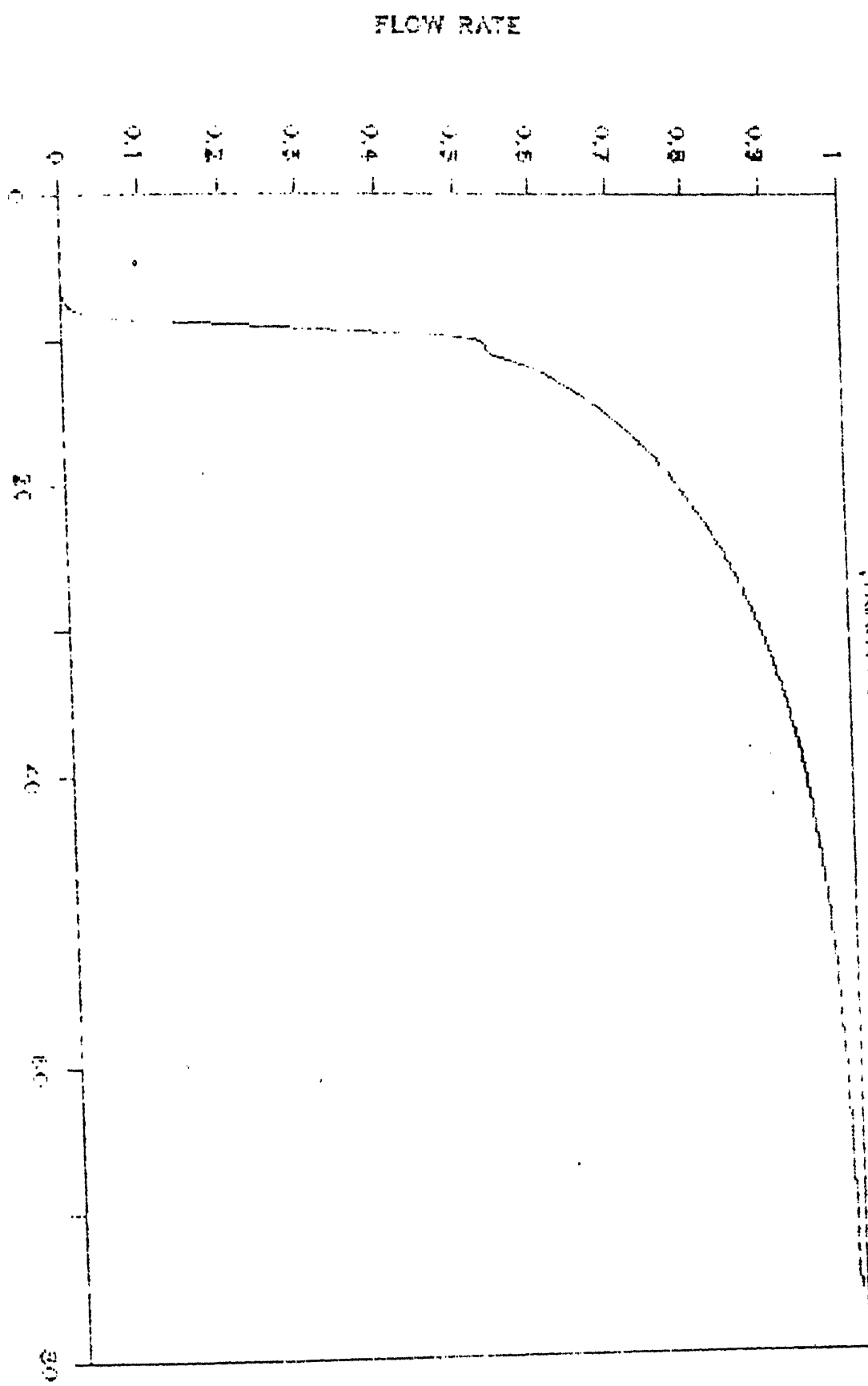
(UNIFORM HEAT FLUX)



FLOW RATE

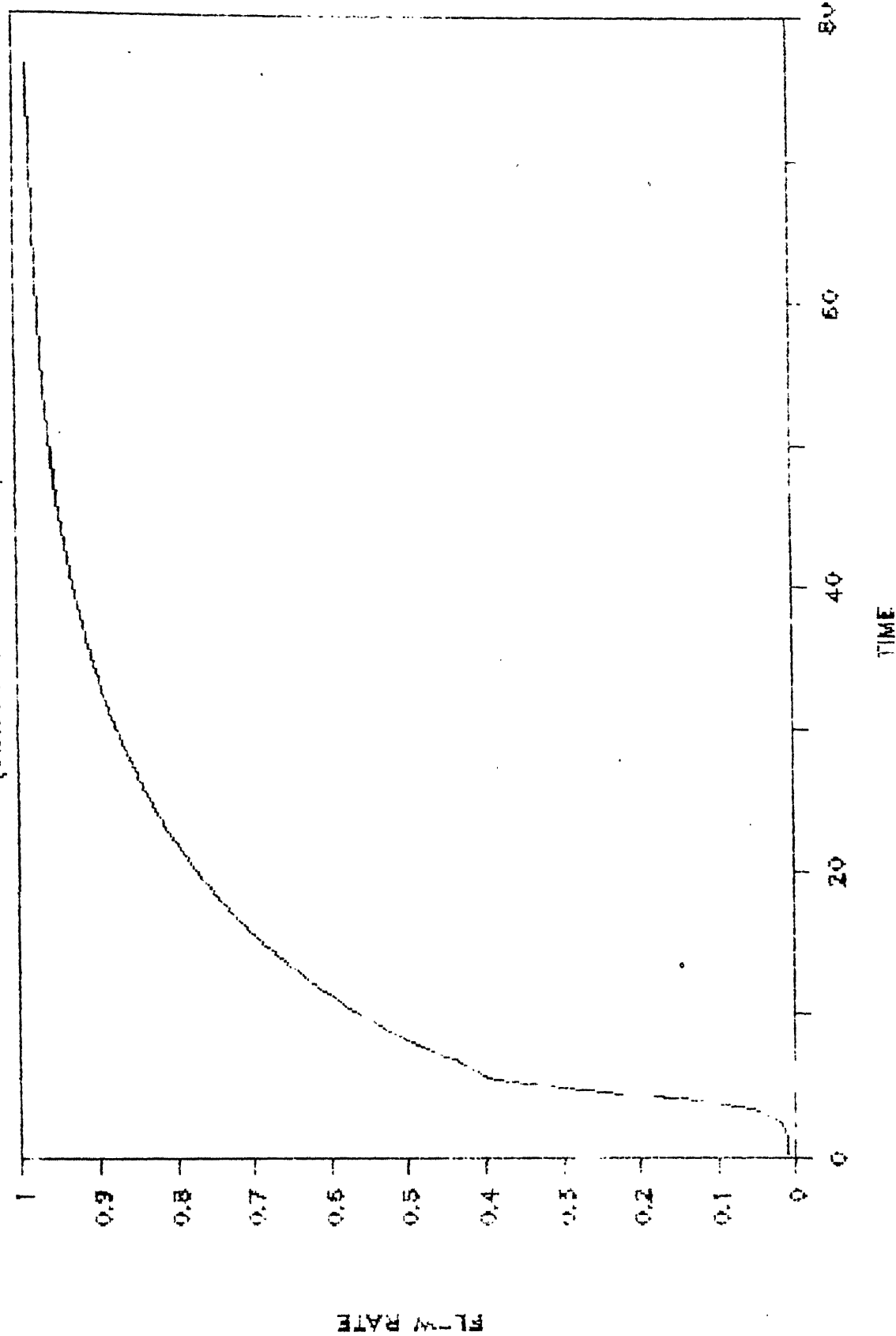
FLOW RATE VS. TIME

(TRIANGULAR HEAT FLUX)



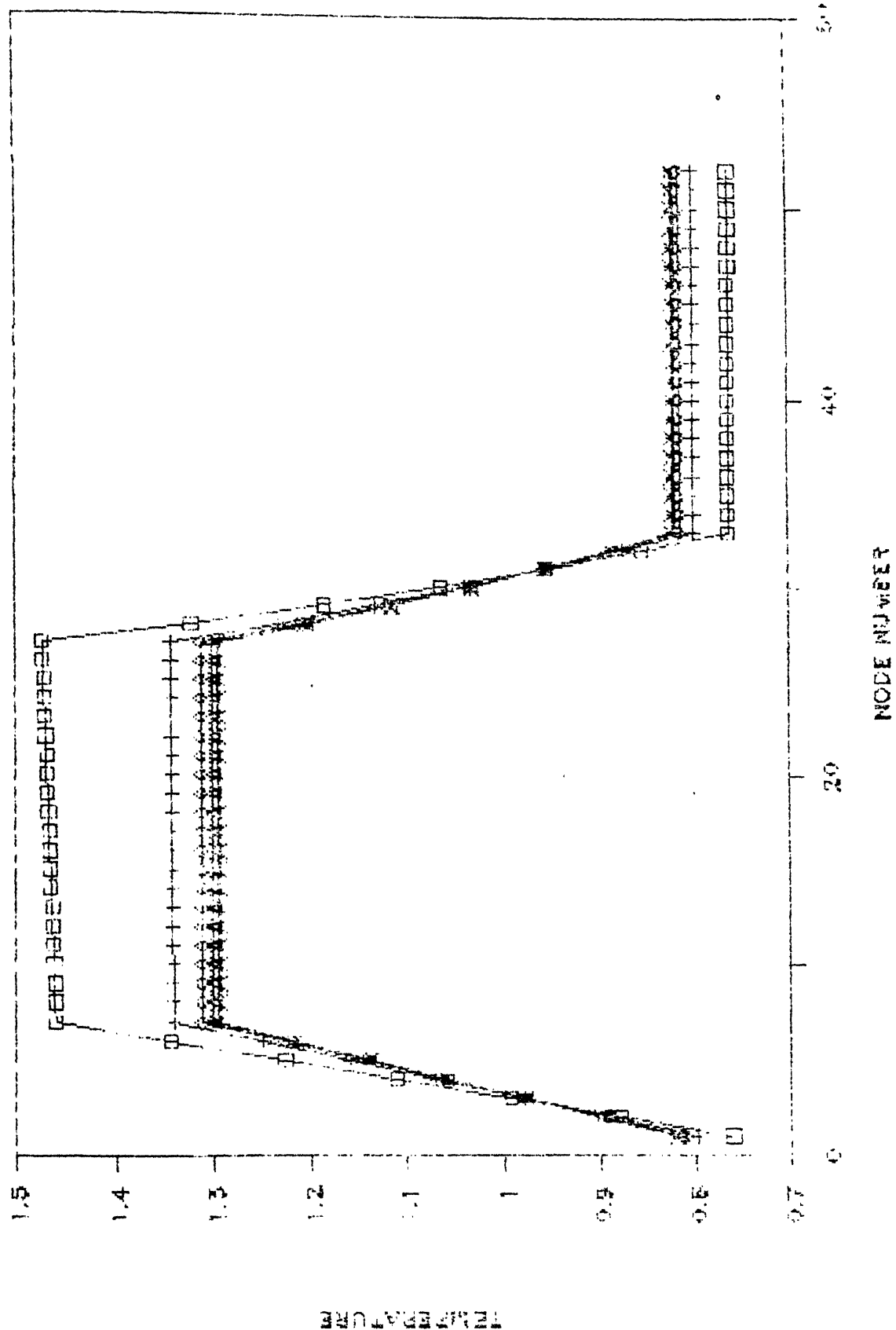
GRAPH 3.2

FLOW RATE V.S. TIME
(RESIDUAL HEAT FLUX)



GRADH. K. Z.

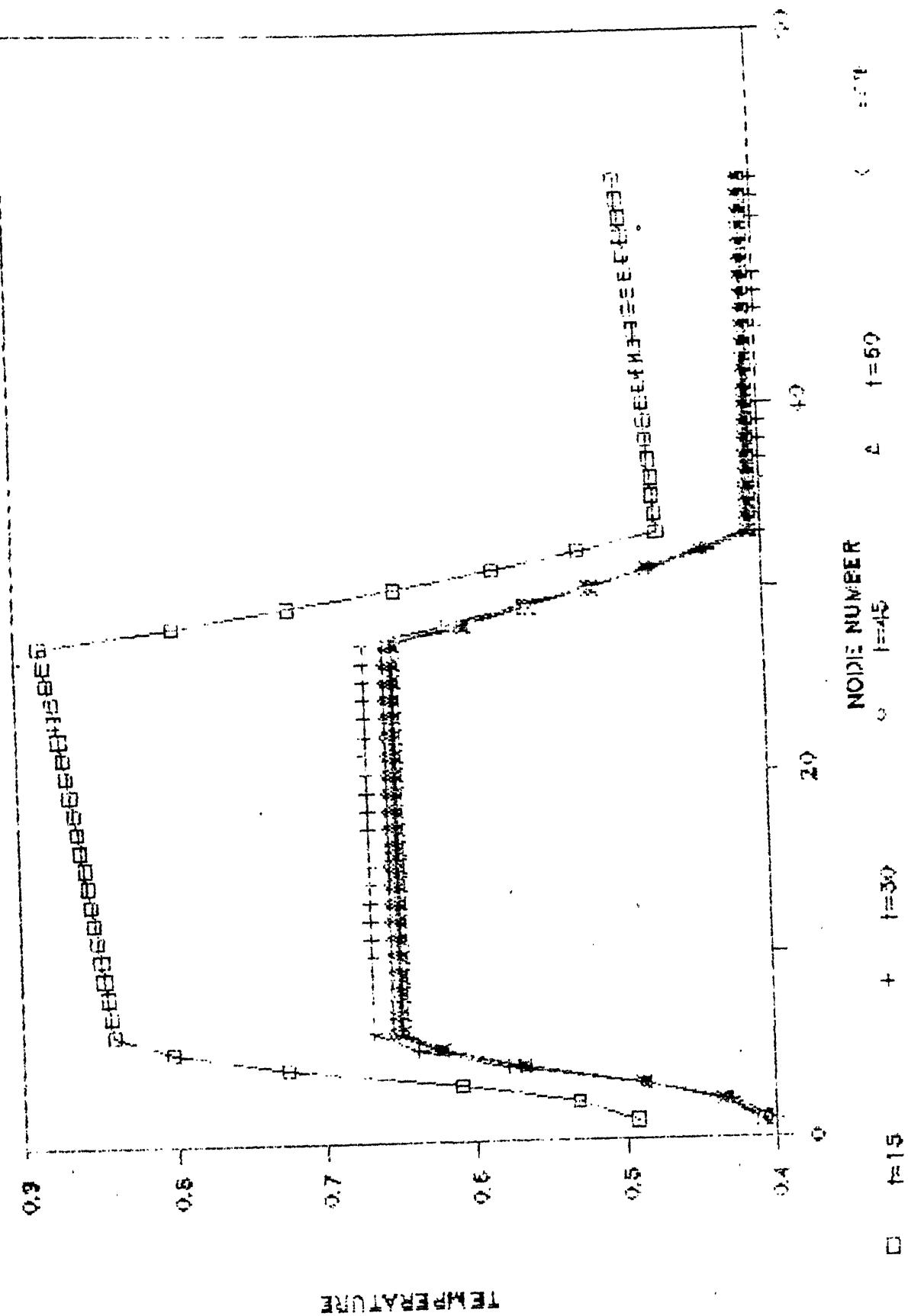
TEMPERATURE-DIST. AT DIFF. TIMES



GRAPH 3.4

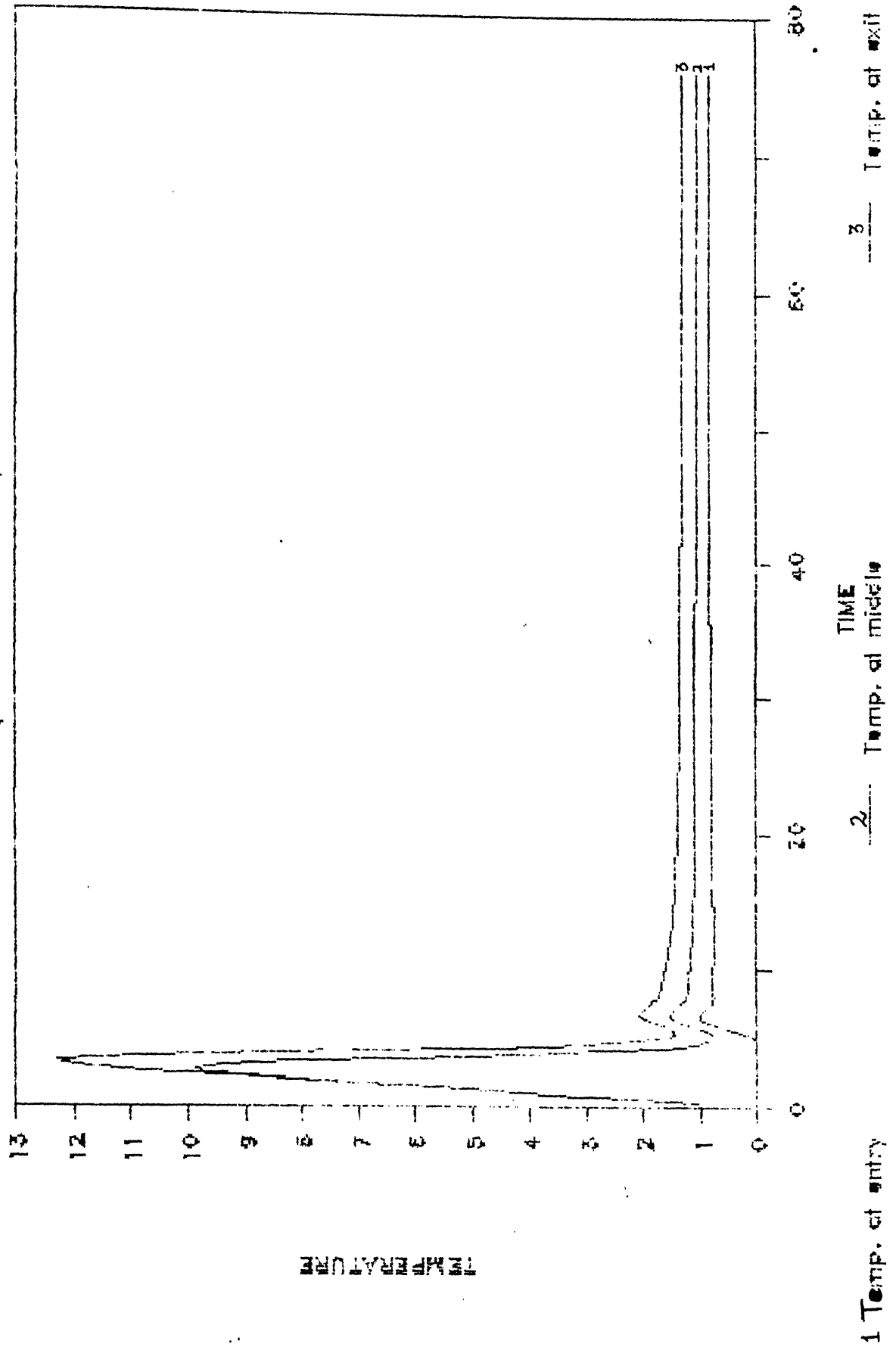
TEMPERATURE DIST. AT DIFF. TIMES

TRIANGULAR HEAT FLUX



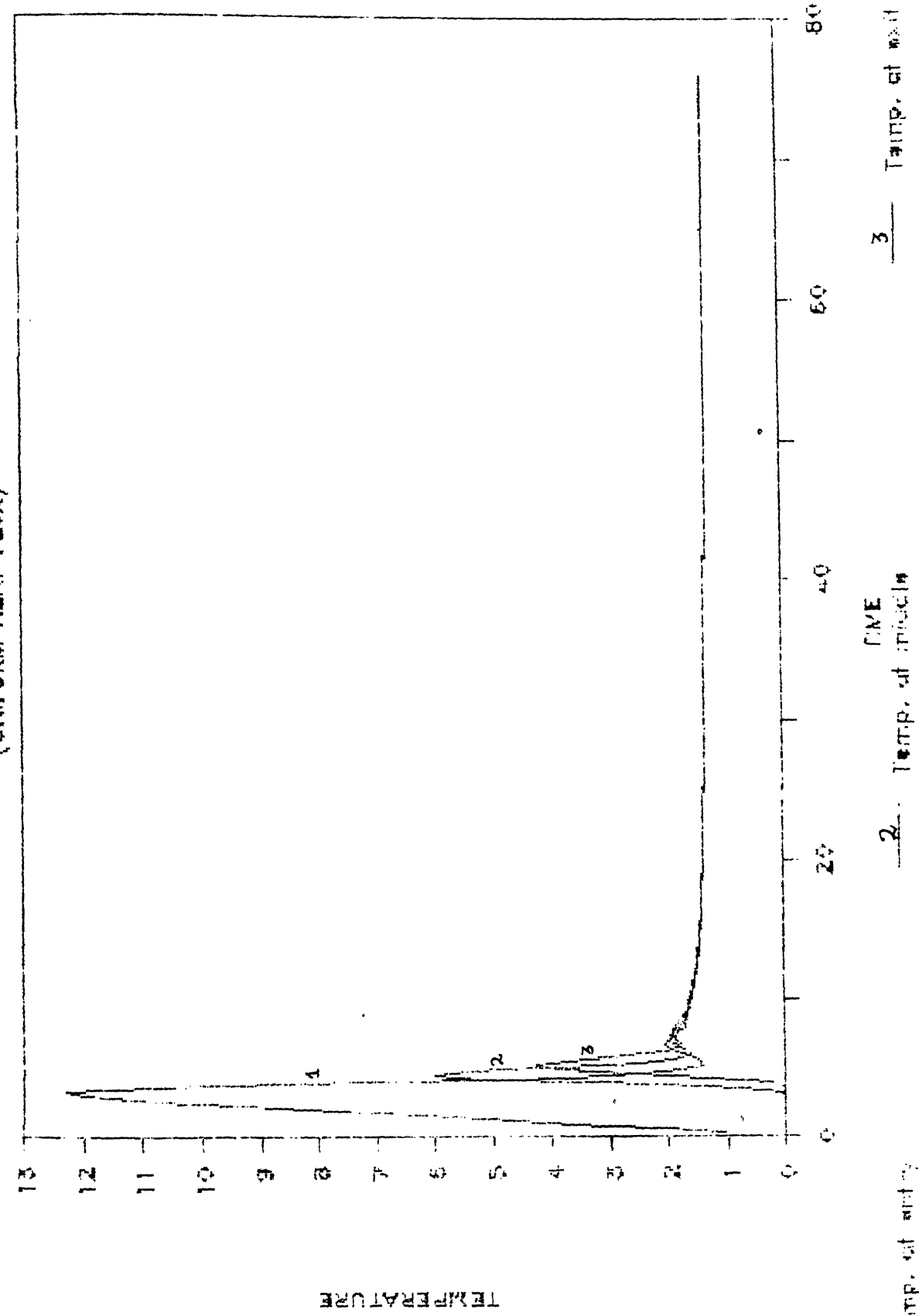
GRADIAZ.

SOURCE TEMPERATURE VS. TIME
(UNIFORM HEAT FLUX)



GRAPH 3.7

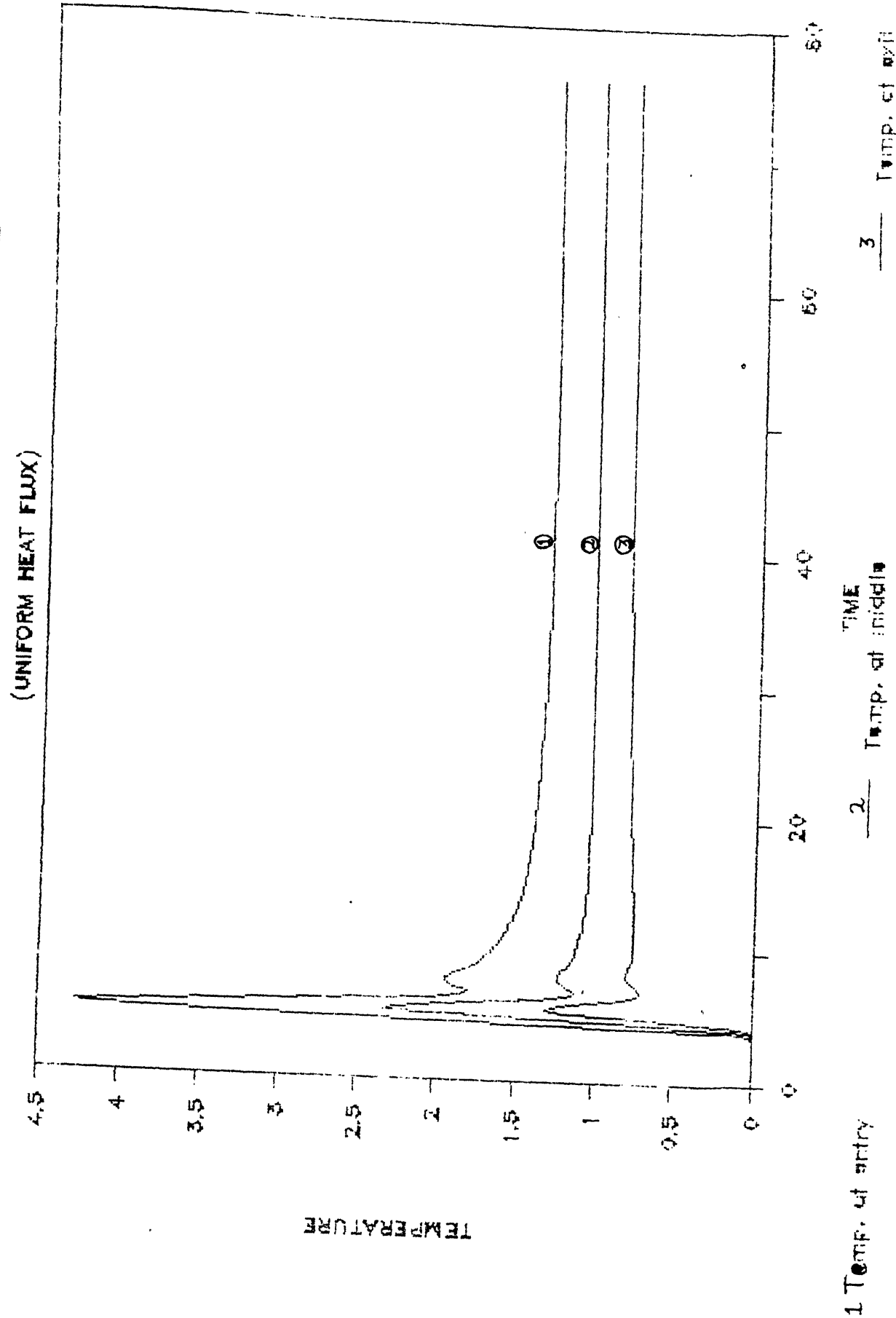
HOT SEGMENT TEMPERATURE VS. TIME (UNIFORM HEAT FLUX)



GRAPH 3.8

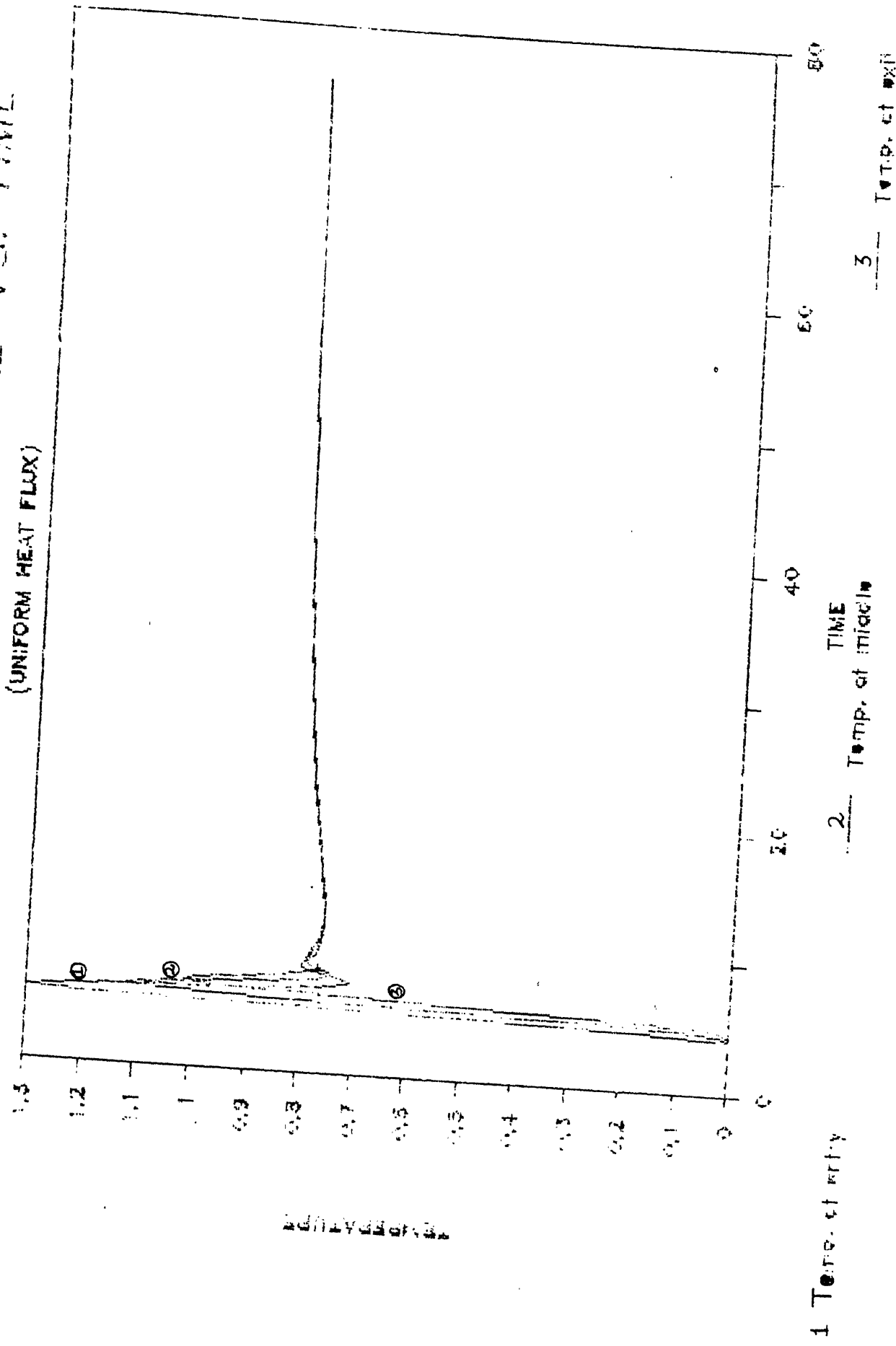
SINK TEMPERATURE VS. TIME

(UNIFORM HEAT FLUX)



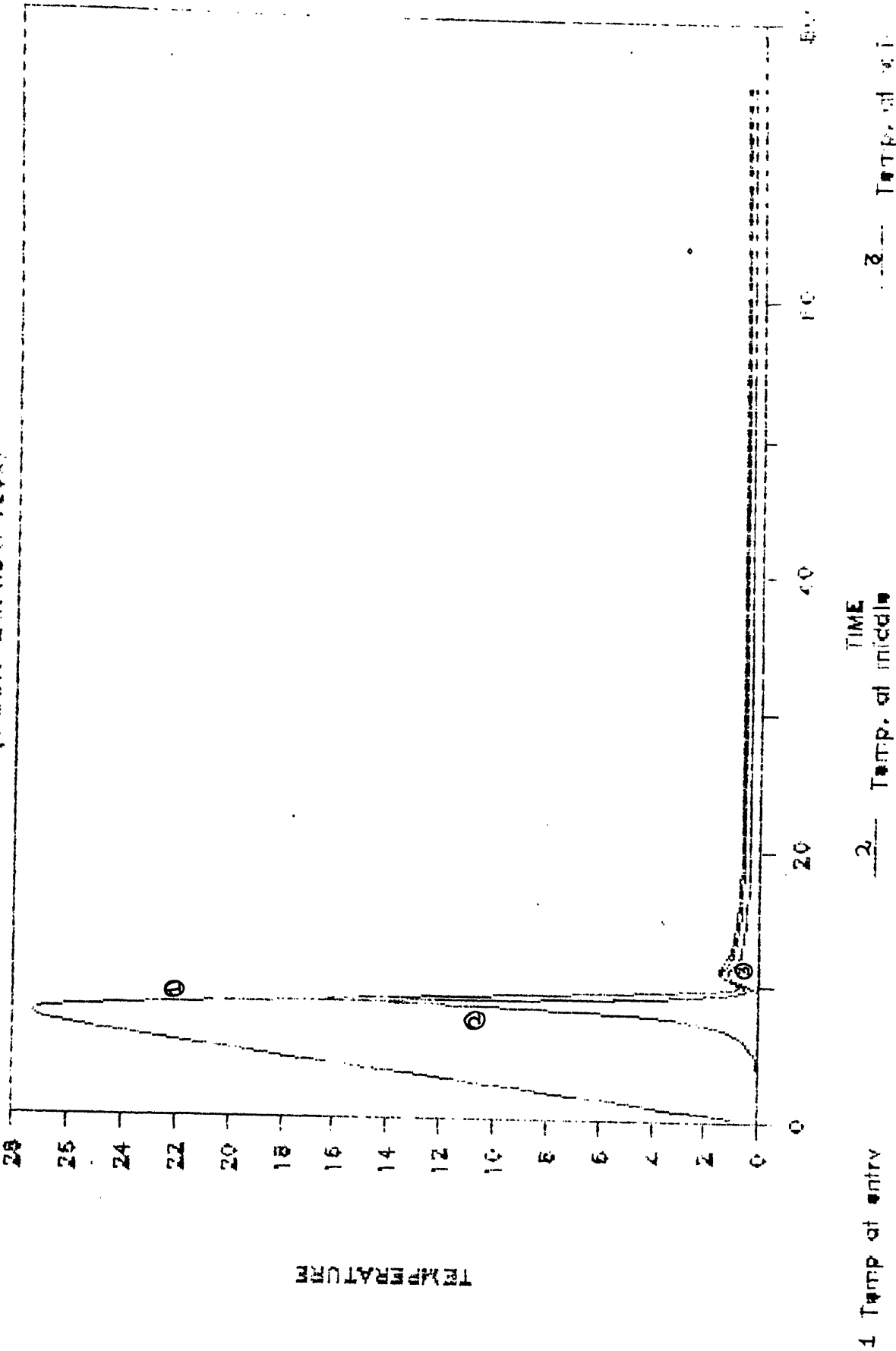
GRAPH 3.9

3-D SEGMENT TEMPERATURE VS. TIME
(UNIFORM HEAT FLUX)



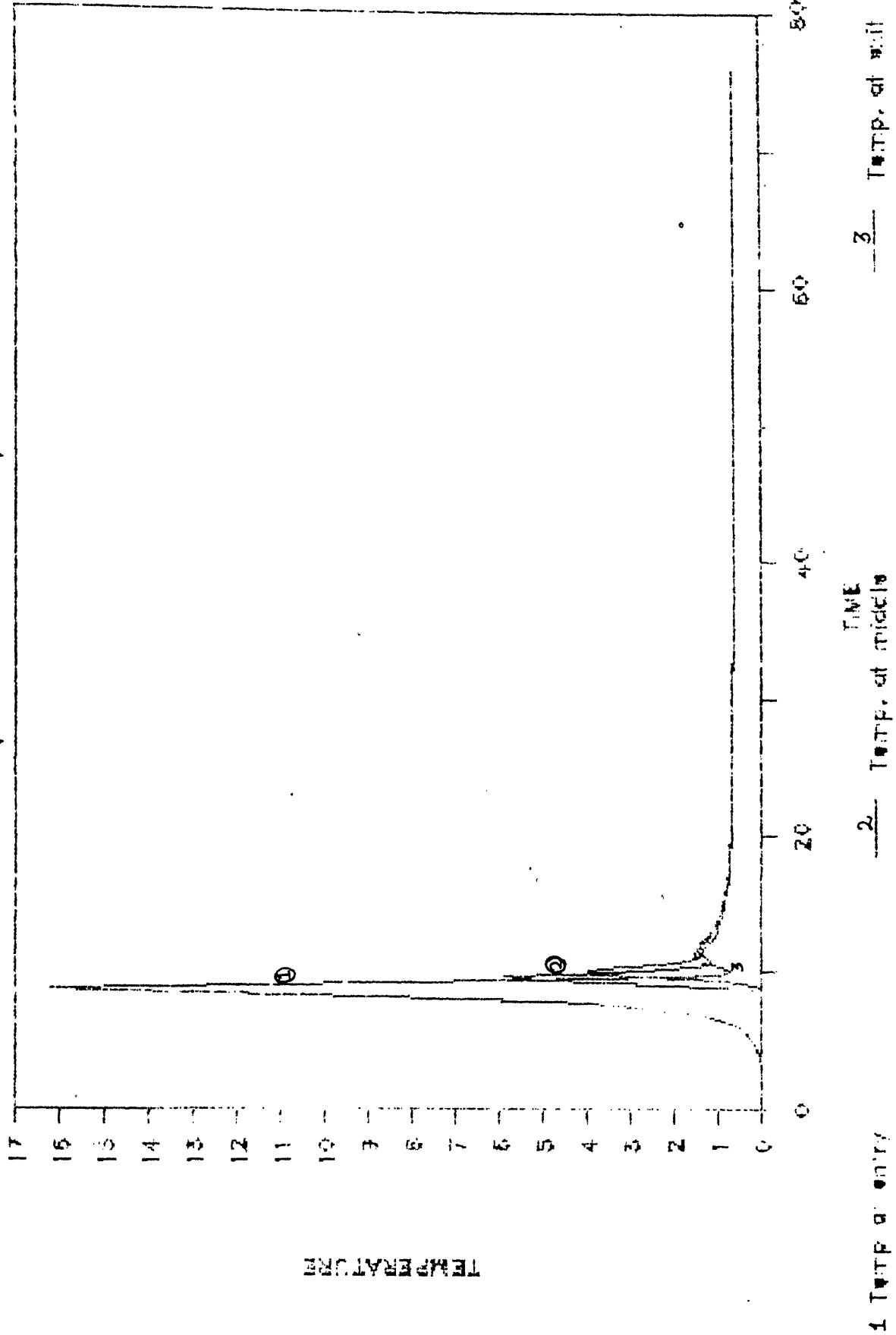
GRAPH 3.10

SOURCE TEMPERATURE VS. TIME
(TRIANGULAR HEAT FLUX)



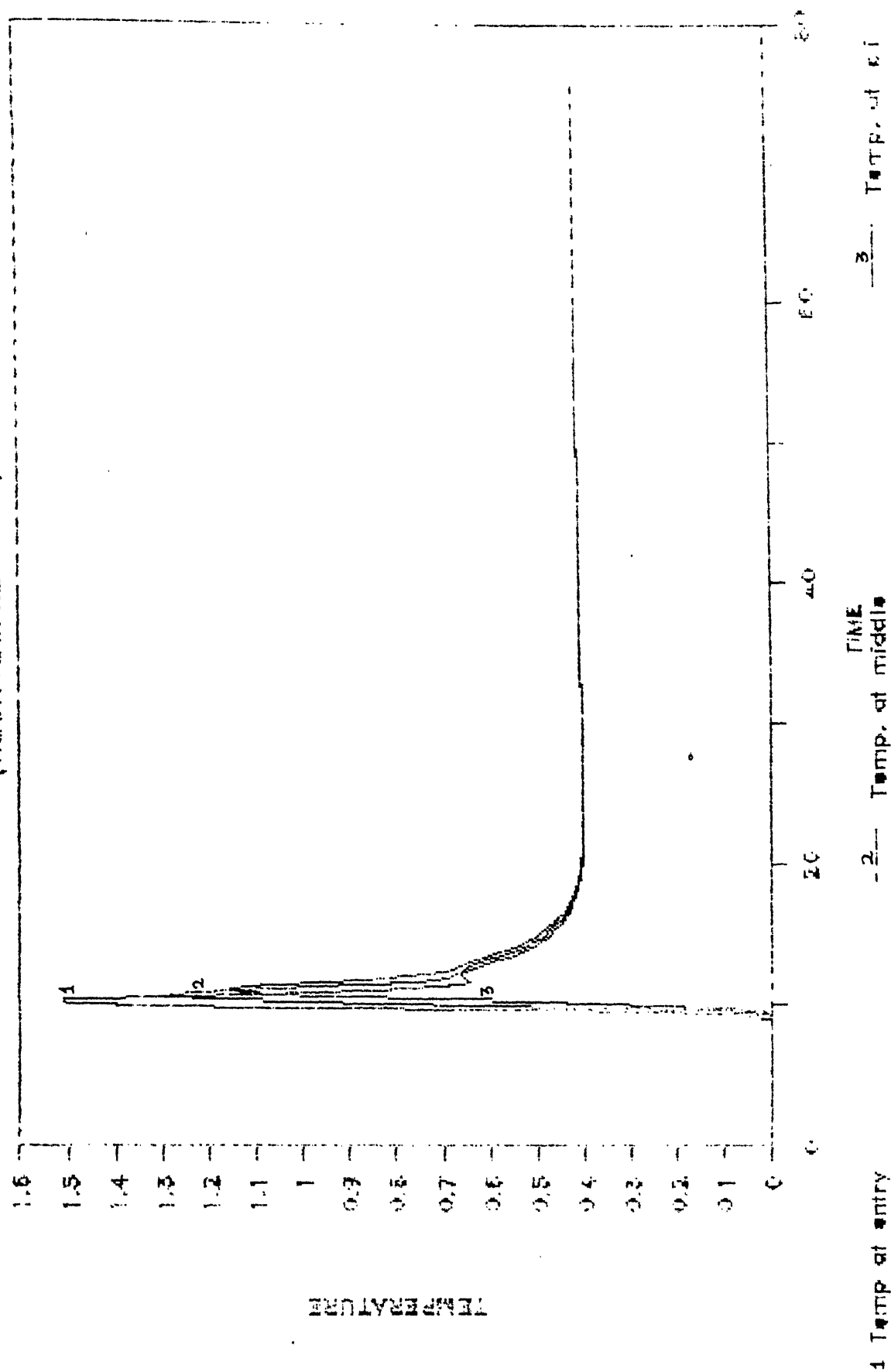
GRAPH 3-11

HOT SEGMENT TEMPERATURE VS. TIME
(TRIANGULAR HEAT FLUX)



COLD SEGMENT TEMPERATURE VS TIME

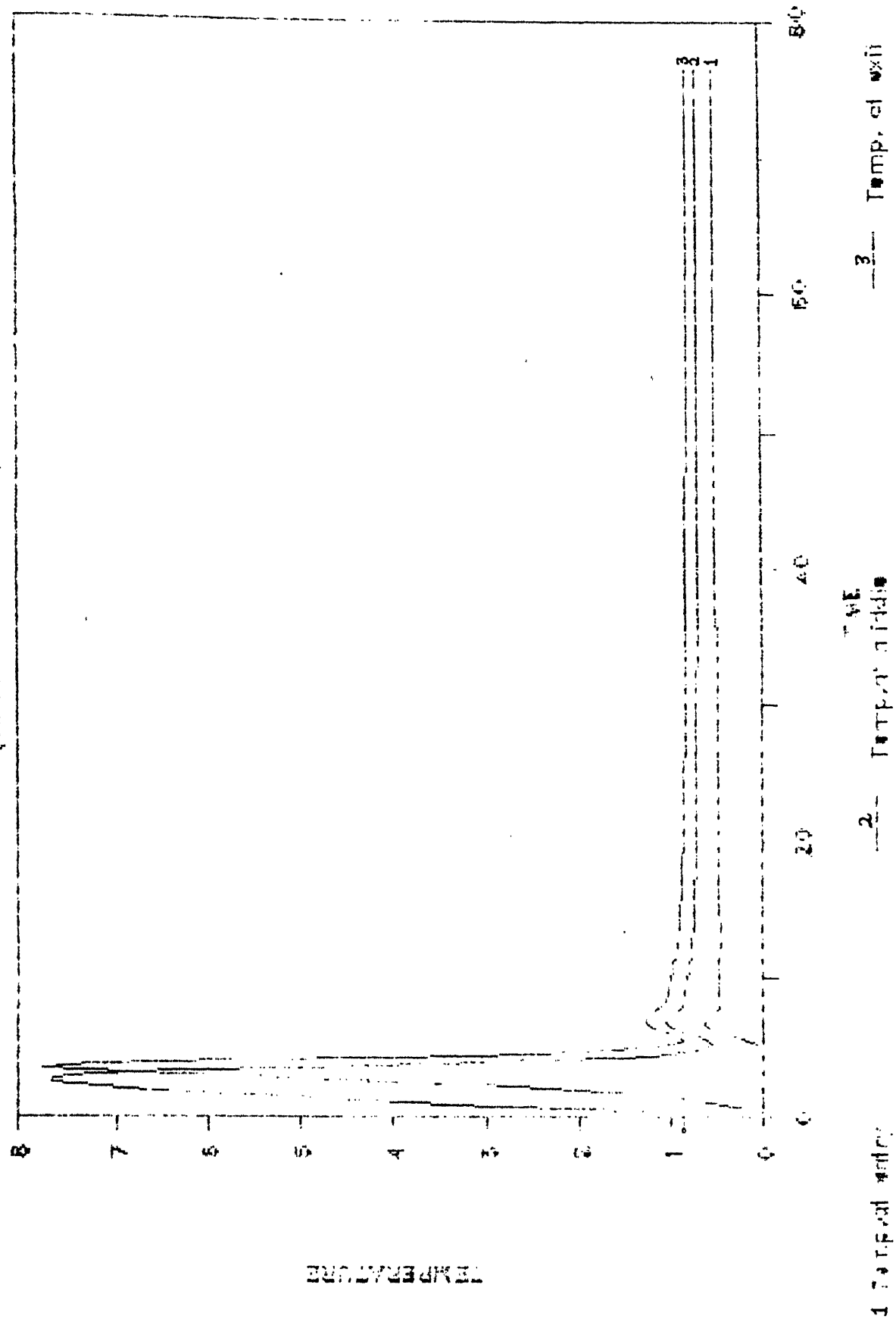
(TRIANGULAR HEAT FLUX)



GRAPH 3.14

SOURCE TEMPERATURE VS. TIME

(SINGULAR HEAT FLUX)



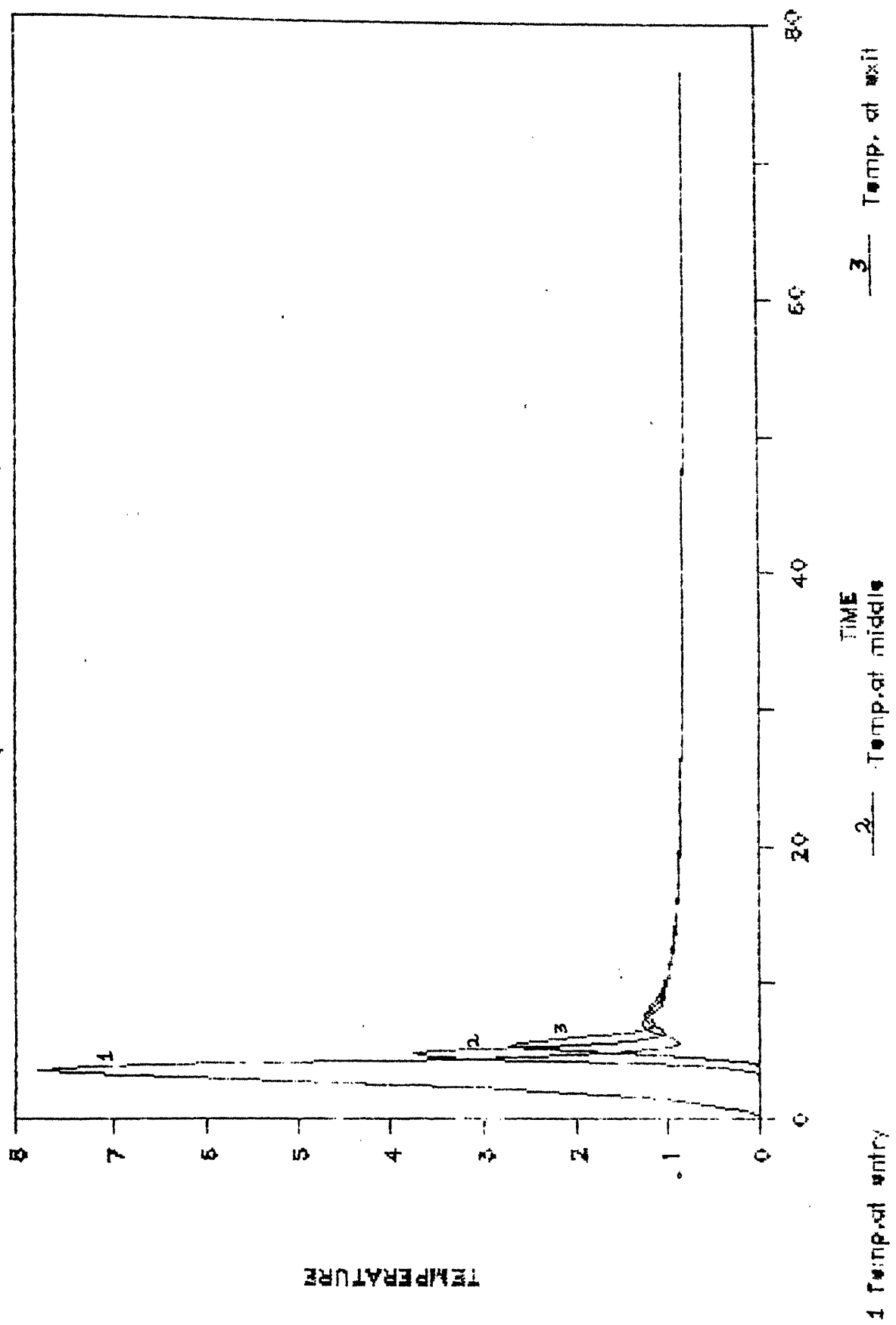
1 - Initial temp.

2 - Temp. at 400 K

3 - Temp. at 600 K

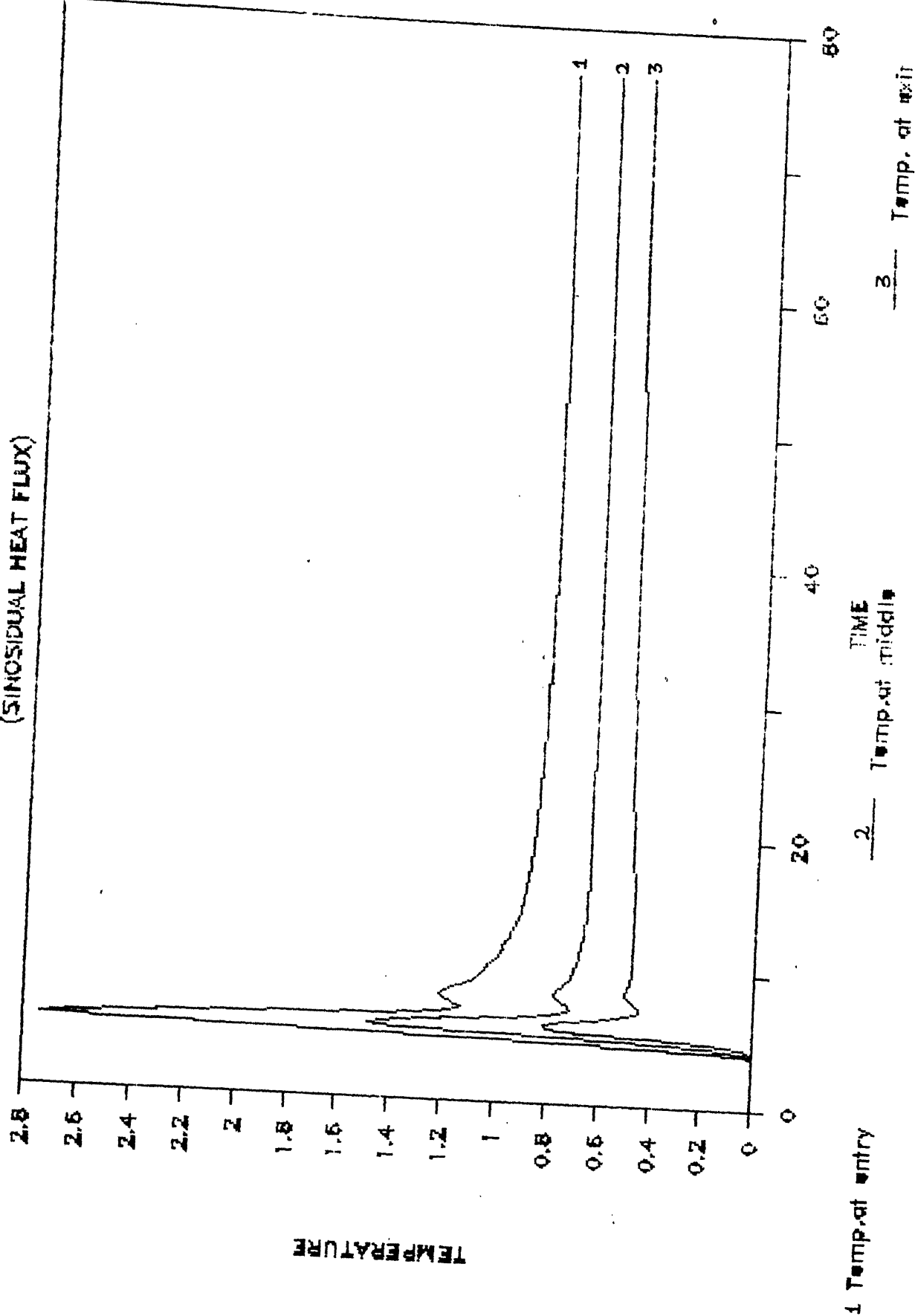
Conclusions

HOT SEGMENT TEMPERATURE VS. TIME
(SINOSIDUAL HEAT FLUX)



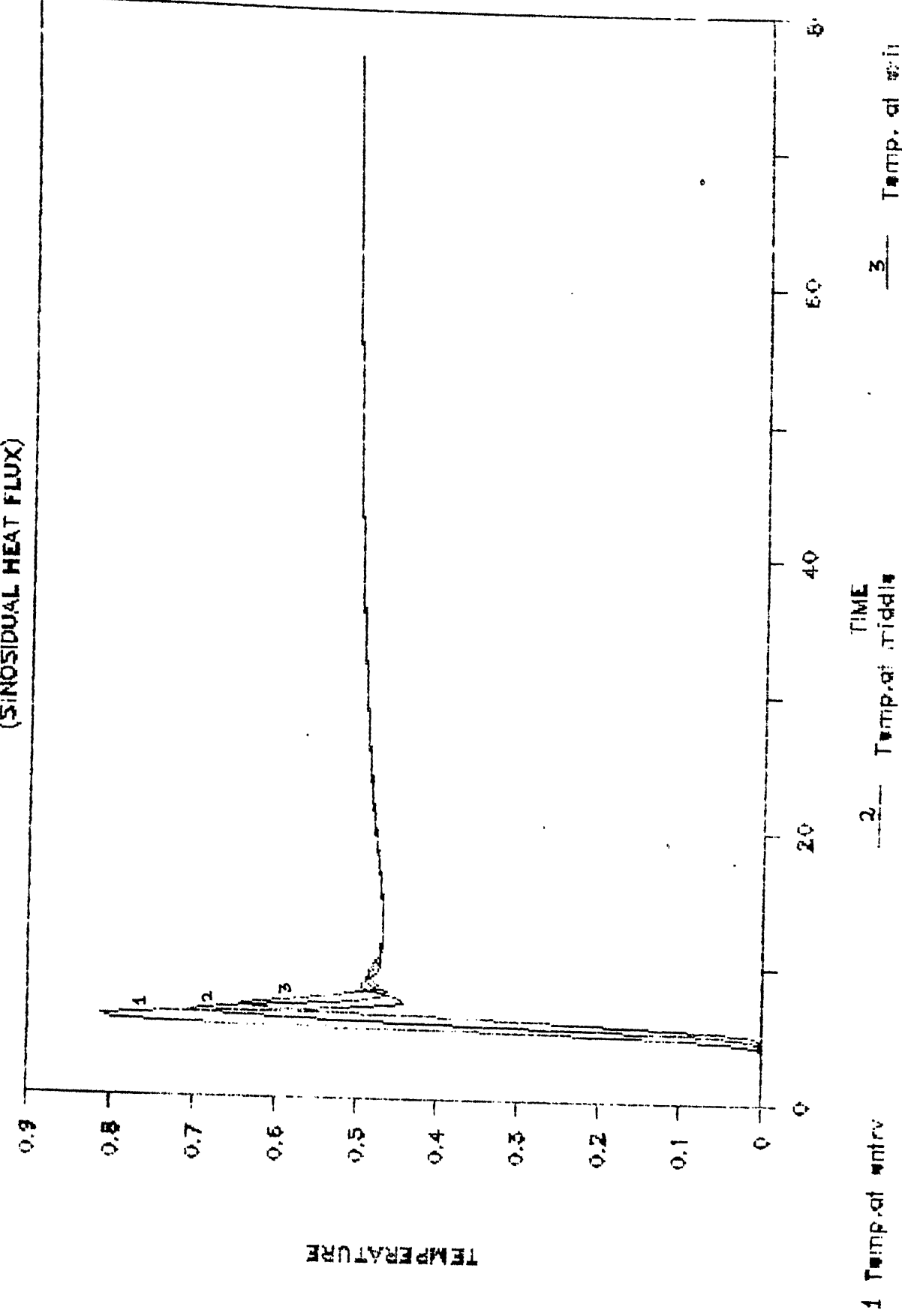
GOAOU 34c

SINK TEMPERATURE VS. TIME
(SINUSOIDAL HEAT FLUX)



GRAPH 3.12

COLD SEGMENT TEMPERATURE VS. TIME (SINUSOIDAL HEAT FLUX)



GRAPH 3.18

CHAPTER-4
MODELLING WITH HEAT EXCHANGER

4.1:Introduction

In the previous chapter, we have considered the rectangular thermosyphon with a constant temperature heat sink for simple analysis. In reality, the heat of the working fluid is transferred to a coolant in a heat exchanger. The heat exchanger may be a parallel flow heat exchanger where the working fluid and the coolant flow in the same direction or a counter flow one where the working fluid and the coolant flow in the opposite direction. The counter flow heat exchanger is an effective one for heat transfer. Here we consider the same case as the previous chapter with a counter flow heat exchanger as a heat sink. The analysis here has been done for the uniform heat flux case. However, this can be extended to the triangular and sinusoidal heat fluxes as well. The thermosyphon loop for analysis has been shown in Figure-4.1.

4.2:Formulation

Here as in the case of Chapter-3, continuity eq.(3.2.2), momentum eq.(3.2.3) and energy eq.(3.2.4) hold along with the boundary conditions (3.2.5). The only change here being T_c , temperature of coolant, in place of T_w , constant wall temperature in the sink portion of energy eq.(3.2.4) and in the initial condition (3.2.5). The coolant temperature T_c in the heat exchanger is not constant. It varies from the inlet to the outlet. Thus we have essentially two eq.s (3.2.3) and (3.2.4) with three variables Q, T and T_c . Thus we need another equation or to express T_c in terms of other two variables T, Q and some known parameters such as coolant inlet temperature T_{ci} , coolant flow rate Q_c .

To obtain the above reduction, we consider the sink portion, i.e., $(W+H)/2 < s < W+H/2$. Considering a section from s and $(s+ds)$ in this portion, we get,

$$\text{heat lost by working fluid} = -\rho Q C_p dT$$

$$\text{heat gained by coolant} = -m_c C_{pc} dT_c$$

$$\text{heat transferred} = h\pi d(T - T_c) ds$$

Equating all these quantities,

$$dQ = -\rho Q C_p dt = -m_c C_{pc} dT_c = h\pi d(T - T_c) ds$$

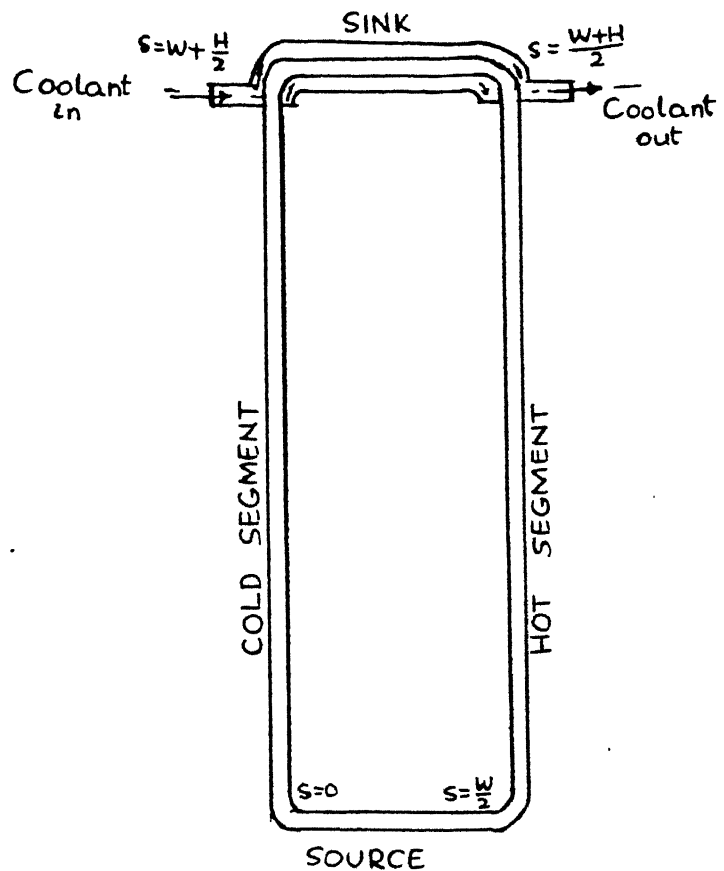


FIGURE 4.1 Rectangular thermosyphon
with heat exchanger as heat sink

$$\text{Now, } d(T-T_c) = dQ \left(-\frac{1}{\rho Q C_p} + \frac{1}{m_c C_{pc}} \right)$$

$$\frac{d(T-T_c)}{T-T_c} = h \pi d \left(-\frac{1}{\rho Q C_p} + \frac{1}{m_c C_{pc}} \right) ds$$

To find the constant C, we have the boundary condition at $s=W+H/2$, $T_c = T_{ci}$, $T = T_{s=W+H/2}$

$$\text{Thus, } C = (T_{s=W+H/2} - T_{ci}) \exp[-h \pi d (W+H/2) \left(-\frac{1}{\rho Q C_p} + \frac{1}{m_c C_{pc}} \right)]$$

Substituting this value of C, we get,

$$T-T_c = (T_{s=W+H/2} - T_{ci}) \exp[h \pi d \left(-\frac{1}{\rho Q C_p} + \frac{1}{m_c C_{pc}} \right) (s-W-H/2)] \quad (4.2.1)$$

Substitution of this equation in energy eq.(3.2.4) for sink portion gives

$$\rho_v C_p \left(\frac{\partial T}{\partial t} + Q \frac{\partial T}{\partial s} \right) = -\frac{4h}{d} (T_{s=W+H/2} - T_{ci}) \exp[h \pi d \left(-\frac{1}{\rho Q C_p} + \frac{1}{m_c C_{pc}} \right) (s-W-H/2)]$$

Now, we have eliminated the variable T_c by known parameters T_{ci} , m_c , C_{pc} and unknown parameters Q and T. Thus we have two equations (3.2.3) and (3.2.4) with two variables Q and T.

4.3: Non-dimensionalisation

The non-dimensionalisation is done as in section 3.4 of Chapter-3. The only difference here is the non-dimensionalisation of T as $T = \frac{T-T_{ci}}{q/h}$. Thus the non-dimensionalised equations are (3.4.1) except for the sink for which energy equation is

$$\frac{1}{2(1+B)} \frac{\partial T}{\partial t} + Q \frac{\partial T}{\partial s} = -MT_{s=1+2B} \exp[h \pi d H/2 \left(-\frac{1}{\rho C_p Q Q_{ch}} + \frac{1}{m_c C_{pc}} \right) (s-1-2B)]$$

$$1+B < s < 1+2B \quad (3.4.1)$$

4.3: Steady state solution

The steady state equations are obtained for each case by making the time derivative zero in the eq.(3.4.1). There exists analytical solution for this case which are given below.

The steady state equations derived from (3.4.1) are

$$G \left[\int_{B}^{1+B} \bar{T} ds - \int_{1+2B}^{2+2B} \bar{T} ds \right] = \bar{Q}^2 \quad (4.4.1)$$

$$\bar{Q} \frac{d\bar{T}}{ds} = M, \quad 0 < s < B$$

$$= 0, \quad B < s < 1+B$$

$$= -MT_{s=1+2B} \exp[h \pi d H/2 \left(-\frac{1}{\rho C_p Q Q_{ch}} + \frac{1}{m_c C_{pc}} \right) (s-1-2B)], \quad 1+B < s < 1+2B$$

$$=0, 1+2B < s < 2+2B$$

with continuity of \bar{T} along the loop.

This coupled equation set is solved by first solving (4.4.2) with \bar{Q} as parameter. After getting the steady temperature profile, (4.4.1) is solved for \bar{Q} and then substituted in the solution of (4.4.2).

Solution of (4.4.2) is given as

$$\bar{T}(s) = Ms/\bar{Q} + K_1, 0 < s < B$$

$$= K_2, B < s < 1+B$$

$$= K_3 - M/G \bar{T}_{s=1+2B} \frac{1}{h\pi dH/2E - \frac{1}{\rho C_p Q Q_{ch}} + \frac{1}{m_c C_{pc}}}$$

$$\exp [h\pi dH/2(-\frac{1}{\rho C_p Q Q_{ch}} + \frac{1}{m_c C_{pc}})(s-1-2B)], 1+B < s < 1+2B$$

$$= K_4, 1+2B < s < 2+2B \quad \text{--- (4.4.3)}$$

The constants are found from continuity condition of $T(s)$.

$$\text{At } s=B, K_2 = MB/\bar{Q} + K_1$$

$$s=1+B, K_2 = K_3 - M/\bar{Q} \bar{T}_{s=1+2B} \left[h\pi dH/2(-\frac{1}{\rho C_p Q Q_{ch}} + \frac{1}{m_c C_{pc}}) \right]^{-1}$$

$$\exp[-h\pi dH/2(-\frac{1}{\rho C_p Q Q_{ch}} + \frac{1}{m_c C_{pc}})] \quad \text{--- (4.4.4)}$$

$$s=1+2B, K_4 = K_3 - M/\bar{Q} \bar{T}_{s=1+2B} \left[h\pi dH/2(-\frac{1}{\rho C_p Q Q_{ch}} + \frac{1}{m_c C_{pc}}) \right]^{-1}$$

$$s=2+2B, K_4 = K_1$$

Now substitution of (4.4.3) in (4.4.1) gives

$$G(K_2 - K_4) = GMB/\bar{Q} \quad [\text{From (4.4.4)}] = \bar{Q}^2$$

$$\text{So, } \bar{Q} = (GMB)^{1/2}$$

Making substitutions (4.4.2) and (3.3.10), $\bar{Q}=1$ --- (4.4.5)

Solution of (4.4.4) set for K_1, K_2, K_3, K_4 and substitution of these constants in (4.5.3) give the steady state temperature distribution.

4.5: Finite difference formulation for transient analysis

For solving the transient equations, we use finite difference method. Explicit scheme has been used for the time derivative part and upwind scheme, here backward difference, is used for the space derivative part. The integro-differential equation is solved by using Simpson's rule for the integrals.

The finite difference equations are given below.

$$1/F \frac{Q^{t+1} - Q^t}{\Delta t} = \frac{G \Delta s}{3} \sum_{i=k}^{k+l-1} a_i T_i^t - \sum_{i=2k+l-2}^n a_i T_i^t - a_{i-1} T_{i-1}^t] - Q^t$$

$$\frac{1}{2(1+B)} \frac{T_i^{t+1} - T_i^t}{\Delta t} + Q^t \frac{T_i^t - T_{i-1}^t}{\Delta s} = M, \quad i=2 \text{ to } k$$

$$= 0, \quad i=k+1 \text{ to } k+l-1$$

$$= -M T_{2k+l-2} \exp[z(1-r/Q^t) \{(i-1)\Delta s - 1 - 2B\}]$$

$$i=k+1 \text{ to } 2k+l-2$$

$$\text{where } z = \frac{h \pi dH/2}{m_c C_p} \text{ and } r = \frac{m_c C_p}{\rho Q_{ch} C_p} = 0, \quad i=2k+l-1 \text{ to } n$$

$$\frac{1}{2(1+B)} \frac{T_i^{t+1} - T_i^t}{\Delta t} + Q^t \frac{T_i^t - T_{i-1}^t}{\Delta s} = 0, \quad i=1$$

$$\text{Thus, } Q^{t+1} = Q^t (1 - F \Delta t Q^t) + \frac{F G \Delta s \Delta t}{3} \sum_{i=k}^{k+l-1} a_i T_i^t - \sum_{i=2k+l-2}^n a_i T_i^t - a_{i-1} T_{i-1}^t \quad (4.5.1)$$

$$T_i^{t+1} = 2(1+B) \Delta t M + T_i^t \left[1 - \frac{2(1+B)Q^t \Delta t}{\Delta s} \right] + \frac{2(1+B)Q^t \Delta t}{\Delta s} T_{i-1}^t, \quad i=2 \text{ to } k \quad (4.5.2.b)$$

$$= T_i^t \left[1 - \frac{2(1+B)Q^t \Delta t}{\Delta s} \right] + \frac{2(1+B)Q^t \Delta t}{\Delta s} T_{i-1}^t, \quad i=k+1 \text{ to } k+l-1 \quad (4.5.2.c)$$

$$, \quad i=2k+l-1 \text{ to } n \quad (4.5.2.f)$$

$$= T_i^t \left[1 - \frac{2(1+B)\Delta t Q^t}{\Delta s} \right] + \frac{2(1+B)\Delta t Q^t}{\Delta s} T_{i-1}^t - 2(1+B)M \Delta t T_{2k+l-2}^t$$

$$\exp[z(1-r/Q^t) \{(i-1)\Delta s - 1 - 2B\}], \quad i=k+1 \text{ to } 2k+l-3 \quad (4.5.2.d)$$

$$= T_i^t \left[1 - \frac{2(1+B)\Delta t Q^t}{\Delta s} \right] - 2(1+B) \Delta t M \exp[z(1-r/Q^t) \{(i-1)\Delta s - 1 - 2B\}]$$

$$+ \frac{2(1+B)\Delta t Q^t}{\Delta s} T_{i-1}^t, \quad i=2k+l-2 \quad (4.5.2.e)$$

$$T_i^{t+1} = T_i^t \left[1 - \frac{2(1+B)\Delta t Q^t}{\Delta s} \right] + \frac{2(1+B)\Delta t Q^t}{\Delta s} T_n^t, \quad i=1 \quad (4.5.2.a)$$

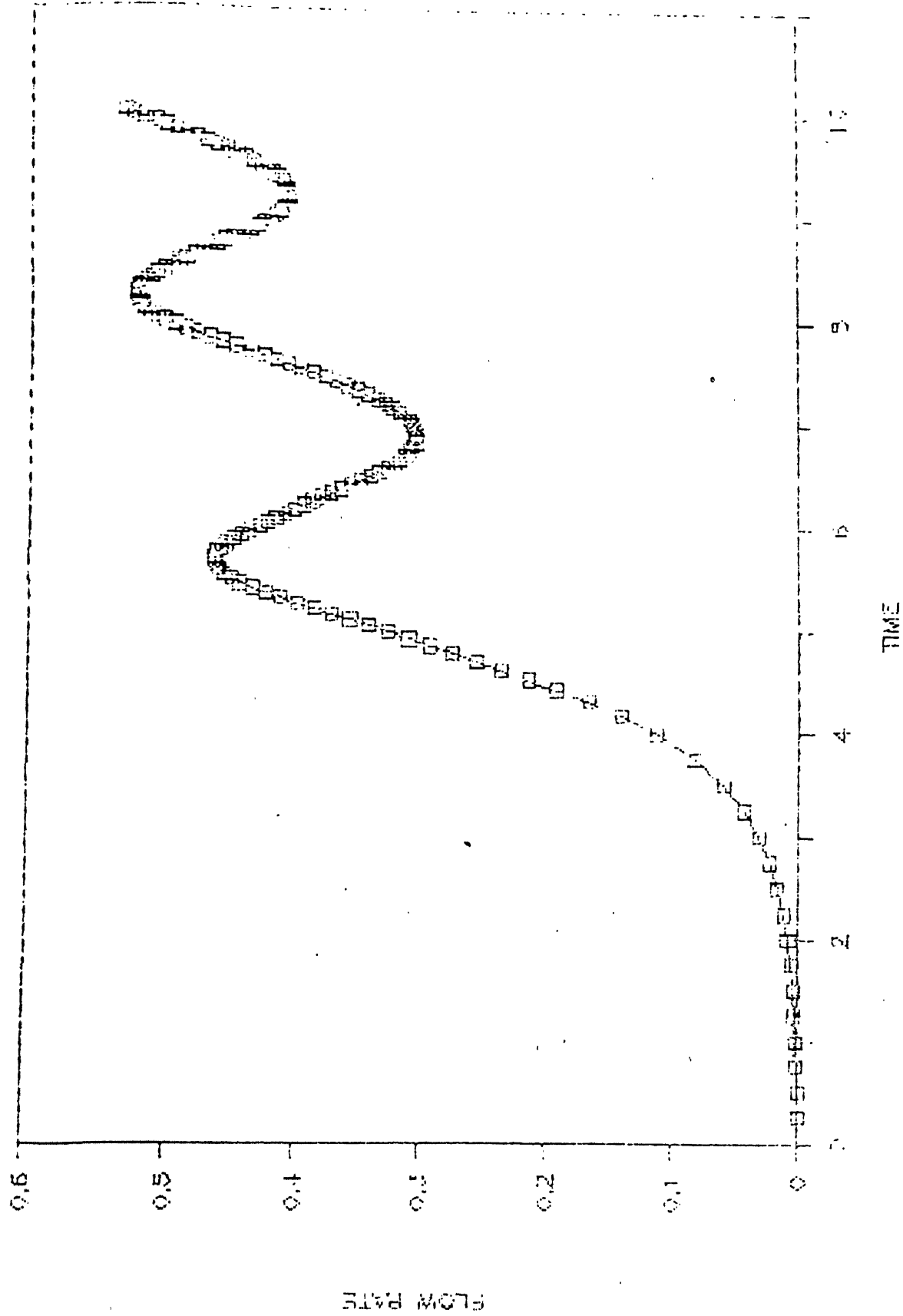
As explicit scheme is susceptible to instability, we choose the time interval at each step so as to satisfy the stability criterion given below.

$$1 - F \Delta t Q^t > 0$$

$$1 - \frac{2(1+B)\Delta t}{\Delta s} Q^t > 0$$

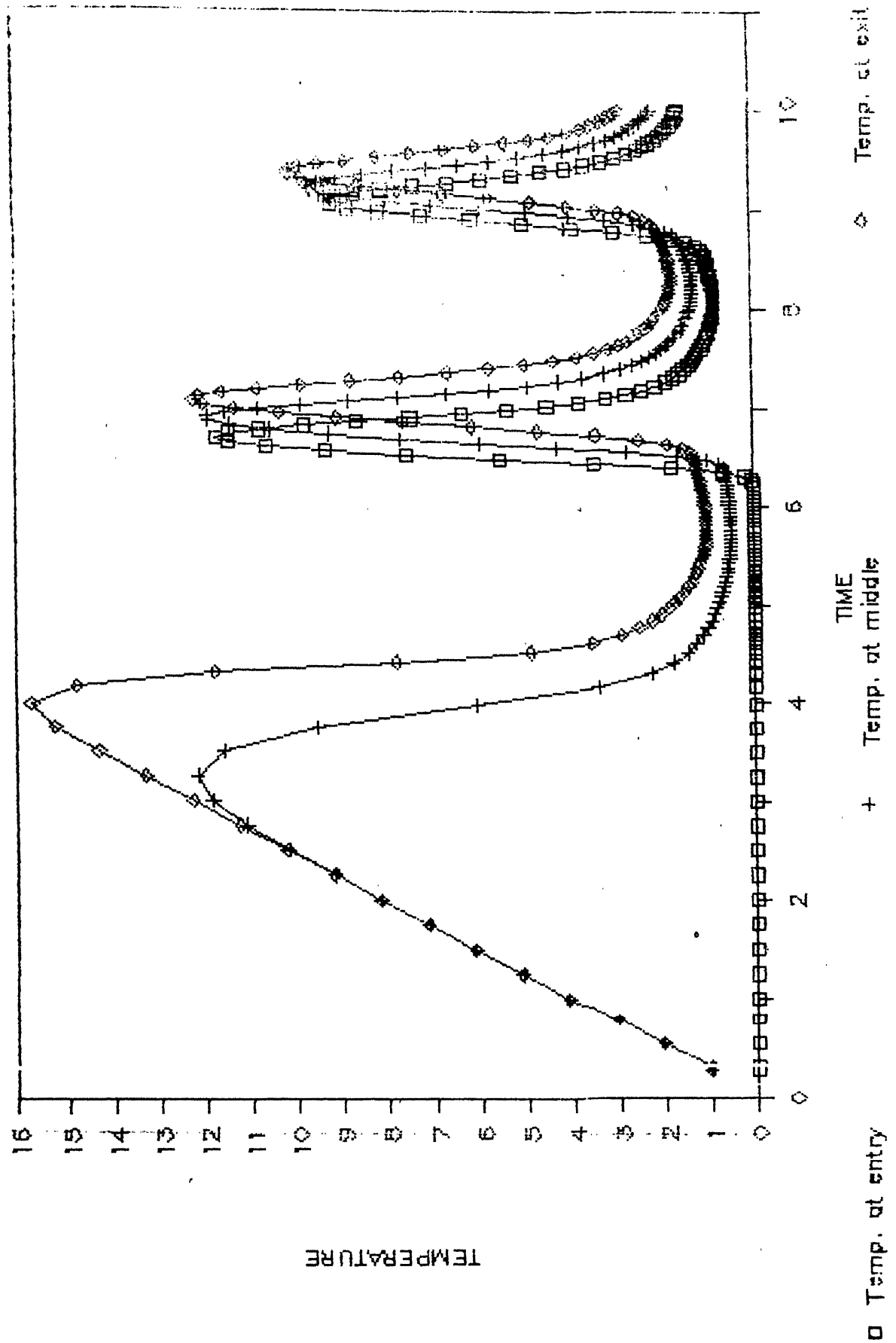
$$1 - \frac{2(1+B)\Delta t}{\Delta s} Q^t - 2(1+B)M \Delta t > 0$$

FLOW RATE VS. TIME



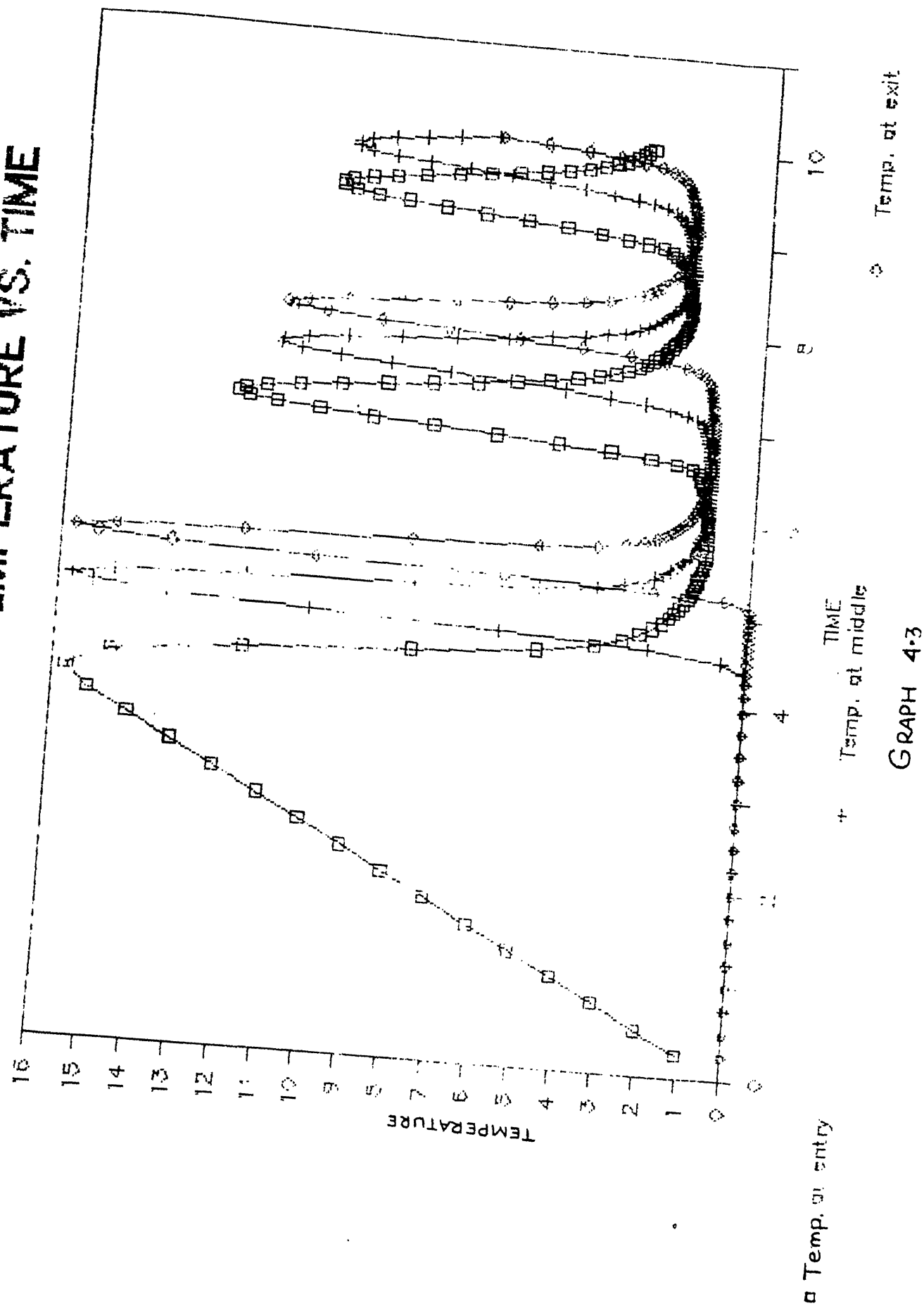
GRAPH 4.1

SOURCE TEMPERATURE VS. TIME

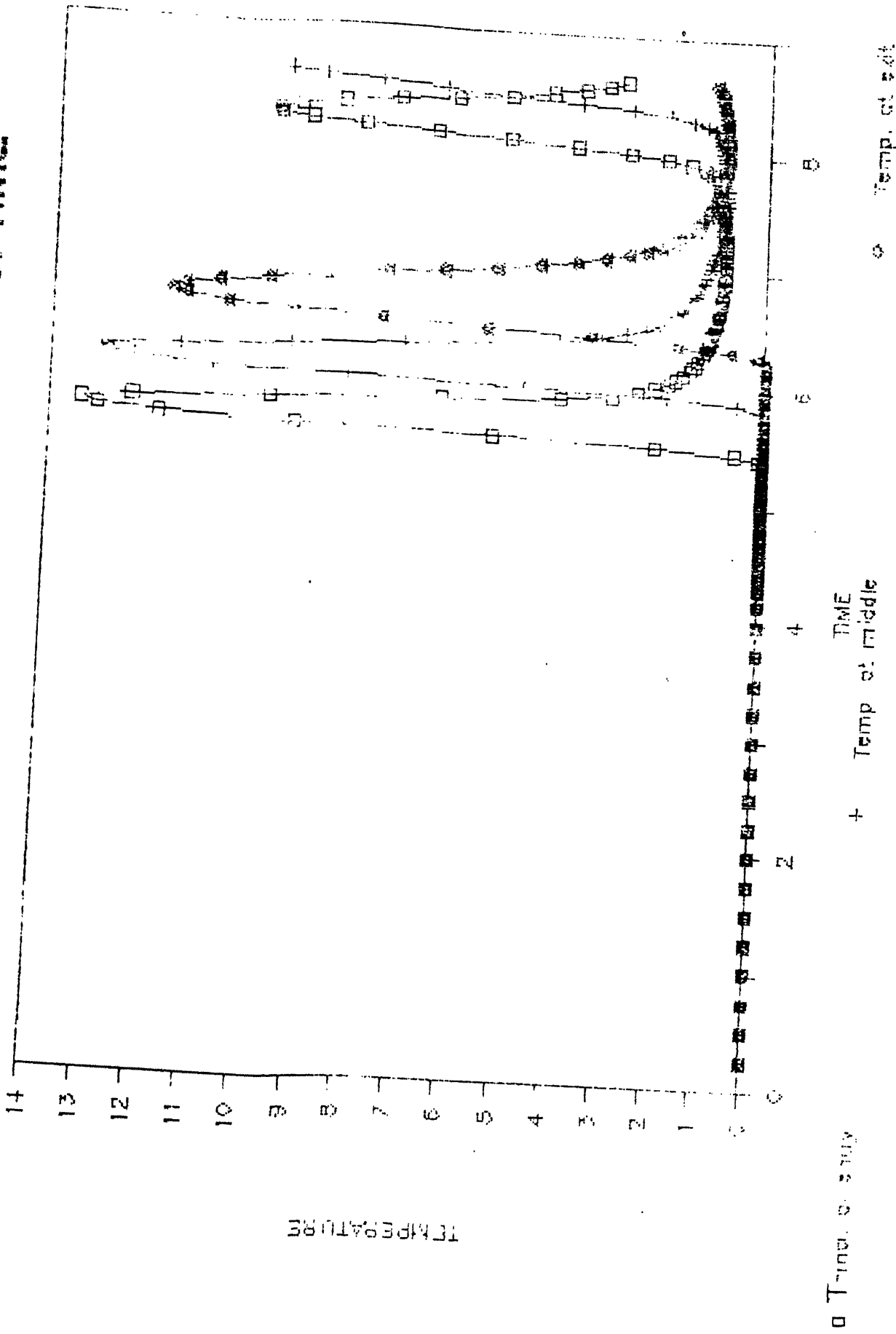


GRAPH 4.2

HOT SEGMENT TEMPERATURE VS. TIME

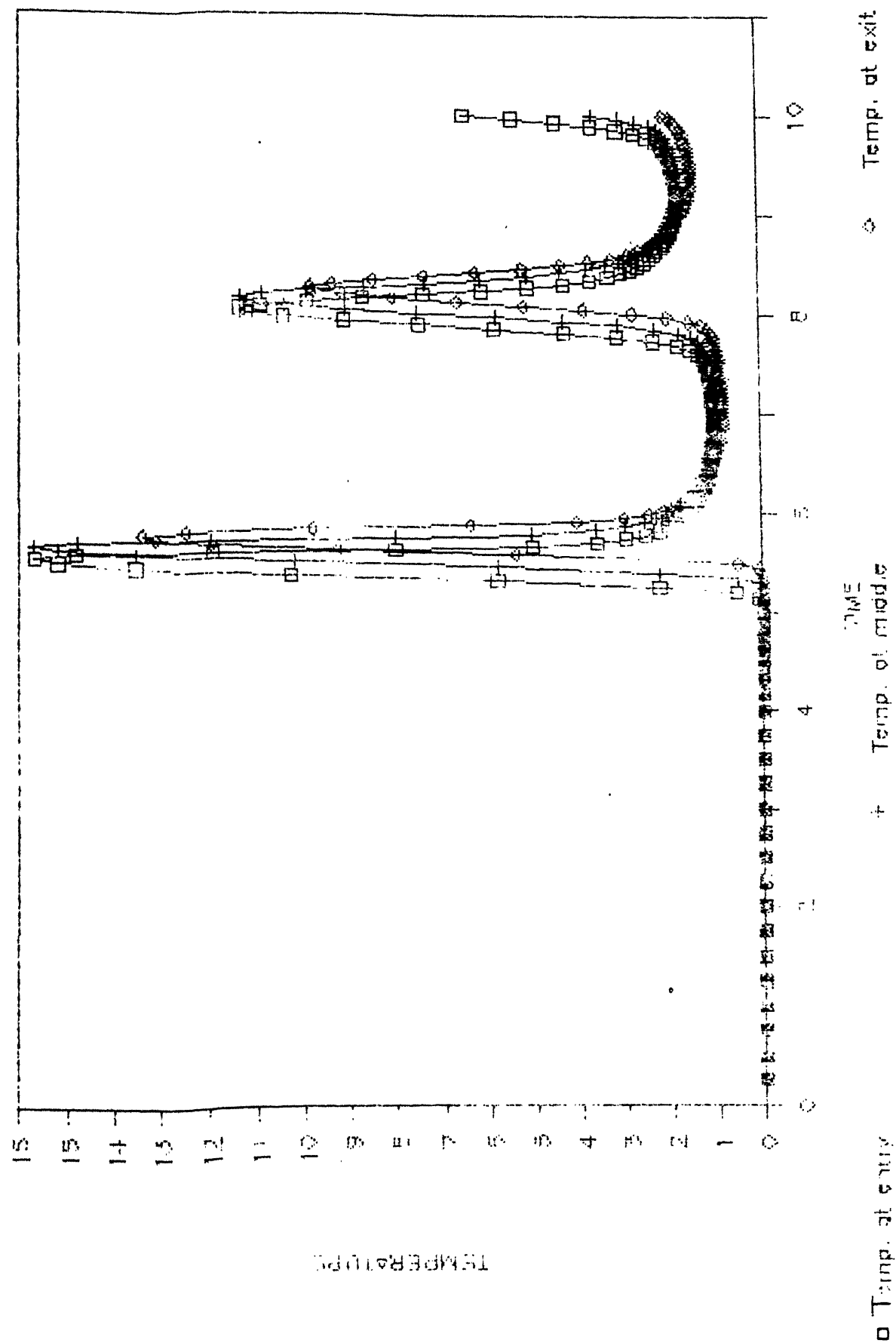


COLD SEGMENT TEMPERATURE VS. TIME



GRAPH 4-4

SINK TEMPERATURE VS. TIME



□ Temp. at entry

+ Temp. at middle

○ Temp. at exit

GRAPH 4.5

4.6: Solution of Finite Difference equations

The finite difference equations here are easy to solve as we have used explicit scheme. Here actually we do not need solution of any equations. Merely by knowing the values of Q and T_i at any time t , we find the values at $(t+1)$ -th time step from eq.s (4.5.1)-(4.5.2.f). The time steps are chosen from the stability criterion at each step.

The marching in time is done till steady state values are obtained, i.e., the error between the values of Q at two consecutive time steps agree within the prescribed tolerance. Provisions are also made to examine oscillatory solutions if there exists no steady state. This is done by allowing the marching for some maximum time.

4.7: Results and discussions

The results have been shown in the plots Graph 4.1 to 4.5. The graphs of flow rate vs. time; source, hot segment, sink, cold segment temperatures vs. time are shown. For each portion the points at entry, exit and middle has been taken into account. The results clearly indicate oscillations. The flow rate and the temperatures oscillate indefinitely without finally coming into any steady state values.

For each portion it indicates that the oscillation is convected along the portion considered. The oscillation initiates from the entry point and gradually passes over to the exit as shown from the time lag between the curves at different sections. The time lag between the flow rate and the temperature may be the cause of the observed instability.

CHAPTER-5
TWO DIMENSIONAL ANALYSIS OF THE THERMOSYPHON PROBLEM

5.1:Introduction

In the previous chapters,we have analysed the rectangular thermosyphon problem in one dimension with the coordinate running along the loop.However, this one-dimensional analysis leads to certain drawbacks.

(1)The actual flow has been observed to be three-dimensional.The one-dimensional analysis gives rise to discrepancies between experimental and theoretical results upto $\pm 30\%$ [6].

(2)In one-dimensional analysis ,some correlations have been used for the friction factor f and the heat transfer coefficient h .The correlations are valid for forced convection case.However,due to their non-availability in natural circulation flows,we have used the same correlations.

To avoid these difficulties,we attempt a two-dimensional analysis of the problem in this chapter.This eliminates the necessity to use any correlations.

5.2 Formulation:

For the two-dimensional formulation of the problem,the following assumptions are made.

(1)The fluid is incompressible.

(2)The flow is two-dimensional,the coordinate s running around the loop and r being in the radial direction.The θ direction is eliminated due to axi-symmetry.

(3)The fluid properties are assumed to be constants.

(4)Boussinesq approximation is valid,i.e.,density is assumed to be constant in all the conservation equations except for the body force term in the momentum equation where linear variation of density with temperature is assumed.

$$\text{i.e., } \rho = \rho_o [1 - \beta(T - T_o)] \text{-----(5.5.1)}$$

(5)The velocity in the radial direction is small compared to the velocity in the axial direction and hence neglected.

(6)Axial conduction and viscous dissipation are negligible compared to the convected energy.

The governing equations in cylindrical coordinate are:

Continuity: $\frac{\partial v}{\partial s} = 0$, i.e., $v = v(r, t)$

i.e., Velocity is a function of time and radial direction.

Momentum: $\rho \frac{\partial v}{\partial t} = -\rho g \cos\theta - \frac{\partial p}{\partial s} + \mu \left(\frac{\partial^2 v}{\partial r^2} + \frac{1}{r} \frac{\partial v}{\partial r} \right)$

Integration along the loop eliminates the pressure term and gives

$$\rho_o L \frac{\partial v}{\partial t} = -g \rho dz + \mu L \left(\frac{\partial^2 v}{\partial r^2} + \frac{1}{r} \frac{\partial v}{\partial r} \right)$$

Using the relation (5.1.1), we get,

$$\rho_o \frac{\partial v}{\partial t} = \frac{q \rho \beta}{L} T dz + \mu \left(\frac{\partial^2 v}{\partial r^2} + \frac{1}{r} \frac{\partial v}{\partial r} \right) \quad \text{---(5.2.2)}$$

$$\text{Energy: } \rho_o C_p \left(\frac{\partial T}{\partial t} + v \frac{\partial T}{\partial s} \right) = k \left(\frac{\partial^2 T}{\partial r^2} + \frac{1}{r} \frac{\partial T}{\partial r} \right) \quad \text{---(5.2.3)}$$

Here axial conduction and viscous dissipation have been neglected.

The equations (5.2.2) and (5.2.3) involve two variables T and q . They represent a coupled partial integro-differential equation set. Velocity v is a function of r and t whereas temperature T is a function of r, s and t . So, we need initial conditions and boundary conditions.

I.C.: At time $t=0$, $T=T_o$, $v=0$

B.C.: i) Continuity of temperature along the loop

ii) At $r=a$, $v=0$

iii) At $r=0$, $\frac{\partial v}{\partial r}=0$

iv) At $r=a$, $k \frac{\partial T}{\partial r}=q$, $0 < s < W/2$ (Source)

$\frac{\partial T}{\partial r}=0$, $W/2 < s < (W+H)/2$ (Hot segment)

$=0$, $(W+H)/2 < s < W+H$ (Cold segment)

$T=T_o$, $(W+H)/2 < s < W+H/2$ (Sink)

v) At $r=0$, $\frac{\partial T}{\partial r}=0$

5.3: Non-dimensionalisation

The above equation sets are non-dimensionalised as:

$$t^* = t v_{ch} / L \quad s^* = 2s / H \quad r^* = r / a$$

$$T^* = \frac{T - T_o}{qa/k} \quad v^* = v / v_{ch}$$

where v_{ch} = Characteristic velocity = Steady state velocity for one-dimensional thermosyphon case with constant heat flux

$$\begin{aligned}
 \text{Thus, } \frac{\partial v}{\partial t} &= \frac{v_{ch}^2}{L} \frac{\partial v^*}{\partial t^*} & \frac{\partial T}{\partial t} &= \frac{v_{ch} q a}{k L} \frac{\partial T^*}{\partial t^*} \\
 \frac{\partial v}{\partial r} &= \frac{v_{ch}}{a} \frac{\partial v^*}{\partial r^*} & \frac{\partial T}{\partial r} &= \frac{q}{k} \frac{\partial T^*}{\partial r^*} \\
 , \frac{\partial^2 v}{\partial r^2} &= \frac{v_{ch}}{a^2} \frac{\partial^2 v^*}{\partial r^*} & \frac{\partial^2 T}{\partial r^2} &= \frac{q}{k a^2} \frac{\partial^2 T^*}{\partial r^*} \\
 ds &= H/2 ds^* & \frac{\partial T}{\partial s} &= \frac{2 q a}{k H} \frac{\partial T^*}{\partial s^*}
 \end{aligned}$$

Substituting these relations in (5.2.2)–(5.2.4) and dropping the * symbol, we get the following non-dimensional set of equations.

$$\text{Momentum: } \frac{\partial v}{\partial t} = Gr \left[\int_{B}^{1+B} T ds - \int_{1+2B}^{2+2B} T ds \right] + IRe \left(\frac{\partial^2 v}{\partial r^2} + \frac{1}{r} \frac{\partial v}{\partial r} \right) \quad (5.3.1)$$

$$\text{Energy: } \frac{\partial T}{\partial t} + 2(1+B)v \frac{\partial T}{\partial s} = IRa \left(\frac{\partial^2 T}{\partial r^2} + \frac{1}{r} \frac{\partial T}{\partial r} \right) \quad (5.3.2)$$

with the boundary and initial conditions

I.C.: At $t=0$, $v=0, T=0$

B.C.: i) Continuity of T along the loop

$$\text{ii) At } r=0, \frac{\partial v}{\partial r}=0$$

$$\text{iii) At } r=0, \frac{\partial T}{\partial r}=0 \quad (5.3.3)$$

$$\text{iv) At } r=1, v=0$$

$$\begin{aligned}
 \text{v) At } r=1, \frac{\partial T}{\partial r} &= 1, 0 < s < B \text{ (Source)} \\
 &= 0, B < s < 1+B \text{ (Hot segment)} \\
 &= 0, 1+2B < s < 2+2B \text{ (Cold segment)} \\
 T &= 0, 1+B < s < 1+2B \text{ (Sink)}
 \end{aligned}$$

with the non-dimensional parameters defined by

$$Gr = \text{Grashof No.} = \frac{g \beta H a}{2 k v_{ch}^2} = \frac{g \beta P}{2 \pi k B v_{ch}^2}$$

$$IRe = \text{Inverse Reynold No.} = \frac{\mu L}{\rho_o a^2 v_{ch}} \quad (5.3.4)$$

$$IRa = \text{Inverse Rayleigh No.} = \frac{L k}{\rho_o C_p a^2 v_{ch}}$$

5.4: Steady state analysis

The steady state equations are derived from (5.3.3) by making the time derivatives zero. Thus, we get,

$$\text{Momentum: } Gr \left[\int_{B}^{1+B} T ds - \int_{1+2B}^{2+2B} T ds \right] + IRe \left(\frac{\partial^2 v}{\partial r^2} + \frac{1}{r} \frac{\partial v}{\partial r} \right) = 0 \quad (5.4.1)$$

$$\text{Energy: } 2(1+B)v \frac{\partial T}{\partial s} = IRa \left(\frac{\partial^2 T}{\partial r^2} + \frac{1}{r} \frac{\partial T}{\partial r} \right) \quad \text{----- (5.4.2)}$$

with the boundary condition

i) Continuity of T along the loop

$$\text{ii) At } r=0, \frac{\partial v}{\partial r}=0$$

$$\text{iii) At } r=0, \frac{\partial T}{\partial r}=0$$

$$\text{iv) At } r=1, v=0 \quad \text{----- (5.4.3)}$$

$$\text{v) At } r=1, \frac{\partial T}{\partial r}=1, 0 < s < B$$

$$=0, B < s < 1+B$$

$$=0, 1+2B < s < 2+2B$$

$$T=0, 1+B < s < 1+2B$$

5.5: Solution for steady state

The complexity involved in the steady state equations eliminates any chance of an analytical solution. The only way to solve these equations is by numerical means. Here we use the finite difference method to solve the equations. For the finite difference formulation, we use, central difference for the second derivatives and backward difference for the first order derivatives. For the integration encountered in the momentum equation, the Trapezoidal rule has been used as the intervals are of non-uniform size due to the presence of bends at the corners.

The discretisation used has been shown in Figure-5.1. Due to symmetry, without taking the total cross-section, only half of it has been taken for analysis. Here l, k, n and m denote the number of nodes in horizontal direction, in vertical direction, total number of axial nodes and number of nodes in radial direction respectively. Thus the source is nodalised from 2 to l; hot segment from l+1 to l+k-2; sink from l+k-1 to 2l+k-2 and cold segment from 2l+k-1 to n=2l+2k-4.

The finite difference equations are given below.

For interior nodes, i.e., j=2 to m-1

$$\text{Gr/2} \left[\sum_{i=1}^{l+k-1} a_{i,j} T_{i,j} - \sum_{i=2l+k-2}^n a_{i,j} T_{i,j} - a_{i,j} T_{i,j} \right] + IRe \frac{v_{j-1} - 2v_j + v_{j+1}}{\Delta r^2} + \frac{1}{r_j} \frac{v_j - v_{j-1}}{\Delta r} = 0$$

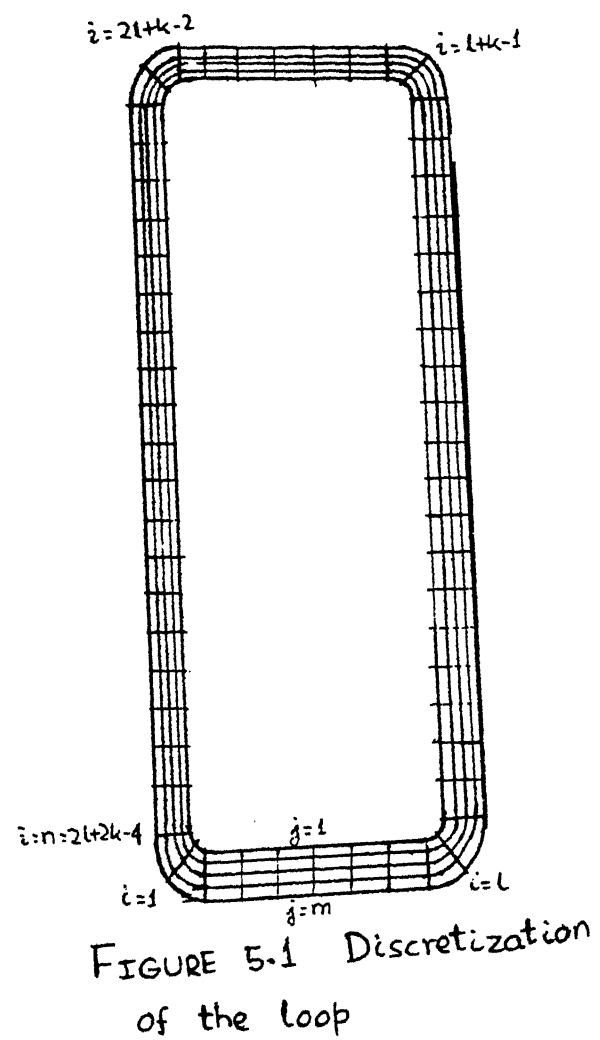


FIGURE 5.1 Discretization
of the loop

$$2(1+B)v_j \frac{T_{i,j} - T_{i-1,j}}{\Delta s_{i,j}} = IRa \left[\frac{T_{i,j-1} - 2T_{i,j} + T_{i,j+1}}{\Delta r^2} \right] \frac{T_{i,j} - T_{i,j-1}}{\Delta r},$$

i=2 to n

$$2(1+B)v_j \frac{T_{i,j} - T_{i,n,j}}{\Delta s_{i,j}} = IRa \left[\frac{T_{i,j-1} - 2T_{i,j} + T_{i,j+1}}{\Delta r^2} \right] \frac{T_{i,j} - T_{i,j-1}}{\Delta r}, \quad i=1$$

where $a_{i,j} = \Delta s_{i+1,j}$, i=1 and 21+k-2
 $= \Delta s_{i,j}$, i=1+k-1 and 1
 $= \Delta s_{i,j} + \Delta s_{i+1,j}$, for other i's
 $= \Delta s_{i,j} + \Delta s_{i-1,j}$, i=21+2k-4

and $\Delta s_{i,j} = \text{Bend length}/2 + \pi/4(j-1)\Delta rd/H$ for i=1,2,1,1+1,
1+k-1,1+k,21+k-2 and 21+k-1

= Δs for other i's

For j=1, i.e., at $r=0$, $\frac{\partial v}{\partial r}=0$ and $\frac{\partial T}{\partial r}=0$

The terms $\frac{1}{r} \frac{\partial v}{\partial r}$ and $\frac{1}{r} \frac{\partial T}{\partial r}$ become $\frac{\partial^2 v}{\partial r^2}$ and $\frac{\partial^2 T}{\partial r^2}$ by L'Hospital's rule.

These conditions also give $v_1 = v_0$ and $T_{i,1} = T_{i,0}$.

During discretisation of second derivatives, we get, for $j=1$, expressions involving v_0 and $T_{i,0}$ for which the above substitutions are made.

Thus, we get, for $j=1$

$$Gr/2 \sum_{i=1}^{l+k-1} a_{i,1} T_{i,1} - \sum_{i=2l+k-2}^n a_{i,1} T_{i,1} - a_{i,1} T_{i,1} + 2IRa \frac{v_2 - v_1}{\Delta r^2} = 0$$

and $(1+B)v_1 \frac{T_{i,1} - T_{i-1,1}}{\Delta s_{i,1}} = IRa \frac{T_{i,2} - T_{i,1}}{\Delta r^2}, \quad i=2 \text{ to } n$

$$(1+B)v_1 \frac{T_{i,1} - T_{i,n,1}}{\Delta s_{i,1}} = IRa \frac{T_{i,2} - T_{i,1}}{\Delta r^2}, \quad i=1$$

At $r=1$, i.e., $j=m$,

$$v=0, \text{ or }, v_j=0$$

$$\frac{\partial T}{\partial r}=1, 0 < s < B, \text{ or }, T_{i,j} = T_{i,j-1} + \Delta r, \quad i=2 \text{ to } l$$

$$= 0, B < s < 1+B, \text{ or }, T_{i,j} = T_{i,j-1}, \quad i=l+1 \text{ to } l+k-2$$

$$T=0, 1+B < s < 1+2B, \text{ or }, T_{i,j}=0, \quad i=l+k-1 \text{ to } 21+k-2$$

$$\frac{\partial T}{\partial r}=0, 1+2B < s < 2+2B, \text{ or }, T_{i,j} = T_{i,j-1}, \quad i=21+k-1 \text{ to } n \text{ and } 1$$

Rearrangement of the above equations give,

Energy equation set(5.5.1) is given by

$$\text{For } j=1: T_{i,j} [v_j + \frac{IRa\Delta s_{i,j}}{(1+B)\Delta r^2}] - \frac{IRa\Delta s_{i,j}}{(1+B)\Delta r^2} T_{i,j+1} = T_{i-1,j}, i=2 \text{ to } n$$

$$= T_{n,j}, i=1$$

$$\text{For } j=2 \text{ to } m-1: T_{i,j-1} [\frac{IRa\Delta s_{i,j}}{2(1+B)\Delta r^2} (-1 + \frac{1}{j-1})] + T_{i,j} [v_j + \frac{IRa\Delta s_{i,j}}{2(1+B)\Delta r^2} (2 - \frac{1}{j-1})]$$

$$+ T_{i,j+1} [\frac{IRa\Delta s_{i,j}}{2(1+B)\Delta r^2}] = T_{i-1,j}, i=2 \text{ to } n$$

$$= T_{n,j}, i=1$$

$$\text{For } j=m: T_{i,j} = T_{i,j-1} + \Delta r, i=2 \text{ to } 1$$

$$= T_{i,j-1}, i=1+1 \text{ to } 1+k-2$$

$$= 0, i=1+k-1 \text{ to } 2l+k-2$$

$$= T_{i,j-1}, i=2l+k-1 \text{ to } n \text{ and } 1$$

The momentum equation set(5.5.2) is given by

$$\text{For } j=1: v_j - v_{j+1} = \frac{Gr\Delta r^2}{4IRe} \sum_{i=1}^{l+k-1} a_{i,j} T_{i,j} - \sum_{i=2l+k-2}^n a_{i,j} T_{i,j} - a_{i,j} T_{i,j}$$

$$j=2 \text{ to } m: v_{j-1} [-1 + \frac{1}{j-1}] + v_j [2 - \frac{1}{j-1}] - v_{j+1}$$

$$= \frac{Gr\Delta r^2}{2IRe} \sum_{i=1}^{l+k-1} a_{i,j} T_{i,j} - \sum_{i=2l+k-2}^n a_{i,j} T_{i,j} - a_{i,j} T_{i,j}$$

$$j=m: v_j = 0$$

5.6: Solution Technique

The above equation sets (5.5.1) and (5.5.2) represent a non-linear set of equations. Hence they are to be solved iteratively. Each set represents a system of tridiagonal matrix with sub-diagonal, diagonal and super-diagonal elements.

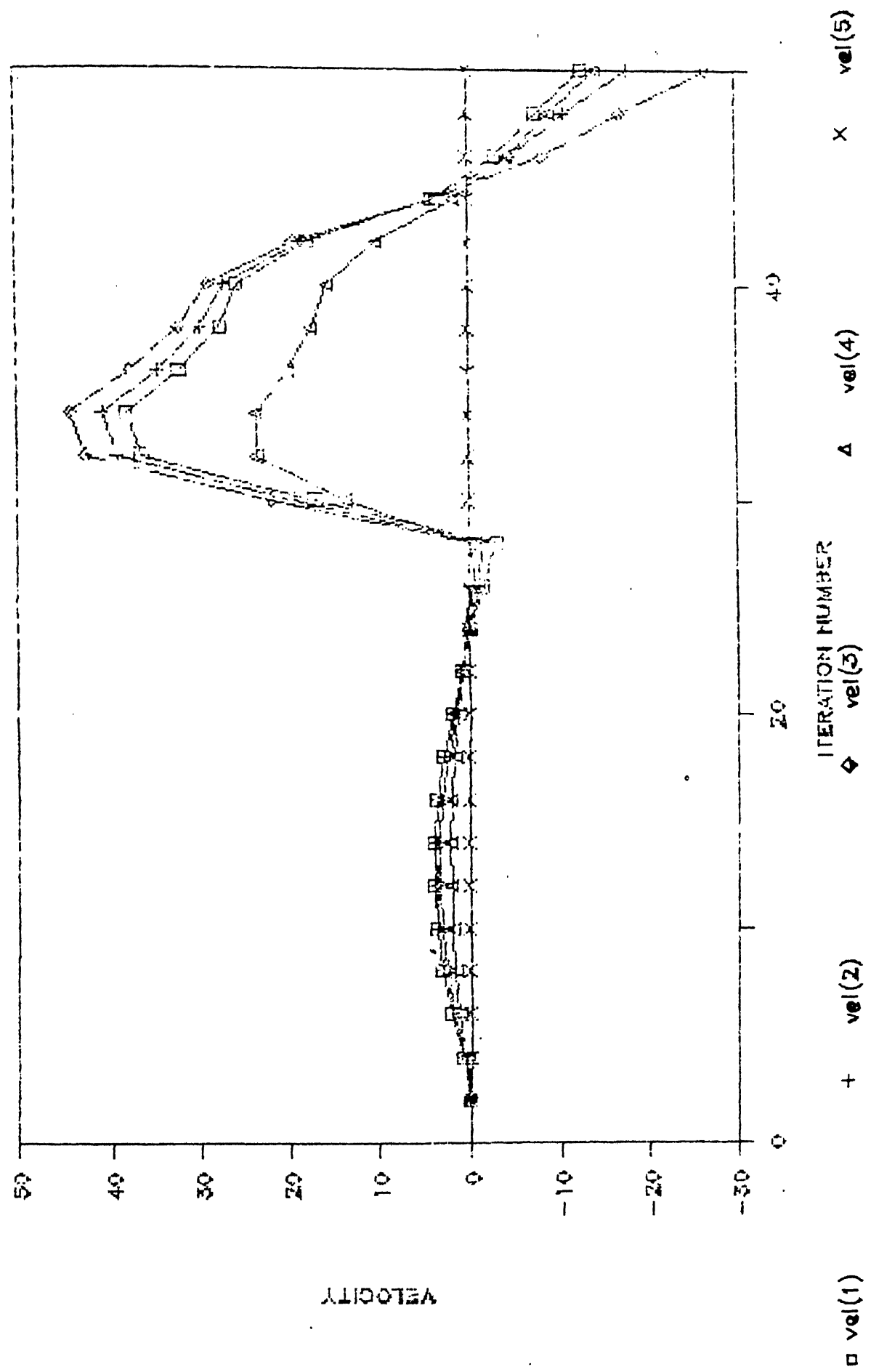
To solve the set of equations, initially some guess values of the vectors $\{v\}^0$ and $\{T\}^0$ are assumed. First, the tridiagonal set (5.5.1) is solved. The quantities v_i and $T_{i,j}$ appearing in the elements of the sub-diagonal, diagonal, super-diagonal or RHS vectors are taken to be v_i^0 and $T_{i,j}^0$ respectively. Thus we get the value of $\{T\}^1$ for first iteration step. Then the tridiagonal set (5.5.2) is solved. The quantities v_j , $T_{i,j}$ appearing in the elements of the sub-diagonal, diagonal, super-diagonal or RHS

vectors are taken to be v_j^0 and $T_{i,j}^0$ respectively. Thus we get the set $\{T\}^0$. Now the sets $\{v\}^0$ and $\{T\}^0$ are compared with the previous set values for convergence. If the system has not converged, then the new values are taken as guess values and the process is repeated till convergence. Provisions are also made to detect if the solution, instead of converging, oscillates. For this purpose, number of oscillations is allowed upto a maximum and the values are noted at each iteration to check if oscillations are present.

5.7:Results and discussions

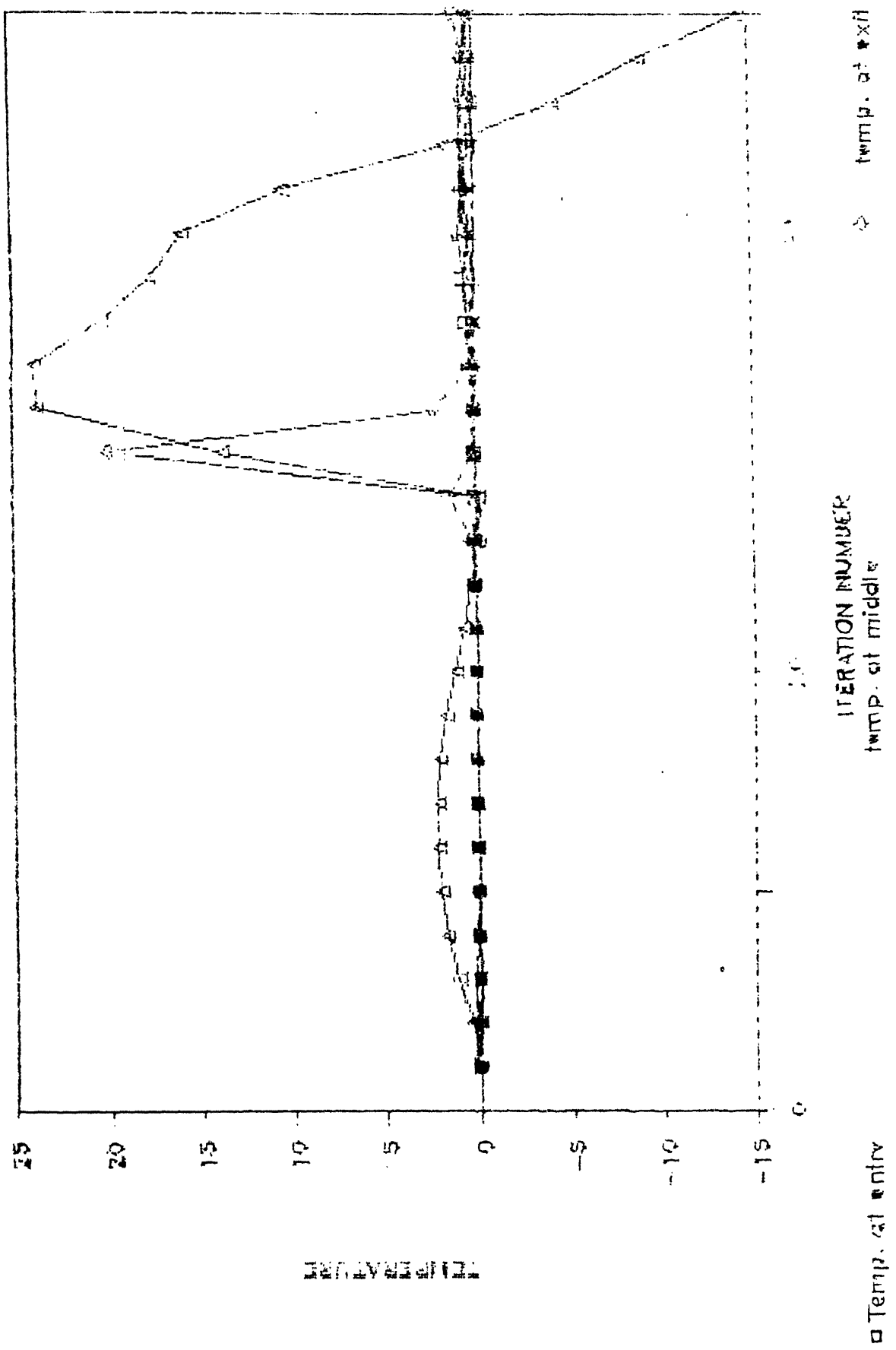
The results are plotted in Graphs 5.1 to 5.5 as velocity vs. iteration numbers and temperature along the source, hot segment, sink and cold segment vs. iteration numbers. The curves show the oscillations in the values of the above quantities with iterations. From the oscillatory behaviour, it can be concluded that there exists no steady state for this case with the chosen values of the parameters. Any small deviation from the steady state results in oscillations. This agrees with the observed instabilities or even flow reversals in the rectangular thermosyphon loop.

VELOCITY V.S. ITERATION



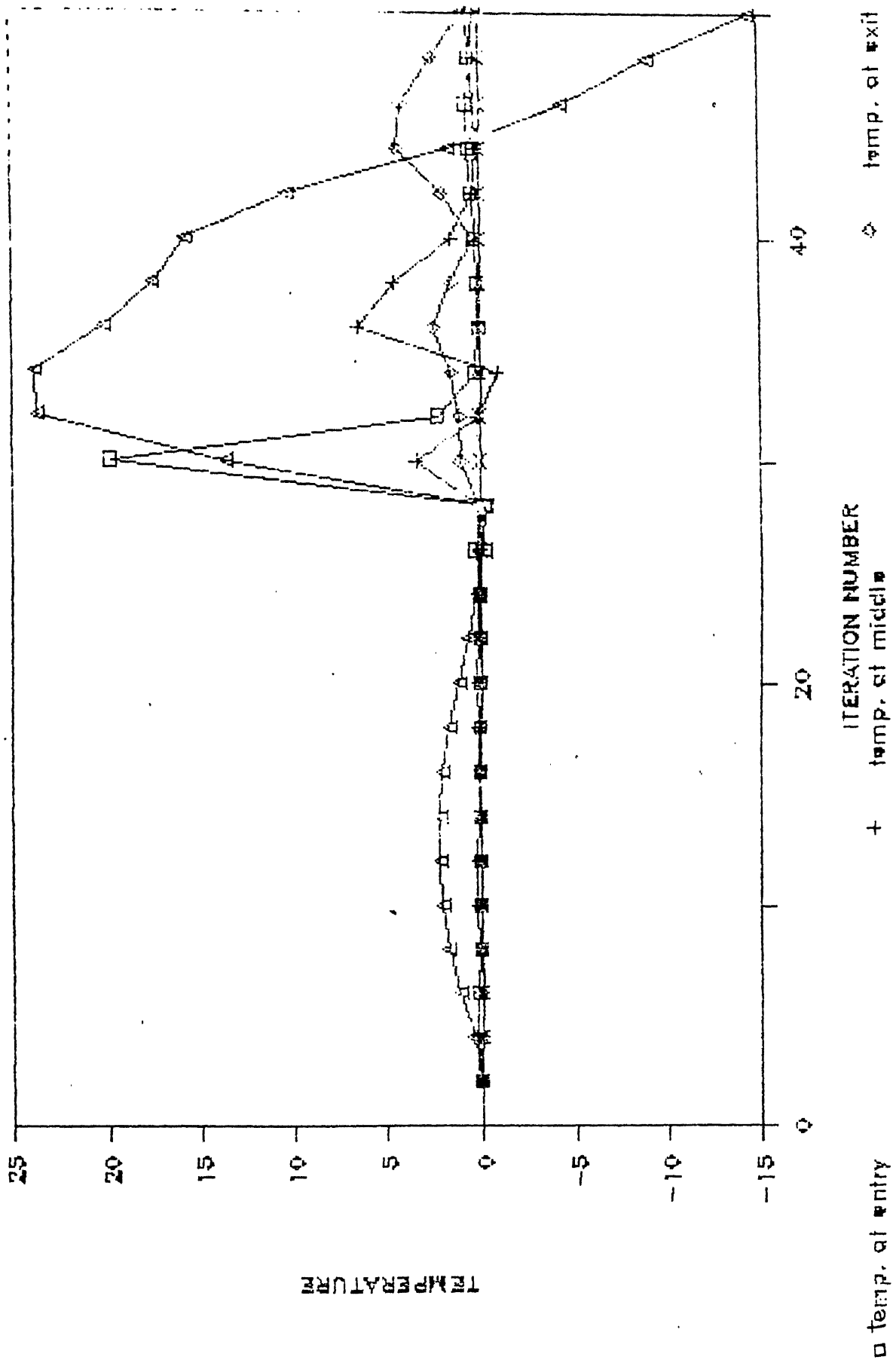
GRAPH 5.1

SOURCE TEMPERATURE VS. INITIATION

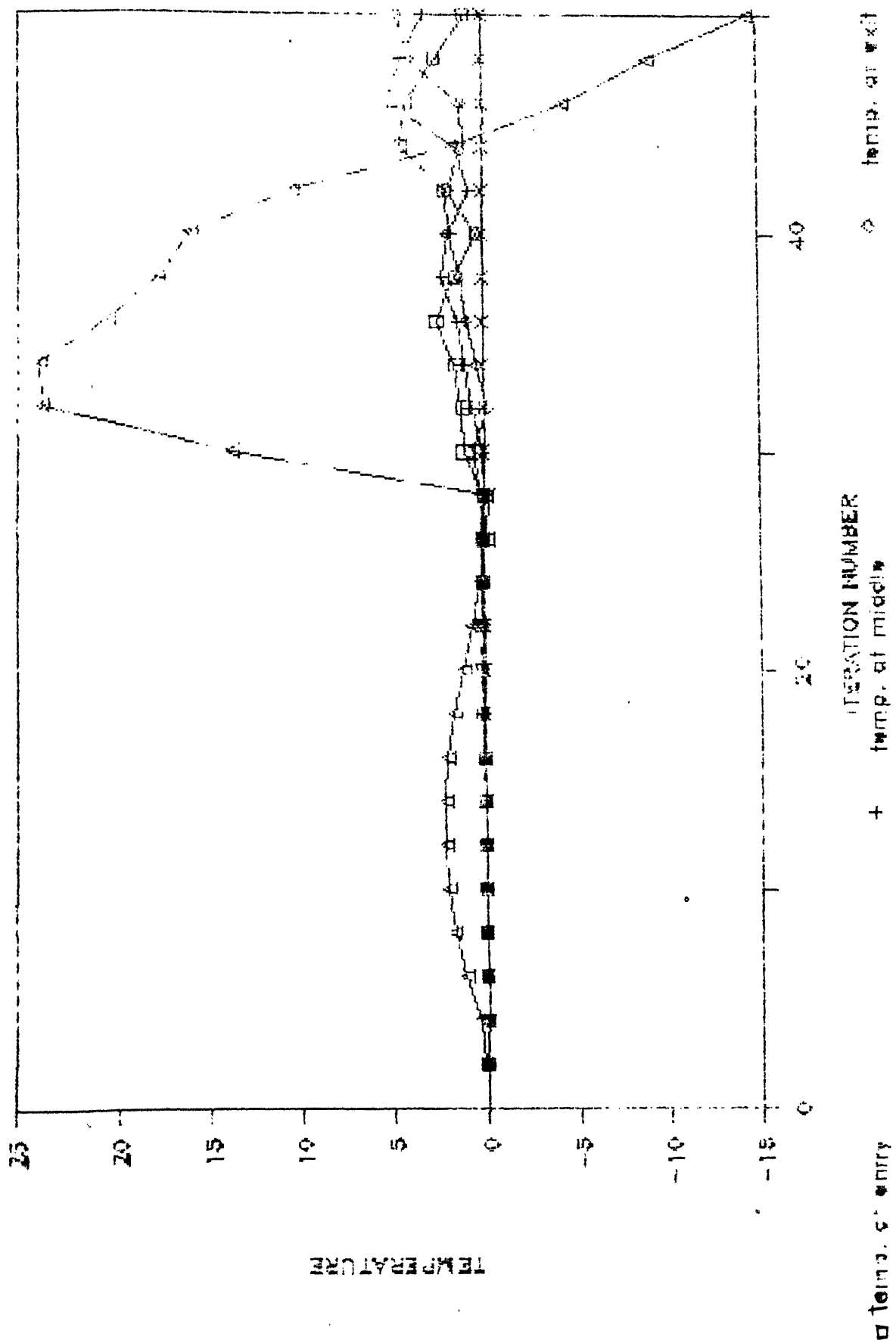


GRAPH 5.2

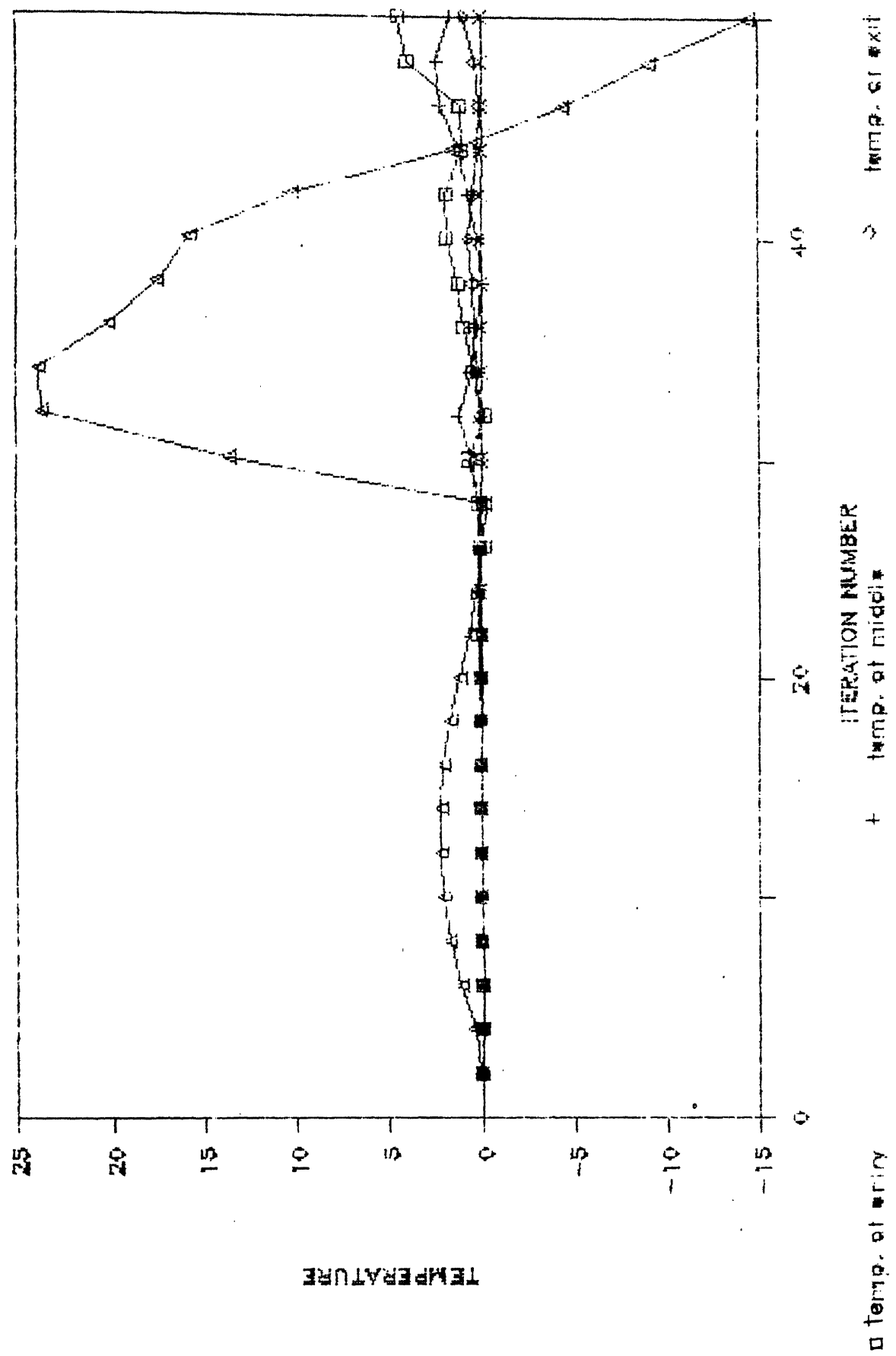
HOT SEGMENT TEMPERATURE VS. ITERATION



SINK TEMPERATURE VS. ITERATION



COLD SEGMENT TEMPERATURE VS. ITERATION



GRAPH 5.5

CONCLUSION

The analysis of the internal natural circulation flow in the rectangular thermosyphon loop has been done starting from the simple case of a thermosyphon loop with point source and point sink to the two-dimensional analysis of the loop with extended source and sink with the heat exchanger as the sink. It has been assumed throughout that there is no initial flow in the loop. The steady state, transient and stability characteristics of each case has been analysed in detail.

It has been shown that the behaviour of the loop depends largely on the prescribed model. The one-dimensional rectangular thermosyphon loop with constant temperature heat sink shows no instability, whereas the same loop gives rise to instability with the introduction of the heat exchanger. The two dimensional analysis also leads to instability.

The loop configuration is one of the few alterable factors in the thermosyphon design. The geometrical dimension of the loop can be changed so as to get rid of the operational and safety problems caused by the periodic instability in the natural convection loops.

However, the actual process occurring in the nuclear power reactors is much more complex than the case analysed. It comprises of a number of such parallel loops with the pressure drop varying largely at different sections. Again, after the failure of the electrical power supply, due to the high inertia of the flywheel of the primary pump, flow is maintained for some period of time and thereafter natural circulation takes over. This transition from forced flow to natural circulation flow has not been taken into account in our case. The improvements in the modelling so as to include the parallel loops, consideration of the pressure drops at different sections of the loop and the initial condition of transition from forced flow to natural circulation flow will throw more light in the design of the primary heat transport system of the nuclear reactor so as to remove the decay heat effectively to ensure safety of the plant.

APPENDIX-I

Let us consider a fluid particle passing through the source at temperature ΔT for a time Δt . Let T_{in} and T_{out} represent the temperature of the fluid particle before and after passing through the source and Q the flow rate.

Now, energy equation gives

$$\frac{\partial T}{\partial t} + \frac{Q}{A} \frac{\partial T}{\partial s} = k(\Delta T - T)$$

As we are considering a particular particle motion, space, i.e., position of the particle becomes a function of time and hence in all we have one independent coordinate t .

So, we get, $\frac{dT}{dt} + kT = k \Delta T$

$$\text{Now, } T_{af} = A \exp(-kt)$$

$$T_{pi} = \Delta T$$

$$\text{So, } T(t) = A \exp(-kt) + \Delta T$$

The boundary conditions are at $t=0, T=T_{in}$

$$\text{at } t=\Delta t, T=T_{out}$$

$$\text{So, } T_{in} = A + \Delta T$$

$$T_{out} = A \exp(-k\Delta t) + \Delta T$$

$$\text{and } T_{out} - T_{in} = A(-1 + e^{-k\Delta t}) = (\Delta T - T_{in})(1 - e^{-k\Delta t})$$

Similarly, for heat sink,

$$T_{out} - T_{in} = (-\Delta T - T_{in})(1 - e^{-k\Delta t})$$

APPENDIX-II

STEADY STATE SOLUTION FOR UNIFORM HEAT SOURCE

The steady state equations derived from (3.4.1) are

$$G \left[s \frac{d\bar{T}}{ds} - \int s \frac{d\bar{T}}{ds} ds \right] = \bar{Q}^2 \quad \text{----- (A2.1)}$$

$$\begin{aligned} \bar{Q} \frac{d\bar{T}}{ds} &= M, \quad 0 < s < B \\ &= 0, \quad B < s < 1+B \\ &= -M\bar{T}, \quad 1+B < s < 1+2B \quad \text{----- (A2.2)} \\ &= 0, \quad 1+2B < s < 2+2B \end{aligned}$$

with continuity of \bar{T} along the loop.

This coupled equation set is solved by first solving (A2.2) with \bar{Q} as parameter. After getting the steady temperature profile, (A2.1) is solved for \bar{Q} and then substituted in the solution of (A2.2).

Solution of (A2.2) is given as

$$\begin{aligned} \bar{T}(s) &= M s / \bar{Q} + K_1, \quad 0 < s < B \\ &= K_2, \quad B < s < 1+B \quad \text{----- (A2.3)} \\ &= K_3 \exp(-Ms/\bar{Q}), \quad 1+B < s < 1+2B \\ &= K_4, \quad 1+2B < s < 2+2B \end{aligned}$$

The constants are found from continuity condition of $\bar{T}(s)$.

So, at $s=B$, $K_2 = MB/\bar{Q} + K_1$

at $s=1+B$, $K_2 = K_3 \exp[-M(1+B)/\bar{Q}]$

at $s=1+2B$, $K_4 = K_3 \exp[-M(1+2B)/\bar{Q}]$

at $s=2+2B$, $K_4 = K_1$

Solving these four equations for K_1, K_2, K_3 and K_4 , we find,

$$\begin{aligned} K_1 &= K_4 = MB/\bar{Q} \frac{\exp(-MB/\bar{Q})}{1 - \exp(-MB/\bar{Q})} \\ K_2 &= MB/\bar{Q} \frac{1}{1 - \exp(-MB/\bar{Q})} \quad \text{----- (A2.4)} \\ K_3 &= MB/\bar{Q} \frac{\exp[M(1+B)/\bar{Q}]}{1 - \exp(-MB/\bar{Q})} \end{aligned}$$

Now, substitution of (A2.3) in (A2.1) gives

$$G(K_2 - K_4) = GMB/\bar{Q} \quad [\text{From A2.4}] = \bar{Q}^2$$

$$\text{So, } \bar{Q} = (GMB)^{1/2}$$

Making substitutions (3.4.2) and (3.3.10), $\bar{Q} = 1$ (A2.5)

The temperature distribution is found by substituting (A2.4) and (A2.5) in (A2.3).

APPENDIX-III

STEADY STATE SOLUTION FOR TRIANGULAR HEAT SOURCE

The steady state equations derived from (3.5.2.1) are

$$G \int_{\frac{B}{2}}^{1+2B} \bar{T} ds - \int_{\frac{B}{2}}^{1+2B} \bar{T} ds = \bar{Q}^2 \quad \text{----- (A2.1)}$$

$$\begin{aligned} \bar{Q} \frac{d\bar{T}}{ds} &= 2sM/B, 0 < s < B/2 \\ &= -2M(s-B)/B, B/2 < s < B \\ &= 0, B < s < 1+B \\ &= -M\bar{T}, 1+B < s < 1+2B \quad \text{----- (A3.2)} \\ &= 0, 1+2B < s < 2+2B \end{aligned}$$

with continuity of \bar{T} along the loop.

This coupled equation set is solved by first solving (A3.2) with \bar{Q} as parameter. After getting the steady temperature profile, (A3.1) is solved for \bar{Q} and then substituted in the solution of (A3.2).

Solution of (A3.2) is given as

$$\begin{aligned} \bar{T}(s) &= Ms^2(\bar{Q}B) + K_1, 0 < s < B/2 \\ &= -2Ms/(\bar{Q}B)(s/2-B) + K_2, B/2 < s < B \\ &= K_4, B < s < 1+B \quad \text{----- (A3.3)} \\ &= K_3 \exp(-Ms/\bar{Q}), 1+B < s < 1+2B \\ &= K_5, 1+2B < s < 2+2B \end{aligned}$$

The constants are found from continuity condition of $\bar{T}(s)$.

$$\text{So, at } s=B/2, MB/(4\bar{Q}) + K_1 = 3MB/(4\bar{Q}) + K_2$$

$$\text{at } s=B, K_2 + MB/\bar{Q} = K_4$$

$$\text{at } s=1+B, K_4 = K_3 \exp[-M(1+B)/\bar{Q}]$$

$$\text{at } s=1+2B, K_5 = K_3 \exp[-M(1+2B)/\bar{Q}]$$

$$\text{at } s=2+2B, K_5 = K_1$$

Solving these five equations for K_1, K_2, K_3, K_4 and K_5 , we find,

$$K_1 = K_5 = MB/(2\bar{Q}) \frac{\exp(-MB/\bar{Q})}{1 - \exp(-MB/\bar{Q})}$$

$$K_2 = -MB/(2\bar{Q}) + K_1 \quad \text{----- (A3.4)}$$

$$K_3 = MB/(2\bar{Q}) \frac{\exp[M(1+B)/\bar{Q}]}{1 - \exp(-MB/\bar{Q})}$$

$$K_4 = K_1 + MB/(2\bar{Q})$$

Now, substitution of (A3.3) in (A3.1) gives

$$G(K_4 - K_5) = GMB/(2\bar{Q}) \quad [\text{From A3.4}] = \bar{Q}^2$$

$$\text{So, } \bar{Q} = (GMB/2)^{1/2}$$

Making substitutions (3.5.2.2) and (3.3.10), $\bar{Q}=1$ ----- (A3.5)

The temperature distribution is found by substituting (A3.4) and (A3.5) in (A3.3).

APPENDIX-IV

STEADY STATE SOLUTION FOR SINOSIDUAL HEAT SOURCE

The steady state equations derived from (3.5.3.1) are

$$G[\int_0^B \bar{T} ds - \int_{1+2B}^{2+2B} \bar{T} ds] = \bar{Q}^2 \quad \text{----- (A4.1)}$$

$$\begin{aligned} \bar{Q} \frac{d\bar{T}}{ds} &= M \sin(\pi s/B), 0 < s < B \\ &= 0, B < s < 1+B \\ &= -M\bar{T}, 1+B < s < 1+2B \quad \text{----- (A4.2)} \\ &= 0, 1+2B < s < 2+2B \end{aligned}$$

with continuity of \bar{T} along the loop.

This coupled equation set is solved by first solving (A4.2) with \bar{Q} as parameter. After getting the steady temperature profile, (A4.1) is solved for \bar{Q} and then substituted in the solution of (A4.2).

Solution of (A4.2) is given as

$$\begin{aligned} \bar{T}(s) &= -MB/(\bar{Q}\pi) \cos(\pi s/B) + K_1, 0 < s < B \\ &= K_2, B < s < 1+B \quad \text{----- (A4.3)} \\ &= K_3 \exp(-Ms/\bar{Q}), 1+B < s < 1+2B \\ &= K_4, 1+2B < s < 2+2B \end{aligned}$$

The constants are found from continuity condition of $\bar{T}(s)$.

So, at $s=B$, $K_2 = MB/(\bar{Q}\pi) + K_1$

$$\text{at } s=1+B, K_2 = K_3 \exp[-M(1+B)/\bar{Q}]$$

$$\text{at } s=1+2B, K_4 = K_3 \exp[-M(1+2B)/\bar{Q}]$$

$$\text{at } s=2+2B, K_4 = K_1 - MB/(\bar{Q}\pi)$$

Solving these four equations for K_1, K_2, K_3 and K_4 , we find,

$$\begin{aligned} K_2 &= 2MB/(\bar{Q}\pi) \frac{1}{1 - \exp(-MB/\bar{Q})} \\ K_3 &= 2MB/(\bar{Q}\pi) \frac{\exp[-M(1+B)/\bar{Q}]}{1 - \exp(-MB/\bar{Q})} \quad \text{----- (A4.4)} \\ K_4 &= K_3 \exp[-M(1+2B)/\bar{Q}] \\ K_1 &= K_4 + MB/(\bar{Q}\pi) \end{aligned}$$

Now, substitution of (A4.3) in (A4.1) gives

$$G(K_2 - K_4) = 2GMB/(\bar{Q}\pi) \quad [\text{From A4.4}] = \bar{Q}^2$$

$$\text{So, } \bar{Q} = (2GMB/\pi)^{1/2}$$

Making substitutions (3.5.3.2) and (3.3.10), $\bar{Q}=1$ (A4.5)

The temperature distribution is found by substituting (A4.4) and (A4.5) in (A4.3).

REFERENCES

[1] Davies T. H. and Morris W. D. ,Ind. Eng. Dig.,26[11/12] 1965, pp.87-91

[2] Ostrach S.,Natural Convections in Enclosures,in:Advances in Heat Transfer,vol.8,ed.T.F.Irvine Jr. and J.P.Hartnet (Academic Press,New York,1972)pp. 156-222

[3] D.Japiske,Advances in Thermosyphon Technology,in:Advances in Heat Transfer,vol.9,ed.T.F.Irvine,Jr. and J.P.Hartnet (Academic Press,New York,1973)pp. 1-111

[4] Gebhart B.,Natural Convection Flows and Stability,in:Advances in Heat Transfer,vol.9,ed.T.F.Irvine,Jr. and J.P.Hartnet (Academic Press,New York,1973)pp 273-348

[5] Gebhart B.,Jaluria Y.,Mahajan R.L.,Sammakia B.,in:Buoyancy Induced Flows and Transport,Hemisphere Publishing Corporation

[6] Keller J.B.,Periodic Oscillation in a model of Thermal Convection,J. Fluid Mech.vol.26,part-3,1966,pp 599-606

[7] Welander P.,On The Oscillatory Instability of a differentially Heated Fluid Loop,J. Fluid Mech.,vol.29,part-1,1967,pp 17-30

[8] Creveling H. F.,De Paz J. F.,Baladi J. Y. and Schoenhals R.J.,Stability Characteristics of a single phase free convection loop,J. Fluid Mech.,vol.67,part-1,1975,pp 65-84

[9] Grief R.,Zvirin Y. and Mertol A.,The Transient and Stability Behaviour of a Natural Convection Loop,ASME Journal of Heat Transfer,vol.101,1979,pp. 684-689

[10] Zvirin Y. and Grief R.,Transient Behaviour of Natural Circulation Loops :Two vertical Branches with Point Heat Source and Sink,Int. J. Heat Mass Transfer,vol.22,1979,pp. 499-504

[11] Chen K.,On the Oscillatory Instability of Closed-loop Thermosyphons,ASME Journal of Heat Transfer,vol.107,1985,pp. 826-832

[12] Zvirin Y.,The Instability Associated with the onset of Motion in a Thermosyphon,Int. J. Heat Mass Transfer,vol.28,No.-11,1985,pp. 2105-2111

[13] Mertol A.,Grief R. and Zvirin Y.,Two-dimensional Study of Heat Transfer and Fluid Flow in a Natural Convection Loop,ASME Journal of Heat Transfer,vol.104,1982,pp. 508-514

[14]Mallinson G. D.,Graham A. D.and De Vahl Davis G.,Three-dimensional Flow in a Closed Thermosyphon,J. Fluid Mech.,vol.109,1981,pp. 259-275

[15]Hart J.E.,A new analysis of the closed loop thermosyphon,Int J. Heat Mass Transfer,vol.27,No.-1,1984,pp. 125-136

[16]Zvirin Y.,The effect of dissipation on free convection loops,Int. J. Heat Mass Transfer,vol.22,1979,pp. 1539-1546

[17]Mertol A.,Grief R. and Zvirin Y.,The transient,steady state and stability behaviour of a thermosyphon with throughflow,Int. J. Heat Mass Transfer,vol. 24 ,No.-4,1981,pp. 621-633

[18]E.E.Lewis,Nuclear Power REactor Safety,A Wiley-Interscience Publication,John Wiley & Sons

[19]Agrawal A.K.,Guppy J.G.,Decay Heat Removal and Natural Convection in Fast Breeder Reactors,Hemisphere Publishing Corporation

[20]Zvirin Y.,A review of natural circulation loops in Pressurised Water Reactors and other systems,Nuclear Engg.and Design,vol. 67,1981,pp. 203-225

[21]Ghosh A.,Bandopadhyay S.K.,Murty L.G.K.,Ramamoorthy N.,Ultimate Heat Sink for PHWR-Evaluation of Existing methods and alternative proposals,Nuclear Engg. and Design,vol. 7,1982,pp. 145-152

[22]Spinks N.J.,Wright A.C.D.,Caplan M.Z.and Prawirosoehardjo S.,Thermosyphoning in the CANDU Reactor,Paper submitted to the April,1983 CSNI Special Meeting on Decay Heat Removal Systems

[23]Chato,J.,Natural Convection Flows in Parallel Channel Systems,ASME Journal of Heat Transfer,vol. 85,1963,pp. 339-345

[24]Zvirin Y.,Jeuck P.R. III,Sullivan C.W.,Duffey R.B.,Experimental and analytical investigation of a natural circulation system with parallel loops,ASME Journal of Heat Transfer,vol. 103,1981,pp. 645-652

[25]Gillette J.L.,Singer R.M.,Tokar J.V.,Sullivan J.E.,Experimental study of the transition from forced to natural circulation in EBR-II at low power and flow,ASME Journal of Heat Transfer,vol. 102,1980,pp. 525-529